

Characterization of complex non-aqueous phase liquids (NAPLs) in the subsurface environment: partitioning and interfacial tracer tests & numerical dissolution assessment

Dissertation
zur Erlangung des Grades eines Doktors der Naturwissenschaften

der Geowissenschaftlichen Fakultät
der Eberhard-Karls-Universität Tübingen

vorgelegt von
Matthias Piepenbrink
aus Lörrach

2007

Tag der mündlichen Prüfung: 23.12.2005

Dekan: Prof. Klaus G. Nickel, Ph.D.

1. Berichterstatter: Prof. Dr. Peter Grathwohl

2. Berichterstatter: PD Dr.-Ing. habil. Thomas Ptak

Characterization of complex non-aqueous phase liquids (NAPLs) in the subsurface environment: partitioning and interfacial tracer tests & numerical dissolution assessment

Matthias Piepenbrink ¹

Abstract. Contamination of the subsurface environment by complex organic non-aqueous phase liquids (NAPLs) and the resulting release of carcinogenic or mutagenic organic compounds impose a serious risk on groundwater quality. Due to the low aqueous solubilities of the individual organic components the rate of mass transfer from the non-aqueous phase to the water phase is very slow, thus NAPL source zones typically represent long-term contamination problems with organic compounds leaching into the ground water, at aqueous concentrations still far in excess of drinking water standards, for decades or centuries until they are finally depleted. Characterizing, understanding and predicting the behaviour of complex multi-component NAPLs at such contaminated sites is given primary attention in site assessment and site remediation. However, up to now even the determination of essential NAPL source zone parameters such as spatial NAPL distribution, NAPL saturation (S_n) and especially NAPL distribution geometry is difficult; conventional invasive methods like soil coring are costly and give only point-scale measurements.

Within this thesis, a numerical model for multi-component NAPL dissolution in porous media (BIONAPL3/D) was used for numerical NAPL dissolution assessment and to gain further insight into interactions between dissolved, persistent organic components being transported within the aqueous phase into a downgradient NAPL phase during the dissolution of a complex source zone. Furthermore, partitioning and interfacial tracer tests (PITTs) were refined, combined and applied, not only to determine the NAPL saturation of the whole tracer flushed section of the aquifer but also to estimate its NAPL distribution geometry. Additionally, ketones were introduced as a new class of oxidation resistant partitioning tracers which can be used for the remediation efficiency assessment of oxidizer techniques.

The calibration procedure of BIONAPL/3D was performed using available BTC data of Indene and Naphthalene that were measured at one representative point sampler (ME 2-7) in the large scale tank experiment at the VEGAS facility. Subsequently the model was able to predict the BTCs of the remaining BTEX and PAH components of the coal tar NAPL with adequate agreement, even for a different point sampler (ME 1-7) located further upgradient in the source zone. The hypothesis of re-partitioning, which leads to an enrichment of residual NAPL phase with persistent compounds delivered in the aqueous phase from upgradient, was confirmed in a numerical experiments using a surrogate NAPL and Benzene as an upgradient constant concentration boundary influencing the NAPL source zone. Sophisticated GC-FID and IC analysis techniques for the different tracer substances were developed, to overcome the problems of previous studies concerning the exact quantification of the individual tracer substances e.g. in the presence of highly volatile organic contaminants or naturally occurring ions like sulphate. This was followed by numerous PITTs at various scales (batch, column, large scale tank), mostly at controlled coal tar NAPL residual saturations, employing a combination of a suite of alcohols and an anionic surfactant. The PITT determined NAPL residual saturations estimates were generally smaller (36%-74%) than the actually existing NAPL volume, due to identified mass transfer limitations. However, the included interfacial tracer clearly distinguished between major different NAPL distribution geometries. As the concerning German authorities were unable to make their decision about the field application of these new tracer substances at a former gasworks site, the field activities had to be shifted to overseas: the emplaced creosote source zone at the Borden field site, Canada. The partitioning tracer tests (PTTs) were adapted to new substances (ketones) being utilizable as pre- and post-remediation PTTs for assessing an oxidizer experiment. After successful column tests using the original creosote and aquifer material, they were employed in a pre-remediation field test. The PTT based average absolute creosote phase volume estimate was at 65% of the initial value (71,84 l); with respect to the ageing of the source zone for more than one decade this value seems to be quite reasonable. Due to the higher partitioning coefficients of the ketones into the creosote the lower detection limit of the PTT was also improved by a factor of ten ($S_n \geq 0.55\%$).

¹ Dissertation am Institut für Geowissenschaften der Universität Tübingen
Anschrift des Verfassers: Matthias Piepenbrink, Jahnstraße 2/1, 72131 Ofterdingen

Charakterisierung von komplexen, mit Wasser nicht mischbaren Flüssigkeiten im Untergrund: Verteilungs- und Grenzflächen-Tracertests & numerische Einschätzung der Lösungsprozesse

Matthias Piepenbrink

Kurzfassung. Die Kontamination des Untergrunds mit komplexen, organischen, mit Wasser nicht mischbaren Flüssigkeiten (Non-Aqueous Phase Liquids: NAPLs) und die daraus resultierende Freisetzung von karzinogenen und mutagenen organischen Verbindungen stellt ein hohes Gefahrenpotential für die Qualität des Grundwassers dar. Aufgrund der geringen Wasserlöslichkeiten der einzelnen organischen Bestandteile läuft der Massentransfer aus der mit Wasser nicht mischbaren Phase in die wässrige Phase nur sehr langsam ab. Daher stellen NAPL Schadensherde typischerweise Langzeitkontaminationen dar, aus welchen über Jahrzehnte oder Jahrhunderte organischen Verbindungen, in Konzentrationen welche die zulässigen Werte der Trinkwasserverordnung bei weitem überschreiten, in das Grundwasser abgegeben werden bevor der Schadensherd schlussendlich abgereichert ist. Der Charakterisierung, dem Prozessverständnis und der Vorhersage des Langzeitverhaltens von komplexen Mehrkomponenten-NAPLs an damit kontaminierten Altstandorten gilt im Zuge der Altlastenerkundung und der Altlastensanierung eine hohe Priorität. Jedoch ist bis dato die Bestimmung der grundlegenden Parameter eines Schadensherds wie zum Beispiel der räumlichen NAPL-Verteilung, der NAPL-Sättigung (S_n) und insbesondere der NAPL-Verteilungsgeometrie sehr schwierig; herkömmliche invasive Methoden wie Kernbohrungen sind teuer und liefern nur punktuelle Informationen.

Im Rahmen dieser Arbeit, wurde ein numerisches Modell für die Auflösung von Mehrkomponenten-NAPLs in porösen Medien (BIONAPL/3D) einerseits für die numerische Einschätzung der Lösungsprozesse benutzt und andererseits eingesetzt um weiteren Einblick in das Zusammenspiel von gelösten persistenten organischen Komponenten welche während der Auflösung eines komplexen Schadensherds mit der wässrigen Phase in den nächstgelegenen unterstromigen NAPL-Phasenkörper transportiert werden zu erhalten. Weiterhin wurden Verteilungs- und Grenzflächen-Tracertests (Partitioning and Interfacial Tracer Tests: PITTs) verfeinert, kombiniert und angewendet, nicht nur um die NAPL-Sättigung der gesamten vom Tracer durchströmten Grundwasserleitereinheit zu bestimmen, sondern auch um deren NAPL-Verteilungsgeometrie abzuschätzen. Zusätzlich wurden Ketone als eine neue Klasse von oxidationsresistenten Partitioning Tracern eingeführt, welche für die Überprüfung der Sanierungseffizienz von Oxidationsverfahren eingesetzt werden können.

Die Kalibration von BIONAPL/3D wurde mittels verfügbarer Durchbruchkurven von Inden und Naphthalin durchgeführt, welche an einer repräsentativen teilverfilterten Kapillare (ME 2-7) in einem großskaligen Tankexperiment in der VEGAS-Forschungseinrichtung gemessen wurden. Anschließend war das Modell in der Lage die Durchbruchkurven der verbleibenden BTEX- und PAK-Komponenten des Teeröls mit adäquater Übereinstimmung vorherzusagen, dies traf ebenfalls für eine weiter oberstromig im Schadensherd angeordnete teilverfilterten Kapillare (ME 1-7) zu. Die Rückverteilungs- (Re-Partitioning) Hypothese, welche zu einer Anreicherung der residualen NAPL-Phase mit persistenten Komponenten, die von oberstrom gelöst in der wässrigen Phase zugeführt werden, führt, wurde in einem numerischen Experiment mit einem Ersatz-NAPL und der Zufuhr von Benzol per konstanter Konzentrationsrandbedingung bewiesen. Für die verschiedenen Tracer-Substanzen wurden ausgefeilte GC-FID und IC Analyseverfahren entwickelt, um die Probleme vorhergehenden Untersuchungen bezüglich der exakten Quantifizierung der einzelnen Tracerstoffe z.B. in der Anwesenheit von hochflüchtigen organischen Kontaminanten oder von natürlich vorkommenden Ionen wie Sulfat zu überwinden. Darauffolgend wurden zahlreiche PITTs in den verschiedensten Skalen (Batch-, Säulen und Tank-Experimente), zumeist mit einer kontrollierten Teeröl NAPL-Sättigung, unter der Anwendung einer Mischung aus verschiedenen Alkoholen und eines Anionischen-Tensids durchgeführt. Die in den Versuchen per PITTs bestimmte NAPL-Sättigung war generell kleiner (36%-74%) als die tatsächlich vorliegende NAPL-Sättigung, was auf Limitierungen beim Massentransfer zurückgeführt werden konnte. Jedoch konnte mittels des integrierten Interfacial Tracers klar zwischen den verschiedenen NAPL-Verteilungsgeometrien unterschieden werden. Da die zuständigen deutschen Behörden nicht in der Lage waren eine endgültige Entscheidung über einen Feldeinsatz dieser neuen Tracersubstanzen an einem ehemaligen Gaswerksstandort zu treffen, mussten die Feldarbeiten nach Übersee verlegt werden: an den künstlich angelegten Kreosot-Schadensherd innerhalb des Borden-Testfelds in Kanada. Die Partitioning Tracer Tests (PTTs) wurden für neue Substanzen (Ketone) angepasst, um diese dann im Rahmen einer vergleichenden Prä- und Post-Sanierungsstudie, d.h. für die Überprüfung der Sanierungseffizienz von Oxidationsverfahren, einsetzen zu können. Nach dem erfolgreichen Einsatz in Säulenversuchen mit original Kreosot und Aquifermaterial, wurden die Ketone schließlich in einem Prä-Sanierungs-PTT eingesetzt. Das per PTT bestimmte mittlere absolute Volumen der Kreosot-Phase beträgt 65% des bekannten Ausgangswerts (71,84 l); in Anbetracht der Alterung des Schadensherds über mehr als ein Jahrzehnt ist dies ein durchaus plausibler Wert. Aufgrund der höheren Verteilungskoeffizienten der Ketone in das Kreosot wurde zudem die untere Nachweisgrenze der PTT-Methode um den Faktor zehn verbessert ($S_n \geq 0.55\%$).

**“An expert is someone who knows some of the worst mistakes
that can be made in his subject, and how to avoid them.”**

Werner Heisenberg (1901-1976)

Acknowledgements

Thanks to:

- Peter Grathwohl and Thomas Ptak for supervising and advising me throughout the work.
- The whole ZAG-laboratory team for the good cooperation.

Special Thanks to:

- Christina Eberhardt & Michael Finkel for their aid with the VEGAS tank experiments and their courtesy of experimental NAPL dissolution data.
- Anne Hartmann-Renz for measuring 1000s of Ion- and SLES-samples.
- Bernice Nisch for assisting the measurement of 1000s of alcohol- and ketone-samples.
- Renate Riehle for technically assisting the drop weight method measurements.

Very special thanks to:

- John Molson for troubleshooting and debugging BIONAPL/3D.
- James F. Barker & Coby Lamarche for conducting the field experiment at CFB Borden, Canada.
- Birgit Stotz for loving encouragement.

Funding:

- Financial support of this work was provided by Deutsche Forschungsgemeinschaft, Priority program 546: "Geochemical processes with long-term effects in anthropogenically-affected seepage- and ground-water".

Contents

1	INTRODUCTION	1
1.1	RESEARCH OBJECTIVES.....	2
1.2	THESIS ORGANISATION.....	2
2	RESIDUAL NAPL PHASE DISSOLUTION	3
2.1	INTRODUCTION.....	3
2.2	THEORY.....	3
2.3	MODELLING.....	5
2.4	NUMERICAL TESTS.....	7
2.4.1	<i>Sensitivity Analysis</i>	7
2.4.2	<i>Re-Partitioning Tests</i>	8
2.4.3	<i>Model Calibration</i>	9
2.4.4	<i>Simulation of Source Depletion</i>	10
2.5	RESULTS AND DISCUSSION.....	14
2.5.1	<i>Sensitivity Analysis</i>	14
2.5.2	<i>Re-Partitioning Tests</i>	16
2.5.3	<i>Model Calibration</i>	17
2.5.4	<i>Simulation of Source Depletion</i>	18
3	PARTITIONING AND INTERFACIAL TRACER TESTS	21
3.1	INTRODUCTION.....	21
3.2	THEORY.....	24
3.2.1	<i>Retardation Factors</i>	24
3.2.2	<i>Retardation of Partitioning Tracers</i>	24
3.2.3	<i>Retardation of Interfacial Tracers</i>	25
3.3	MATERIALS AND METHODS.....	26
3.3.1	<i>Tracer Chemicals</i>	26
3.3.2	<i>Tar oil DNAPL</i>	26
3.3.3	<i>Aquifer Material</i>	27
3.3.4	<i>Analytical Methods</i>	27
3.3.5	<i>Batch Experiments</i>	29
3.3.6	<i>Column Experiments</i>	30
3.3.7	<i>Large scale tank experiments</i>	33
3.4	RESULTS AND DISCUSSION.....	37
3.4.1	<i>Batch Experiments</i>	38
3.4.2	<i>Column Experiments</i>	39
3.4.3	<i>Large scale Tank experiments</i>	53
3.5	SUMMARIZED RESULTS OF THE PITT EXPERIMENTS.....	60

4	KETONE PARTITIONING TRACER TESTS AT BORDEN.....	63
4.1	INTRODUCTION.....	63
4.2	THEORY.....	64
4.3	MATERIALS AND METHODS.....	64
4.3.1	<i>Tracer Chemicals</i>	64
4.3.2	<i>Creosote DNAPL</i>	65
4.3.3	<i>Analytical Methods</i>	65
4.3.4	<i>Batch Experiments</i>	66
4.3.5	<i>Column Experiments</i>	66
4.3.6	<i>Field Tests</i>	67
4.4	RESULTS AND DISCUSSION.....	68
4.4.1	<i>Batch Experiments</i>	68
4.4.2	<i>Column Experiments</i>	69
4.4.3	<i>Field Experiment</i>	71
4.5	SUMMARIZED RESULTS OF THE KETONE PTTs.....	72
5	SUMMARY AND CONCLUSIONS.....	74

1 Introduction

Liquid complex organic multi-component mixtures like coal tars, tar oils and creosote can contain hundreds of different chemicals with only a few present at greater than 1% by weight (Mueller et al., 1989). For example the composition of creosote depends on the coal tar from which it was produced; it generally contains 85% polycyclic aromatic hydrocarbons (PAHs), 10% phenolics and 5% heterocyclic compounds (nitrogen, sulfur and oxygen containing aromatics) (Mueller et al., 1989). Liquid complex organic mixtures are associated with manufactured gas plants, tar distillation works and wood preservative plants, most of them are dense non-aqueous phase liquids (DNAPLs) thus after being released they will migrate through the unsaturated zone and then further across the water table downward the saturated zone until they meet an impermeable boundary. At these boundaries DNAPL pools are formed, which may occupy up to 100% of the pore space. Residual DNAPL blobs are typically formed at the trailing edge of a migrating DNAPL body due to hysteresis (Bear, 1972) and typically occupy from 1 to 20% of the pore space. The individual compounds of a DNAPL commonly have low aqueous solubilities, but nevertheless they are permanently released into groundwater at aqueous concentrations far in excess of drinking water standards. Because of their low aqueous solubilities the rate of mass transfer from the non aqueous phase to the water phase is very slow, thus DNAPL source zones represent long-term contamination problems with organic compounds leaching into the ground water for decades or centuries until the source is depleted. The resulting contamination of the ground water with the released substances, e.g. polycyclic aromatic hydrocarbons (PAHs) is of great

concern because many of the PAHs are carcinogenic or mutagenic. Furthermore, recent studies have shown, that not only contact with the neat coal tar but also with coal tar contaminated soil is sufficient to produce the typical DNA adducts that indicate the tumorigenic potential of this substance (Koganti et al., 2001).

Contamination by complex organic multi-component DNAPLs is a global problem. In the 19th and 20th century approximately 1,000 manufactured gas plants were operated just in Germany (Zamfirescu, 2000). Assessing, understanding and predicting the behaviour of complex multi-component NAPLs at such contaminated sites is given primary attention in environmental hydrogeology and site remediation. However, up to now the amount and location of a NAPL source zone is difficult to determine; conventional invasive methods like soil coring are costly and give only point-scale measurements, which must then be regionalized throughout the site yielding site assessment at a high level of uncertainty. For these reasons, innovative methods for source characterisation have to be being developed. Partitioning and interfacial tracer tests are some of these innovative techniques which offer the possibility not only to determine the DNAPL saturation of the whole tracer flushed section of the aquifer but also to estimate the DNAPL distribution geometry which is one of the major parameters required for the prediction of the long-term behaviour of the source zone.

1.1 Research Objectives

The objectives of this research were to investigate the capability of a numerical model for multi-component NAPL dissolution in porous media (BIONAPL3/D) in predicting the long-term source depletion behaviour of a multi-component NAPL. Furthermore to numerically test the hypothesis of re-partitioning, which leads to an enrichment of former depleted residual NAPL phase with soluble compounds delivered in the aqueous phase from upgradient, which was already observed in the field (Zamfirescu, 2000).

Partitioning and interfacial tracer tests need to be combined in one experimental run, the so called PITT experiments, to determine the NAPL saturation and the interfacial area between NAPL and water phase in one single experiment.

A new class of oxidation resistant partitioning tracers had to be implemented in the PTT methodology to use them as pre- and post-remediation evaluation tool when employing an innovative source zone oxidation technique.

1.2 Thesis organisation

Following the introduction, this thesis is divided into three main sections: Chapter 2 investigating the residual NAPL Phase dissolution, Chapter 3 examining the application of partitioning and interfacial tracer tests and Chapter 4 presenting the introduction of ketones as oxidation resistant partitioning tracers for a field tests at Borden. Chapter 5 presents a summary and conclusions for the entire thesis, but because chapters two, three and four were developed as separate stand-alone sections they also have their own introduction and summary and conclusions.

2 Residual NAPL Phase Dissolution

This chapter describes NAPL dissolution simulations in porous media using BIONAPL/3D. An extensive sensitivity analysis was used to identify the influence of the governing mass transfer parameters. This initial work was followed by testing the re-partitioning capabilities (mass transfer from the aqueous phase back into the NAPL phase) of the code and the model calibration by a limited amount of data from the VEGAS tank experiment. The final forward modelling of the source depletion in the transient tank experiment was validated by the whole available dataset.

2.1 Introduction

The relevant contaminant spectra and processes at the 'Testfeld-Süd', a former gasworks site with intense DNAPL contamination which was in focus for the applied part of this research, were identified by Zamfirescu (2000) as follows:

(1) The relevant contaminant spectra at the 'Testfeld-Süd' consisted of the 16 EPA-PAH, BTEX (plus 8 other volatile aromatic hydrocarbons) and several NSO-heterocyclic compounds which are present in the groundwater at elevated concentrations and are all original coal tar / tar oil constituents.

(2) In column experiments with disturbed and undisturbed field cores the dissolution of contaminants out of residual coal tars and tar oils was identified as relevant contaminant release process. Other processes like diffusion limited contaminant desorption out of aquifer material or diffusion limited contaminant desorption out of low conductivity zones are

only of minor importance, as long as any residual NAPL phase is present.

(3) The maximum aqueous contaminant concentrations determined in lab experiments and multilevel wells at the 'Testfeld-Süd' equal the saturation concentrations attained by equilibrium dissolution out of the respective NAPL phase according to the Raoult's law. This fact permits the use of simple equilibrium based back on the envelope calculations/models for a rough, but fast prediction of the total dissolution behaviour of NAPL source zones.

The subsequent research of this work consequently focussed on the incorporation of these results into numerical modelling for more precise predictions of the long-term source zone dissolution behaviour of multi-component NAPLs and also on the complex interactions (a) within a multi-component NAPL source zone itself and (b) within a multi-component NAPL source zone under the influence of upgradient aqueous contaminant concentrations.

2.2 Theory

The equilibrium aqueous concentration of an individual compound m (C_s^m) out of a liquid, complex organic mixture (e.g. NAPLs like coal tar, tar oil) can be calculated according to Raoult's law, which describes the equilibrium behaviour of a solute between two phases:

$$C_s^m = \chi_m \gamma_m S_m \quad (2-1)$$

where χ_m , γ_m and S_m denote the mole fraction [-], the activity coefficient in the organic mixture [-] and the solubility of the pure compound in water [g/l].

The activity coefficient is often assumed to equal unity. For pure compounds that are solid under ambient temperature and pressure conditions, the hypothetical subcooled liquid solubility (Lane & Loehr, 1992; Loyek, 1998) must be used instead of S_m .

Under these assumptions the concentration of a compound in the aqueous phase is proportional to its mole fraction in the complex organic phase. Validation of this theory was given in different studies and for numerous complex NAPLs e.g. by Grathwohl (1998) for creosote, a coal tar and two of its distillation products, by Lee et al. (1992) for eight different coal tars and by Ferreira-Reckhorn et al. (2001) for gasoline constituents. Mukherji et al. (1997) and Loyek (1998) showed that deviations of the activity coefficients of individual compounds from unity can often be explained by errors associated with the estimates of the subcooled liquid solubility.

The dissolution behaviour of entrapped NAPLs in a natural porous media depends on the mass transfer between the residual NAPL phase and the mobile aqueous phase. This process can be described by stagnant boundary layer models. In practice the mass transfer coefficient is predicted from empirical correlations using the dimensionless Sherwood number Sh , which relates the interface mass transfer resistance to the properties of the porous media and water:

$$Sh = \frac{k_{diss} d}{D_{aq}} \quad (2-2)$$

where k_{diss} , d and D_{aq} denote the mass transfer coefficient [cm/s], the characteristic length of the porous medium, e.g. the mean grain diameter [cm] and the aqueous diffusion coefficient of the component [cm²/s]. These correlations are in general functions of other dimensionless numbers:

$$Sh = f(Re, Sc, \theta) \quad (2-3)$$

Many of these correlations have been published in literature covering different ranges of Reynolds numbers Re [-], Schmidt numbers Sc [-] and NAPL filled porosities θ [-].

The Re number is given as:

$$Re = \frac{v_a d}{\eta_w} \quad (2-4)$$

where v_a is the linear water velocity [cm/s] and η_w is the cinematic viscosity of water [cm²/s].

The Sc number is the ratio between the cinematic viscosity (η_w) and the aqueous diffusion coefficient ($Sc = \eta_w / D_{aq}$). The NAPL filled porosity (θ) is given by the residual NAPL saturation (S_n) and the porosity of the porous medium ($\theta = S_n n$).

Khachikian and Harmon (2000) give graphical comparisons (Sh number versus Peclet number) for different kinds of empirical Sh correlations that were reported in the chemical and environmental engineering literature.

For laminar flow in packed beds Fitzer et al. (1995) determined:

$$Sh = 1.9 Sc^{1/3} Re^{1/2} \quad (2-5)$$

For the dissolution of naphthalene spheres in column experiments Powers et al. (1994) derived:

$$Sh = 36.8 Re^{0.654} \quad (2-6)$$

Miller et al. (1990) found in column experiments with glass beads and different levels of toluene residual saturation, that the mass transfer is related to aqueous phase velocity and the NAPL filled porosity, giving:

$$Sh = 12 Re^{0.75} \theta^{0.6} Sc^{0.5} \quad (2-7)$$

For investigation of dissolution fingering phenomena Imhoff and Miller (1996) and Imhoff et al. (1996) used the following term:

$$Sh = 186 \theta^{0.87} Re^{0.71} \quad (2-8)$$

Figure 2-1 gives a graphical plot of the four empirical Sherwood number correlations listed above versus a range of Reynolds numbers typical for natural flow in porous media.

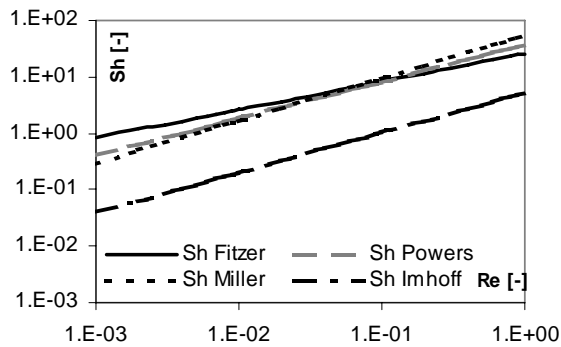


Figure 2-1: Sherwood numbers (Sh) given by the empirical correlations of different authors versus Reynolds number (Re). Settings: Sc number=2600 [-], $n=0.33$ [-], $Sn=0.05$ [-].

The abundance of correlations reported in literature suggests that the knowledge at the homogeneous column scale has grown, but has yet to yield a universal theory. As it should be noted that all these relationships only reflect the specific settings of the individual experiment and are not necessarily valid for other settings.

Therefore it is not astonishing, that Bradford et al. (2000) were unable to fit all observed concentration time series of dissolving PCE obtained in 23 column experiments (with varying parameters for NAPL filled porosity, median grain size and uniformity index) by one single correlation.

Experiments conducted in a heterogeneous 2D tank set-up by Nambi and Powers (2000) confirmed this, as they found that the aqueous flow patterns within the system are largely responsible for the establishing effluent concentrations.

For complex mixtures, this emphasises the need for an adequate modelling tool which incorporates Raoult's law and combines both, the mechanistically correct mass transfer functions as well as the changes in flow patterns due to varying NAPL saturation.

2.3 Modelling

Modelling was carried out using a numerical model, BIONAPL/3D (Frind et al., 1999; Molson, 2000; Molson, 2001), which was designed for simulating multi-component NAPL dissolution in porous media. The capabilities and limitations of the code concerning the used spectra of available functions are listed in Table 2-1 (modified after Molson, 2001).

Table 2-1. Summary of the capabilities, assumptions and limitations of BIONAPL/3D.

Capabilities	Assumptions and Limitations
<ul style="list-style-type: none"> Fully coupled flow (steady state or transient) and mass transport in 1D, 2D or 3D domains Domain can be heterogeneous and anisotropic Sources can originate in the aqueous phase or from a dissolving NAPL phase, possible source location within the domain or on a boundary Sources can be composed of multi contaminant mixtures Relative permeability changes with respect to NAPL saturation and dissolution Versatile boundary conditions Output includes concentration breakthrough curves, 1D profiles, 2D sections and 3D volumes 	<ul style="list-style-type: none"> Fluid is incompressible and the aquifer is non-deforming Saturated flow domain is a non-fractured or equivalent porous media Gas phase transport is neglected NAPL phase (if included) is immobile Multiple NAPL phase source zones are possible, but only with an identical NAPL composition

The major equations with respect to the relative permeability changes and the mass transfer process are presented below. For the complete description of the solution approach and all governing equations see the BIONAPL/3D user guide (Molson, 2001) or Molson (2000) and Frind et al. (1999).

The equation for saturated groundwater flow in the presence of a dissolving residual NAPL can be written as:

$$\frac{\partial}{\partial x_i} \left(K_{ij} k_{rw} \frac{\partial h}{\partial x_j} \right) + S_w S_s \frac{\partial h}{\partial t} + n \frac{\partial S_w}{\partial t} = 0 \quad (2-9)$$

where h [m] is the hydraulic head, K_{ij} [m/day] is the hydraulic conductivity tensor, n [-] is the porosity, k_{rw} [-] is the relative permeability with respect to water, x_i [m] are the spatial coordinates (x, y, z), t [days] is the time, S_s [m⁻¹] is the specific storage and S_w [m³_{water}/m³_{voids}] is the water saturation.

The presence of NAPL will affect the hydraulic properties of the source zone, thus it is required to express the relative hydraulic conductivity k_{rw} as a function of S_n :

$$k_{rw} = \left(\frac{(1 - S_n) - S_{rw}}{1 - S_{rw}} \right)^4 \quad (2-10)$$

where S_{rw} is the irreducible degree of water saturation. The degrees of saturation with respect to water (S_w) and NAPL (S_n) are given by: $S_w + S_n = 1$.

A graphical plot of the relationship between S_n and k_{rw} (Eq. 2-10) is given in Figure 2-2.

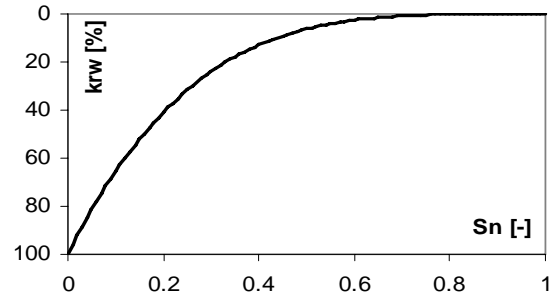


Figure 2-2: Relative permeability k_{rw} as a function of NAPL saturation S_n . Settings: $S_{rw} = 0$.

The equation for advective-dispersive transport of a NAPL component m undergoing kinetic dissolution from a residual NAPL source can be written as:

$$n S_w D_{ij}^m \frac{\partial^2 C_w^m}{\partial x_i^2} - q_i \frac{\partial C_w^m}{\partial x_i} - n S_w \lambda^m (C_s^m - C_w^m) = n S_w R \frac{\partial C_w^m}{\partial t} \quad (2-11)$$

where D_{ij}^m [m²/day] is the hydrodynamic dispersion tensor, C_w^m [kg/m³] is the aqueous concentration of an individual component m , q_i [m/day] is the Darcy flux component, λ^m [day⁻¹] is the mass transfer rate coefficient, C_s^m [kg/m³] is the equilibrium aqueous concentration of an individual compound out of a given NAPL according to the Raoult's law (eq. 2-1) and R [-] is the retardation factor.

The mass transfer rate coefficient of component m (λ^m) in equation 2-11 at point i is defined empirically as (Frind et al., 1999):

$$\lambda_i^m = \frac{Sh D_{aq}^m}{d^2} \left(\frac{f_i^m S_{n,i}}{S_{n,0}} \right)^{\beta^m} \quad (2-12)$$

where Sh [-] is the Sherwood number, D_{aq}^m [m²/s] is the aqueous diffusion coefficient of component m , d [m] is the median grain diameter, $S_{n,i}$ [-] is the NAPL saturation at point i , with $S_{n,0}$ [-] being the initial saturation, f_i^m [-] is the local fraction of component m in the NAPL mixture and β^m [-] is an empiric non-linear exponent of component m , which is assumed to range between zero and one. This lumped parameter represents the possible time dependence of the mass transfer process (degree

of accessibility to water phase) and will influence the long-term transient dissolution behaviour of the source zone (prolonged concentration tailings during dissolution). Note that λ^m is less sensitive to changes in NAPL saturation as β^m decreases. A linear mass transfer rate coefficient can be achieved by setting $\beta^m = 0$, which simplifies equation 2-12 to:

$$\lambda_i^m = \frac{ShD_{aq}^m}{d^2} \quad (2-13)$$

The description of the iterative algorithm of BIONPL/3D for each time step is available in Frind et al. (1999) and briefly summarized as follows: (1.) Solve equation (2-9) for hydraulic head h using the previous settings of S_n and k_{rw} from equation (2-10). (2.) Calculate the Darcy fluxes q_i according to Darcy's law. (3.) Solve the transport equation (2-11) for all components m regarding to their aqueous concentrations C_w^m using the previous values of S_n , S_w , C_s^m and λ^m .

Afterwards the mass of each component m remaining in the NAPL is calculated. Subsequently the new aqueous equilibrium concentration C_s^m is calculated according to equation (2-1), k_{rw} and S_n are updated and finally λ^m is adjusted with respect to the new S_n .

2.4 Numerical Tests

2.4.1 Sensitivity Analysis

The influence of the two governing mass transfer input parameters Sh and β^m on the total NAPL dissolution time and attained aqueous concentration was tested in a fully saturated, homogeneous 2-D model domain (20 m in length, 1 m in width and 10 m in height) described below. The aquifer properties were chosen according to the effective parameters determined in the 'Testfeld-Süd', see Table 2-2.

Table 2-2: Representative properties of the model domain aquifer according to values determined in 'Testfeld-Süd'

Property	Value
Hydraulic conductivity [m/s]	2.5e-03
Porosity [-]	0.13
Linear velocity [m/day]	1
Median grain size [m]	0.005

S_s and S_{rw} were set to zero

For general assessment of the source dissolution behaviour the source zone geometry was assumed to be a cube of 1m³. In order to save computation time the first model calculations were run with a surrogate DNAPL composed of only three representative components (Tab. 2-3), that are taken to be non-degradable (thus the focus being solely on mass transfer processes).

The discretisation within the 2-D grid was set to 0.05 m in the source area to 0.1 m in the downstream vicinity to 0.5 m elsewhere in each of the two coordinate directions, giving a grid of $81 \times 2 \times 57 = 9234$ nodes (Fig. 2-3). The discretisation satisfies the grid Peclet constraint ($\Delta x \leq 2\alpha_L$). A time step of 0.04 days, satisfying the Courant constraint ($\Delta t \leq \Delta x/v_a$), and a total run time of 720 days was used for all simulations.

The hydraulic gradient is controlled by a fixed-flow upgradient boundary face and a fixed-head downgradient boundary face, while all other boundary conditions were set to no-flow. For transport the upgradient boundary face is set to fixed concentration of zero, all other boundaries are assigned zero-gradient boundary conditions. To minimize the influence of transverse as well as upstream dispersion, dispersivity values of $\alpha_L = 0.3$ m and $\alpha_{TH} = 0.001$ m were used.

Table 2-3: Properties of the surrogate DNAPL used for sensitivity analysis

	Benzene	Xylene	Naphthalene
Molecular weight [kg/mol]	0.078	0.106	0.128
Solubility of the pure compound in water [kg/m ³]	1.8	0.2	0.12*
Number of Moles	50	18.4	15.2
Aqueous diffusion coefficient [m ² /s]	5.0 e-10	5.0 e-10	5.0 e-10

DNAPL density was set to 1200 [kg/m³], initial saturation is 0.05 [-] and * is the subcooled liquid solubility

The grid spacing, the position of the source zone ($S_{n,0} = 0.05$) and of the nested sampling wells Well 1 and Well 2 (one well per well nest is fully screened, the other is just screened in the z -range of the source zone) is indicated in Figure 2-3, a cross section of the model domain.

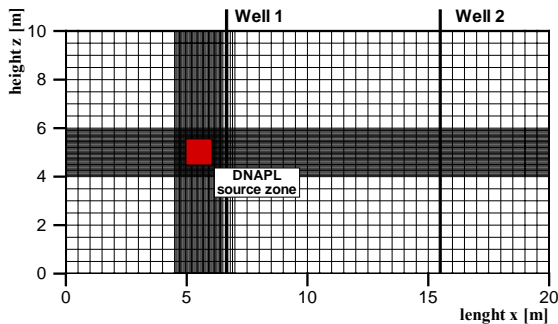


Figure 2-3. Cross section of the 2-D model domain indicating the dimensions and discretisation of the grid, location of the DNAPL source zone and position of the well nests Well 1 and Well 2.

As stated before, the mass transfer input parameters that can be varied in this sensitivity testing are Sh and β^n , which here are assumed to be the same for all three NAPL constituents. An initial estimate of Sh was obtained by equations 2-5 to 2-8, the results were all close to 5 besides the correlation of Imhoff that delivers 0.2. As there was no available correlation for an initial guess of β^n the mean (0.5) of its possible range (0.0-1.0) was used.

To evaluate the sensitivity of the individual input variables the following settings were used, $\beta = 0.5$ with five different Sh number values: 0.15, 1.5, 5, 15 and 150 as well as $Sh = 5$ with three β values: 0.0, 0.5 and 1.0.

The only component specific input parameters playing a role in the mass transfer process, the aqueous diffusion coefficient D_{aq}^m and the solubility of the pure compound in water S_m ,

were obtained independently (Tab. 2-3) and not fitted.

2.4.2 Re-Partitioning Tests

The capability of BIONAPL/3D to account for partitioning of high aqueous concentrations from upgradient sources back into the NAPL phase at regions where the local aqueous equilibrium concentration is lower (due to a different NAPL composition) was tested in the same fully saturated, homogeneous 2-D model domain (20 m in length, 1 m in width and 10 m in height) described above.

The NAPL phase source zone composition as well as the grid discretisation, time steps, flow boundaries and all other settings were identical as before.

The conditions for transport were changed as follows: the upper half (5 m to 10 m) of the upgradient boundary face is set to fixed concentration of 1.5 kg/m³ of Benzene and zero concentration for the other compounds while the lower half is set to zero concentration for all compounds, at all other boundaries a zero concentration gradient is assumed.

The position of the NAPL source zone ($S_{n,0} = 0.05$) and of the new upstream input boundary source of benzene at a constant aqueous concentration of 1.5 kg/m³ is indicated in Figure 2-4.

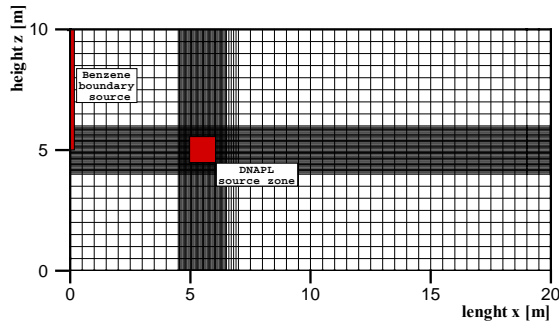


Figure 2-4. Cross section of the 2-D model domain indicating the location of the grid, location of the DNAPL source zone and the position of the constant benzene boundary source: 1.5 kg/m^3 .

The mass transfer input parameters Sh and β^n , were assigned as 5 and 0.5. The component specific parameters were already given in Table 2-3.

2.4.3 Model Calibration

The calibration of the model was done with the aid of PAH and BTEX concentration time series that were measured by Eberhardt and Grathwohl (2002) in the downgradient proximity of a dissolving coal tar source zone ($0.5 \text{ m} \times 1 \text{ m} \times 1 \text{ m}$) in a large scale tank experiment ($8 \text{ m} \times 1 \text{ m} \times 3 \text{ m}$) at the VEGAS facility, University of Stuttgart.

Calibration was based on the component concentrations observed at a representative point-sampler (ME 2-7) 0.1 m downgradient of the homogeneous NAPL-blob source zone.

Using Sh from a given correlation (equation 2-6) the model was calibrated with respect to the mass transfer parameter β^n , that was used to fit the concentration tailings observed within 177 days.

Model runs were conducted in a fully saturated, homogeneous 2-D model domain (1.2 m in length, 0.1 m in width and 0.5 m in height) described below. The aquifer properties were chosen according to the effective parameters in the large scale tank experiment, see Table 2-4.

Table 2-4: Properties of the model domain aquifer according to values determined in the large scale tank

Property	Value
Hydraulic conductivity [m/s]	$5.5\text{e-}03$
Porosity [-]	0.39
Linear velocity [m/day]	1.7
Median grain size [m]	0.0015

S_s and S_{rw} were set to zero

The emplaced source zone was represented by a source zone domain of 0.5 m in length (i.e. the real streamtube length of the source zone in the experiment), 0.1 m in width and 0.5 m in height. These calibration calculations were run with a surrogate DNAPL: a coal tar composed of 11 representative components that are again taken to be non-degradable (so the focus is solely on mass transfer processes). The individual component fractions were set according to the results determined by Eberhardt and Grathwohl (2002) for the Rüttgers coal tar that was used in the tank experiment (Tab. 2-5 and Tab. 2-7).

The discretisation within the 2-D grid varied from 0.02 m in the source x -direction and downgradient x -direction to 0.05 m elsewhere in each of the two coordinate directions, giving a grid of $49 \times 2 \times 11 = 1078$ nodes. The discretisation satisfies the grid Peclet constraint ($\Delta x \leq 2\alpha_L$). A time step of 0.01 days, satisfying the Courant constraint ($\Delta t \leq \Delta x/v_a$), was used for all simulations. The hydraulic gradient is controlled by a fixed flow upgradient boundary and a fixed head downgradient boundary, while all other boundaries were set to no-flow. For transport, the upgradient boundary is set to fixed concentration of zero, all other boundaries are assigned zero-gradient boundary conditions. To minimize the influence of upstream dispersion a dispersivity value of $\alpha_L = 0.015 \text{ m}$ was used, which is a reasonable value for the small scale transport processes (0.1 m between the downgradient end of the source zone and the sampling well) considered here.

The grid spacing, the position of the coal tar DNAPL source zone ($S_{n,0} = 0.05$) and of the

point-sampling well is indicated in Figure 2-5, a cross section of the model domain.

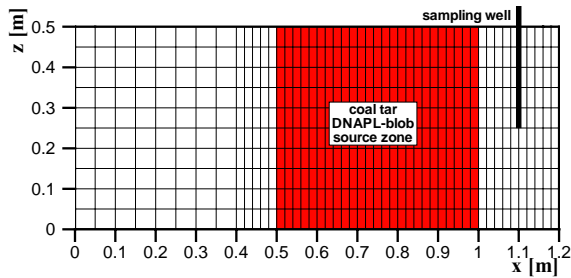


Figure 2-5. Cross section of the 2-D model domain indicating the dimensions and discretisation of the grid, location of the coal tar DNAPL source zone and position of the point-sampling well.

As stated before, the only fitting parameter in this calibration is β^n , which here is assumed to be the same for all 11 NAPL compounds. An initial estimate of Sh was obtained by equation 2-6 which delivered a value of 3.2. To evaluate the best fit of the β^n input variable the following settings were used: $Sh = 3.2$ with varying β^n values between 0.0 and 1.0.

The component specific input parameters e.g. the solubility of the pure compound in water S_m and the composition of the coal tar were obtained independently (Tab. 2-5.) and not fitted.

The composition of the coal tar was set according to the data of Eberhardt and Grathwohl (2002); the complete BTEX and PAH spectra of the Rüttgers coal tar and a comparison to several coal tar samples obtained from 'Testfeld Süd' are presented in Table 2-7.

2.4.4 Simulation of Source Depletion

Forward modelling of the tank experiment under transient flow conditions (see Tab. 2-6) was used to validate the model performance after the successful finalisation of the calibration procedure described in the previous chapter.

The validation was done with the aid of PAH and BTEX concentration time series that were measured under transient flow conditions by Eberhardt and Grathwohl (2002). Validation target thus consists of the component concentrations observed at two selected point-samplers: ME 1-7 that is located 0.1 m within the NAPL-blob source zone (measured from the upstream edge of the source zone) and ME 2-7 that is located 0.1 m downgradient the downstream edge of the NAPL-blob source zone (Fig. 2-6).

Table 2-5: Properties of the 11 component surrogate coal tar DNAPL used in calibration studies

Component	MW [kg/mol]	S_m [kg/m ³]	D_{aq}^m [cm ² /s]	M [mole]
Benzene	0.078	1.780	5.0e-10	6.970e-3
Toluene	0.092	0.534	5.0e-10	6.619e-3
Indene	0.116	0.332	5.0e-10	5.204e-2
BTEX-remnant [§]	0.113	0.348	5.0e-10	1.207e-2
Naphthalene	0.128	0.105*	5.0e-10	6.247e-1
Methyl-Naphthalene	0.142	0.029*	5.0e-10	6.418e-2
Acenaphthylene	0.152	0.044*	5.0e-10	7.436e-2
Fluorene	0.166	0.012*	5.0e-10	5.777e-2
Phenanthrene	0.178	0.0042*	5.0e-10	1.758e-1
Fluoranthene	0.202	0.0012*	5.0e-10	8.287e-2
PAH-remnant [§]	0.289	0.0017*	5.0e-10	1.386

DNAPL density was set to 1200 [kg/m³], initial saturation is 0.05 [-], * is the subcooled liquid solubility and [§] are hypothetical remnant creations to represent the properties of the whole coal tar used in the tank experiment

Table 2-6. Properties of the model domain aquifer according to values determined in the large scale tank

Property	Value
Hydraulic conductivity [m/s]	5.5e-03
Porosity [-]	0.39
v_a [m/day] at time 0-177 [days]	1.7
v_a [m/day] at time 177-219 [days]	5.1
v_a [m/day] at time 219-228 [days]	3.4
v_a [m/day] at time 228-293 [days]	1.7
v_a [m/day] at time 293-308 [days]	5.1
v_a [m/day] at time 308-368 [days]	1.7
Median grain size [m]	0.0015

S_s and S_{rw} were set to zero

Using Sh from a given correlation (equation 2-7) and β^n , that was retrieved in the previous calibration, the model results were evaluated with respect to their fit to the concentration tailings observed under transient flow conditions within 368 days. Model runs were conducted in the same fully saturated, homogeneous 2-D model domain (1.2 m in length, 0.1 m in width and 0.5 m in height) as described above. The aquifer properties and transient flow conditions were chosen according to the effective parameters of the large scale tank experiment, see Table 2-6.

The composition and position of the emplaced source zone in the model domain is already given in chapter 2.4.3 (Model Calibrations). Besides the placement of a second well the 2-D grid discretisation is identical to the calibration setup. The time steps were adapted to the specific flow conditions, satisfying the Courant constraint ($\Delta t \leq \Delta x/v_a$). The hydraulic gradient is now controlled by a fixed head upgradient boundary and a fixed head downgradient boundary, while all other boundaries were set to no-flow. Transient flow was handled by using separate time intervals for each flow velocity and adding/subtracting the respective head increment to/from the existing upgradient boundary head, increasing or decreasing the velocity. For transport the upgradient boundary face is set to fixed concentration of zero, all other boundaries are assigned zero-gradient boundary conditions. The grid spacing, the position of the coal tar DNAPL source zone

($S_{n,0} = 0.05$) and of the two point-sampling wells are indicated in Figure 2-6.

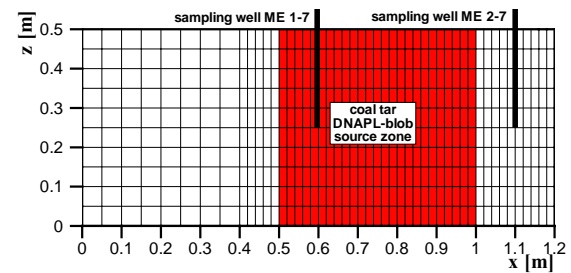


Figure 2-6. Cross section of the 2-D model domain indicating the dimensions and discretisation of the grid, location of the coal tar DNAPL source zone and position of the two point-sampling wells ME 1-7 and ME 2-7.

The component specific input parameters, i.e. the solubility of the pure compound in water S_m and the composition of the coal tar were kept at their independent values already presented in Table 2-5.

These synthetic model applications were consequently followed by an extensive search for 'model-adequate' source zone data (composition, volume and spatially distribution of the coal tar/tar oil NAPL) at the 'Testfeld-Süd'.

The analyses of the residual phase sampled from wells B16, B56 and B55 (Zamfirescu, 2000) and of the commercial, 'fresh' Rüttgers coal tar (Eberhardt and Grathwohl, 2002) are given in Table 2-7.

Two of the analysed coal tar samples (B56 and B55) from the field site show significant lower PAH content than the 'fresh' Rüttgers coal tar, but the composition of the third sample (B16) is very similar. Therefore, it can be assumed that the initial composition of the coal tars spilled at the 'Testfeld-Süd' was at least to some extent comparable to that of the Rüttgers coal tar. Coal tar sample B56 shows extremely low BTEX and PAH content and therefore represents a very aged NAPL phase close to depletion of the soluble components. The sample B55 supports the hypothesis of re-partitioning that was numerically simulated in Chapter 2.3.2 (Re-Partitioning Tests), as its composition is

extremely enriched in Acenaphthene (a relatively well soluble PAH) while all other PAHs behave according to their properties.

Table 2-7: Composition of the 'fresh' industrial Rüttgers coal tar and three residual coal tar phases sampled in well B16, B56 and B55 at 'Testfeld-Süd'.

Compound	Rüttgers coal tar* [wt %]	B16 [§] [wt %]	B56 [§] [wt %]	B55 [§] [wt %]
Benzene	0.095	0.099	0.0007	0.00003
Toluene	0.107	0.418	0.0014	0.00003
Ethylbenene	0.004	0.277	0.0012	0.00003
p-Xylene	0.069	0.753	0.0028	0.00006
o-Xylene	0.025	0.268	0.0012	0.00027
Isopropylbenzene	n.d.	0.006	n.d.	0.00005
Propylbenzene	0.001	0.007	n.d.	0.00001
1,2,4-Trimethylbenzene	0.024	0.356	0.0026	0.00027
1,2,3-Trimethylbenzene	0.006	0.085	0.0013	0.00008
1,3,5-Trimethylbenzene	0.012	2.41	0.0018	0.0029
Benzofurane	0.091	0.025	0.0013	0.002
Indane	0.009	0.168	0.0007	0.0016
Indene	1.065	1.59	0.0027	0.00004
Naphthalene	14.087	12.0	1.35	0.200
2-Methylnaphthalene	1.608	3.62	0.054	3.77
1-Methylnaphthalene	0.693	1.25	0.024	0.265
Acenaphthylene	1.991	0.963	0.048	0.013
Acenaphthene	0.310	2.03	0.104	4.19
Fluorene	1.689	1.93	0.161	1.77
Phenanthrene	5.513	2.86	0.214	2.44
Anthracene	1.351	0.544	0.038	0.034
Fluoranthene	2.949	0.782	0.036	0.337
Pyrene	2.132	0.510	0.021	0.246
Benz(a)anthracene	1.082	0.218	0.0012	n.d.
Chrysene	0.758	0.269	0.0019	n.d.
Benzo(b)fluoranthene	1.169	0.209	n.d.	n.d.
Benzo(k)fluoranthene	n.d.	n.d.	n.d.	n.d.
Benz(a)pyrene	0.742	0.086	n.d.	n.d.
Indeno(1,2,3-cd)pyrene	0.396	0.041	n.d.	n.d.
Dibenz(a,h)anthracene	0.068	n.d.	n.d.	n.d.
Benzo(g,h,i)perylene	0.274	0.047	n.d.	n.d.
∑ determined compounds [wt%].	38.321	33.821	2.070	13.272

* Eberhardt and Grathwohl (2002), [§] Zamfirescu (2000), n.d. – not detected

A representation of all point data, that were available from several drilling campaigns (Years: 1968, 1969, 1988, 1990, 1996 and 1998) is given in Figure 2-7, a map of the 'Testfeld-Süd' indicating all boreholes where residual NAPL phase was detected (note: not all these boreholes are still existing as monitoring wells).

A depth-orientated plot of this information is given in two pseudo-cross-sections of the field site (Fig. 2-8a and 2-8b) where all NAPL bearing boreholes are projected on two perpendicular planes, one is parallel to the northing and the other to the easting. These

figures clearly indicate that even under these 'increased' information density conditions no single governing source zone domain can be located but all individual source zones are more or less evenly distributed between approximately 320 m in S-N and 175 m in W-E direction. In contrast to this, the depth-orientation of the source zones is clearly towards the lower part of the aquifer, something which has to be expected for DNAPLs.

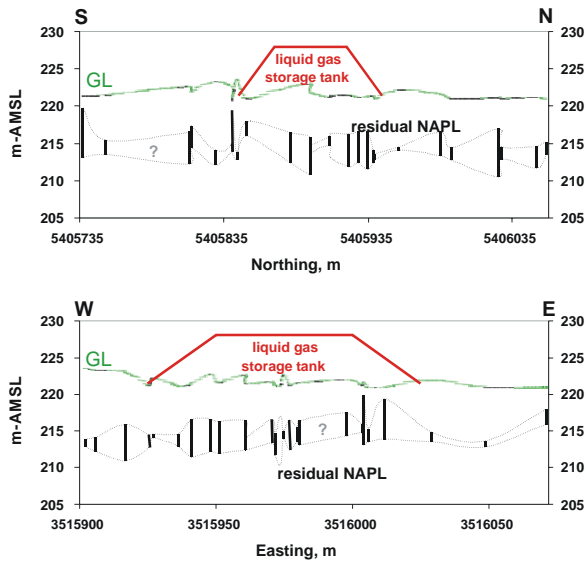


Figure 2-8: (a) S-N and (b) W-E cross section with projected residual NAPL bearing boreholes. GL-Ground level.

This situation indicates the need for improved integrating exploration/testing methods as it is impossible to determine neither the extent of the source area nor to resolve the spatially distribution and saturation of the individual sub-elements solely by the means of standard point-scale sampling techniques (boreholes).

Due to this insufficient data base, the modelling of source depletion at 'Testfeld-Süd' would only be possible with additional results from Partitioning and Interfacial Tracer Tests (PITTs). For a first estimate, a scenario model of the total dissolution time of different NAPL phases (B16, B55) at field scale (under the rough assumption of the lacking input parameters) that was carried out by Zamfirescu (2000) using a self provided Fortran code is included in the following.

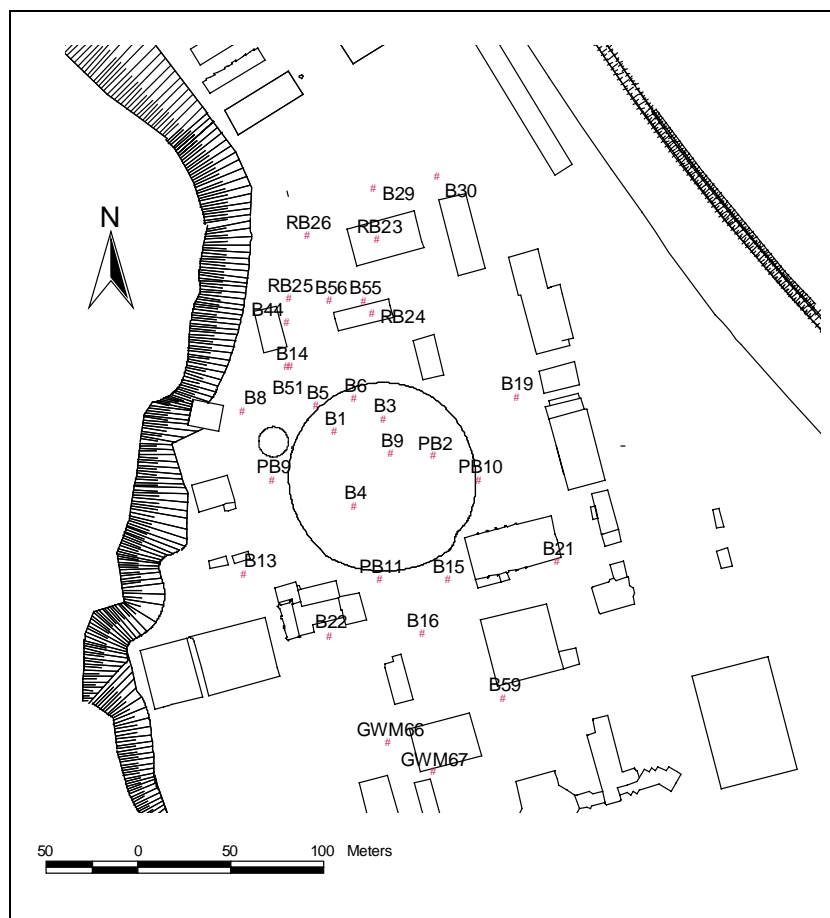


Figure 2-7. Map of the 'Testfeld-Süd' indicating all boreholes where residual NAPL phase was detected during several drilling campaigns.

The following settings were used by Zamfirescu (2000): the starting composition of the respective coal tars is already listed in Table 2-7, initial residual saturation was set to 0.02, the coal tar density is 1200 kg/m^3 and the average molar weight of the coal tars was set to 0.25 kg/mole, the downgradient length of the source zone was set to 4 m, the porosity is 0.15 and the groundwater velocity was set to 2 m/day.

It has to be noted, that under these conditions (i.e. due to the lack of validated/verified input data) the gain in absolute precision of the results modelled by the more sophisticated, but very computation time intensive, BIONAPL/3D compared to the simplistic equilibrium based code by Zamfirescu (2000) is negligible.

2.5 Results and Discussion

2.5.1 Sensitivity Analysis

The sensitivity of the total NAPL dissolution time and resulting aqueous concentrations with respect to variations of the mass transfer parameters Sh and β^m is shown in the following graphs (Fig. 2-9 - Fig. 2-16). The compilation of the concentration time series calculated for a surrogate NAPL (Benzene, Xylene and Naphthalene) with a fixed setting of $Sh = 5$ combined with three varying β values: 0.0, 0.5 and 1.0 is given in Figure 2-9.

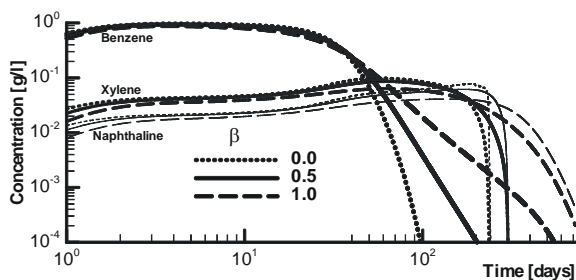


Figure 2-9. Simulated peak concentrations for Benzene (bold lines), Xylene (medium lines) and Naphthalene (thin lines) at well 1 (partially screened) with $Sh = 5$ and $\beta = 0.0, 0.5$ and 1.0.

It can be noted that tailing increases with increasing β values especially for Benzene but less for Xylene and Naphthalene. This behaviour is due to the use of the NAPL volume fraction which is raised to the power of β in the mass transfer rate coefficient (equation 2-12); this NAPL volume fraction becomes larger for Xylene and Naphthalene at times when Benzene is completely dissolved. The plateau as well as the maximum aqueous concentrations of the individual compounds are only slightly affected.

For the sake of clarity the breakthrough curves of each compound are also plotted in separate graphs (Fig. 2-10 – Fig. 2-12).

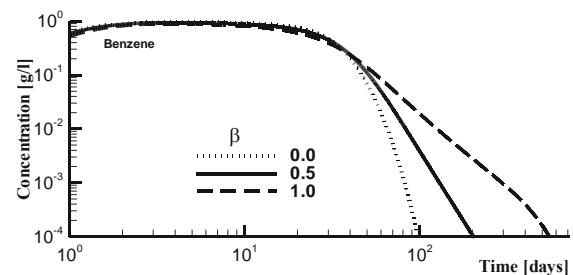


Figure 2-10. Simulated peak concentrations for Benzene (bold lines) at well 1 (partially screened) with $Sh = 5$ and $\beta = 0.0, 0.5$ and 1.0.

Figure 2-10 gives a total dissolution time (definition: the aqueous concentrations of the individual components drop below $1\text{E-}04 \text{ g l}^{-1}$) for Benzene between approx. 100 days ($\beta = 0.0$) and 500 days ($\beta = 1.0$).

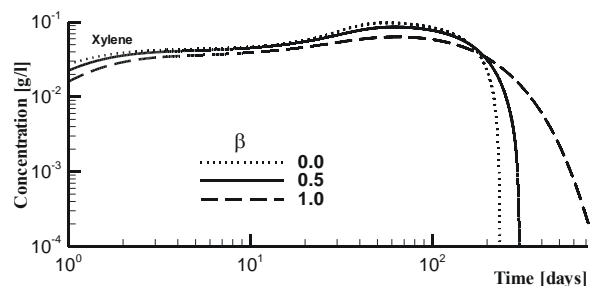


Figure 2-11. Simulated peak concentrations for Xylene (medium lines) at well 1 (partially screened) with $Sh = 5$ and $\beta = 0.0, 0.5$ and 1.0.

Figure 2-11 gives a total dissolution time for Xylene between approx. 250 days ($\beta = 0.0$) and 750 days ($\beta = 1.0$).

Whereas Figure 2-12 gives a total dissolution time for Naphthalene that is just slightly longer

than for Xylene, i.e. approximately 250 days ($\beta = 0.0$) and 750 days ($\beta = 1.0$).

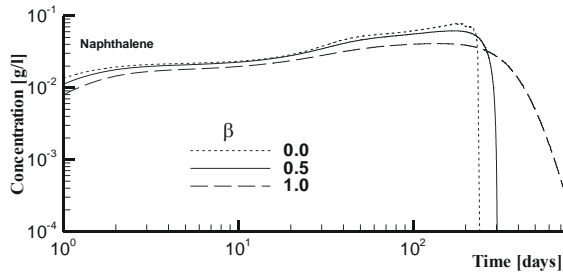


Figure 2-12. Simulated peak concentrations for Naphthalene (thin lines) at well 1 (partially screened) with $Sh = 5$ and $\beta = 0.0, 0.5$ and 1.0 .

The compilation of the concentration time series calculated for the surrogate NAPL with a fixed setting of $\beta = 0.5$ combined with 5 varying Sh values: 0.15, 1.5, 5, 15 and 150 is given in Figure 2-13.

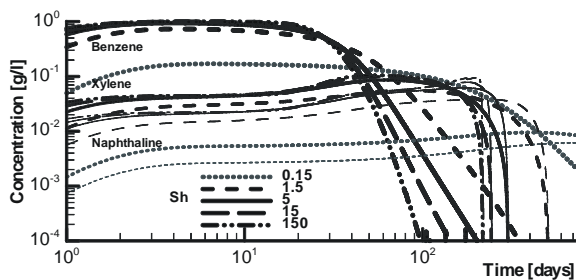


Figure 2-13. Simulated peak concentrations for Benzene (bold lines), Xylene (medium lines) and Naphthalene (thin lines) at well 1 (partially screened) with $\beta = 0.5$ and $Sh = 0.15, 1.5, 5, 15, 150$.

Here we have to deal with an inverse correlation: the tailing decreases with an increasing Sh number. However, the influence of the Sh is not compound specific and is less sensitive than for β except for the very small Sh value (0.15) when the aqueous concentrations drop dramatically. This means the mass transfer resistance increased so much that the length of the mass transfer zone is longer than the actually existing source zone (1 m). Consequently the concentrations are dropping for all compounds and the total dissolution time then exceeds the simulation period.

In general the plateau and maximum aqueous concentrations of the individual compounds as well as the total dissolution time are only

slightly affected by an increase (3- and 30fold) relative to the estimated starting value of $Sh = 5$. The effects of a Sh decrease are more obvious, as they finally lead to non-equilibrium source dissolution conditions. For the sake of clarity the breakthrough curves of each compound are again plotted in separate graphs (Fig. 2-14 – Fig. 2-16).

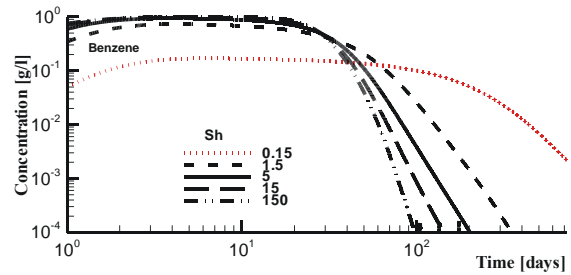


Figure 2-14. Simulated peak concentrations for Benzene (bold lines) at well 1 (partially screened) with $\beta = 0.5$ and $Sh = 0.15, 1.5, 5, 15, 150$.

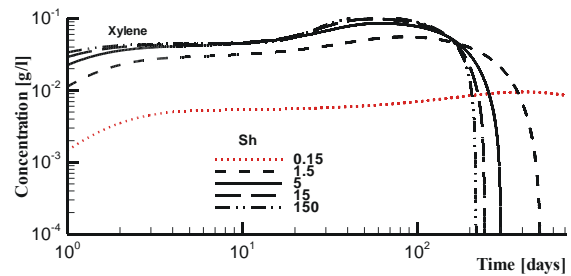


Figure 2-15. Simulated peak concentrations for Xylene (medium lines) at well 1 (partially screened) with $\beta = 0.5$ and $Sh = 0.15, 1.5, 5, 15, 150$.

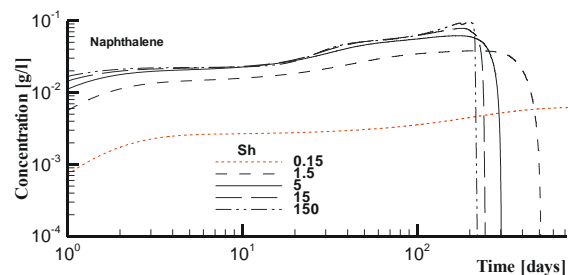


Figure 2-16. Simulated peak concentrations for Naphthalene (thin lines) at well 1 (partially screened) with $\beta = 0.5$ and $Sh = 0.15, 1.5, 5, 15, 150$.

Simulated well effects were evaluated by a comparison of concentration time series recorded at a fully screened well (filter-screen over the complete 10 m thickness of the model domain aquifer) and a partially screened well (filter-screen only over the 1 m vertical extent of

the model domain source zone) both were located in well nest Well 1 (Fig. 2-17).

It has to be noted, that the monitoring at the fully filtered well yields concentrations that are much smaller than the locally attained equilibrium concentrations, which can only be resolved by the partially screened well. In the real world of field site evaluation, data obtained from the 'fully screened well scenario' (which is still standard at many sites) can thus erroneously be taken as evidence for non-equilibrium NAPL dissolution.

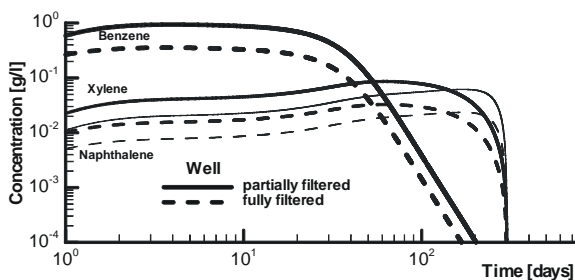


Figure 2-17. Simulated peak concentrations for Benzene (bold lines), Xylene (medium lines) and Naphthalene (thin lines) at well nest Well 1 (one well is only partially screened in the vertical extent of the source zone, the other is fully screened). Settings: $\beta = 0.5$ and $Sh = 5$.

2.5.2 Re-Partitioning Tests

The capability of BIONAPL/3D to transfer dissolved compounds from a relatively high aqueous concentration (here emitted by a upgradient constant boundary source of Benzene) back into the complex NAPL phase (at downgradient regions where the local aqueous equilibrium concentration of Benzene is lower) is demonstrated in Figure 2-18 to Figure 2-20. Figure 2-18 shows the aqueous Benzene concentrations in a cross section of the whole model domain with a constant plume emitting from the benzene boundary source zone at 1.5 g/l and hitting the upper half of the DNAPL source zone further downgradient.

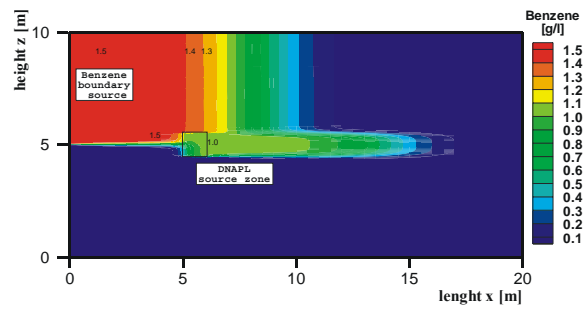


Figure 2-18. Cross section of the model domain indicating aqueous Benzene concentrations, the location of the benzene boundary source and its plume as well as the location of the DNAPL source zone and its plume.

The abrupt change in colour (red to green, at the upstream edge of the source zone) indicates, that the high aqueous concentration (1.5 g/l) of the upgradient plume on its passage through the DNAPL is immediately decreased to the lower values of the local equilibrium aqueous concentrations of the source zone (1.0 g/l).

A focus on the processes that are going on in the residual DNAPL phase of the source zone is given in Figure 2-19, a cross section of the enlarged source zone area. The upper half of the source zone is under the influence of the boundary source zone Benzene plume and is therefore enriched with respect to the mole fraction of Benzene. The lower half of the source zone is flushed with clean water and thus shows the standard dissolution behaviour, i.e. Benzene dissolves first (with respect to Xylene and Naphthalene) and is hence diminished in its mole fraction.

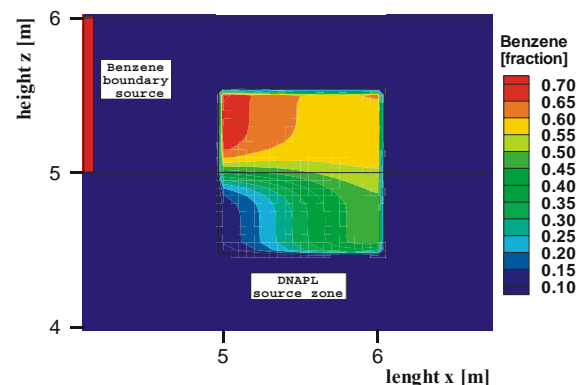


Figure 2-19. Cross section of the enlarged source zone area indicating the mole fraction of Benzene in the residual DNAPL source zone, the schematic location of the benzene boundary source as well as the location of the initial DNAPL source zone

A profile through the upper half of the plume dominated DNAPL source zone shows the respective mole fractions of all three compounds (Fig. 2-20), it displays that Benzene is strongly enriched at the upstream edge of the DNAPL source zone which is dominated by the upgradient boundary source zone.

Over time Benzene enrichment will protrude (from the left to the right) through the whole extent of the DNAPL source zone (Fig. 2-20).

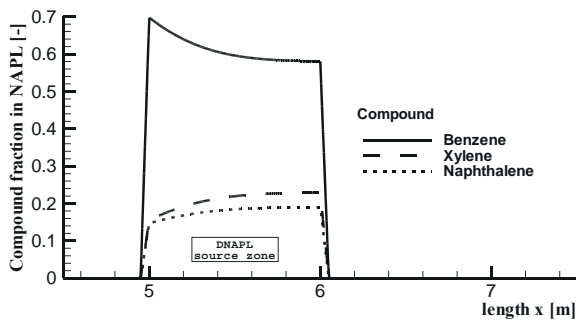


Figure 2-20. Profile through the upper half of the plume dominated DNAPL source zone area indicating the mole fractions of Benzene, Xylene and Naphthalene in the residual DNAPL phase.

Under the assumption of an upgradient plume of constant concentration the Benzene dissolution processes in the DNAPL source zone will not start until all other components are so depleted (or Benzene is so enriched), that the local equilibrium concentration exceeds the 1.5 g/l that are delivered from upstream.

2.5.3 Model Calibration

The calibration targets were BTEX and PAH concentrations, that were measured in the large scale tank experiment within the first 177 days of steady state flow source zone dissolution at point sampler ME 2-7, 0.1 m downgradient the source zone. Due to scattering in the BTEX and absence of tailing in most PAH experimental data Indene and Naphthalene were selected as governing calibration substances. Sh was independently set to 3.2 (result of the empiric correlations). The only mass transfer fitting parameter left for this calibration was β^n , best fit was obtained with a value 0.2 and is displayed in Figure 2-21 and Figure 2-22. While the fit for

Indene is quite good it was impossible to fit the other components with the identical settings. It is believed that the unexpected shape of the Benzene and Toluene experimental BTCs (especially the scattering at late times) is due to analytical problems or cross contamination rather than kinetic dissolution processes because these would even increase over time but they are obviously not present for Indene (the last declining BTC).

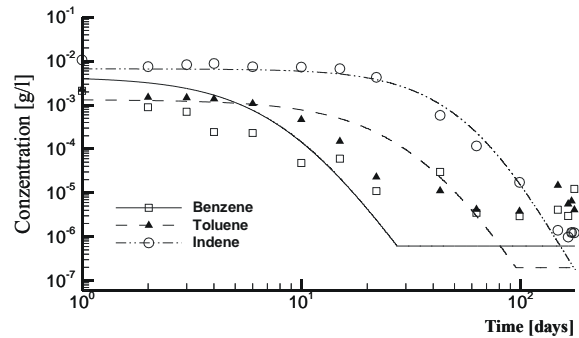


Figure 2-21. Breakthrough curves of Benzene, Toluene and Indene at point sampler ME 2-7. Points indicate measured data and lines are the fitted model results: $Sh = 3.2$ and $\beta^n = 0.2$.

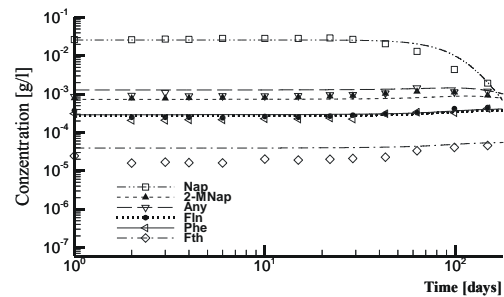


Figure 2-22. Breakthrough curves of Naphthalene (Nap), 2-Methyl-Naphthalene (2-M Nap), Acenaphthylene (Any), Fluorene (Flu), Phenanthrene (Phe) and Fluoranthene (Fth) at point sampler ME 2-7. Points indicate measured data and lines are the fitted model results: $Sh = 3.2$ and $\beta^n = 0.2$.

As it was stated above only the Naphthalene BTC yields a short tailing; but this and also the equilibrium aqueous plateau concentrations for the other PAHs were quite well fitted by the same β parameter (0.2) that was also applied for the BTEX compounds.

2.5.4 Simulation of Source Depletion

After the successful calibration procedure the model was ready to be used in forward modelling runs. The data sets of the of BTEX and PAH concentrations that were measured within the large scale tank experiment over the first 368 days of transient flow source zone dissolution at point sampler ME 1-7 (0.1 m within the source zone) and ME 2-7 (0.1 m downgradient the source zone) were used for this model validation run. Figure 2-23 and Figure 2-24 show the data of ME 2-7. Due to the strong scattering of the BTEX data (Benzene, Toluene) the gain in information, compared to the calibration done before is just small, but a positive evaluation was obtained for the Indene data which decrease another order of magnitude according to the modelled line before the data scattering also starts. The majority of the measured PAH data do not change much in the additional time period, therefore the focus is again on Naphthalene. The measured Naphthalene data first tend to decline faster than the model predictions but finally the concentrations rise again and fit to the predicted model. This may be a indication for dissolution fingering processes that were amplified under the influence of the transient velocity field in the tank experiment.

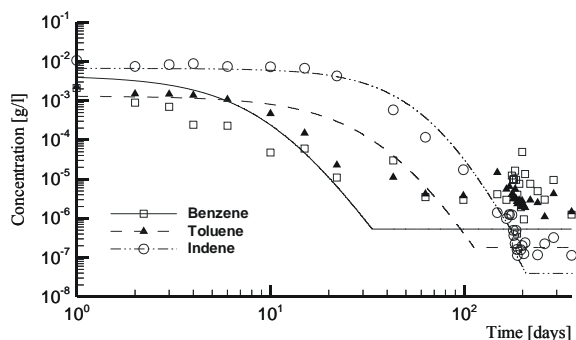


Figure 2-23. Breakthrough curves of Benzene, Toluene and Indene at point sampler ME 2-7, transient flow. Points indicate measured data and lines are the forward prediction model results: $Sh = 3.2$ and $\beta^n = 0.2$.

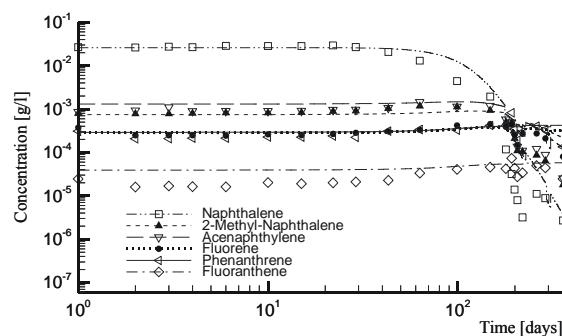


Figure 2-24. Breakthrough curves of Naphthalene, 2-Methyl-Naphthalene, Acenaphthylene, Fluorene, Phenanthrene and Fluoranthene at point sampler ME 2-7, transient flow. Points indicate measured data and lines are the forward prediction model results: $Sh = 3.2$ and $\beta^n = 0.2$.

Figure 2-25 and Figure 2-26 show the BTCs of ME 1-7. This data set is relatively independent from the calibration data set used before (as it is located further upstream, thus being faster dominated by the mass transfer length and a protruding dissolution front) and is therefore an important database for the quality assessment of single point BTC calibrations.

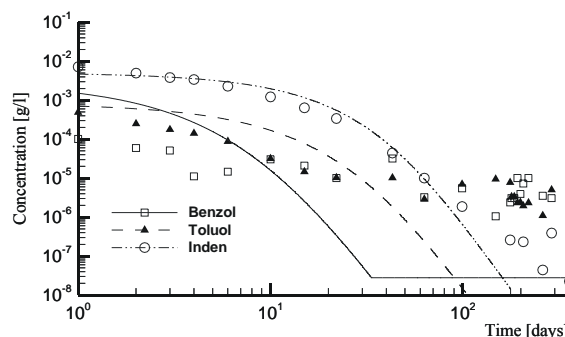


Figure 2-25. Breakthrough curves of Benzene, Toluene and Indene at point sampler ME 1-7, transient flow. Points indicate measured data and lines are the forward prediction model results: $Sh = 3.2$ and $\beta^n = 0.2$.

Once again the scattering in the BTEX data (Benzene and Xylene) prevents any clear statements. But the measured Indene-BTC displays an adequate agreement with the predicted line. Only the late part of the tailing ($< 10^{-6}$ g/l) is underestimated by the model.

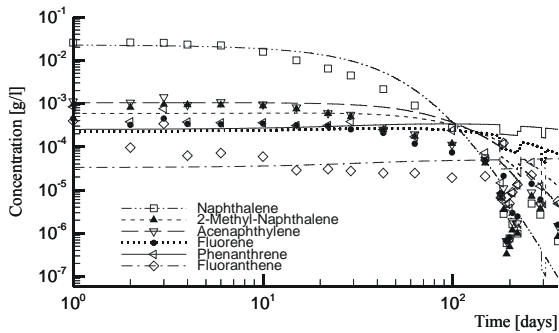


Figure 2-26. Breakthrough curves of Naphthalene, 2-Methyl-Naphthalene, Acenaphthylene, Fluorene, Phenanthrene and Fluoranthene at point sampler ME 1-7, transient flow. Points indicate measured data and lines are the forward prediction model results: $Sh = 3.2$ and $\beta^n = 0.2$.

The modelled plateau concentrations of the PAHs are in good agreement with the measured data, but the concentration decrease in the tailing is underestimated by the model. This indicates that either the length of the mass transfer zone in the model was overestimated with respect to the experiment (where dissolution is obviously faster i.e. it is for longer times at equilibrium conditions), and in the tailing we again have to deal with some sampling artefacts or that real kinetic dissolution effects govern the long-term behaviour of these BTCs.

Figure 2-27, a concentration profile through the center of the source zone at 30 days gives further insight in these complex interactions and moving boundaries between non-equilibrium and equilibrium dissolution processes.

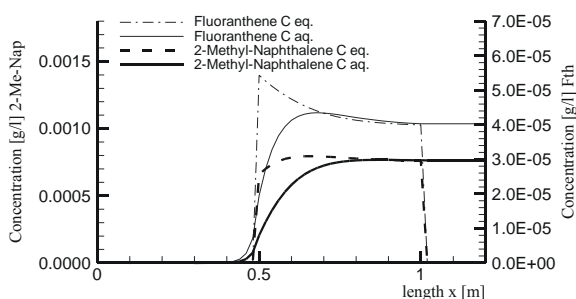


Figure 2-27. Fluoranthene (right y-axis) and 2-Methyl-Naphthalene (left y-axis) concentration profiles across the center of the DNAPL source zone; at 30 days. Dashed lines represent the theoretical equilibrium aqueous concentration according to the local component fraction in the DNAPL while the solid lines represent the actually obtained aqueous concentration.

The concentration profile of 2-Methyl-Naphthalene is representative for all well soluble compounds that get depleted at the upstream edge of the source zone from the very beginning of the dissolution process. Their actually aqueous concentrations approach the equilibrium aqueous concentrations within a certain mass transfer zone. When this concentration is once achieved it is kept at its constant level for the rest of the passage through the source zone (the equilibrium is established with respect to the then constant downgradient molar fraction). When the length of the DNAPL source zone shrinks to values under the length of the mass transfer zone, then these compounds will leave the source zone with lower aqueous concentrations according to their local equilibrium concentration at the downstream source zone edge.

The concentration profile of Fluoranthene is representative for all medium to low solubility compounds that get enriched at the upstream edge during the beginning of the dissolution process. Their actually aqueous concentrations first approach higher local concentrations (due to their local enrichment at the upstream end) than the aqueous equilibrium concentration at which they are finally leaving the source zone at the downstream end. This means that the higher aqueous concentrations are transported from the upgradient source zone nodes to the downgradient source zone nodes, where the local aqueous equilibrium concentration is lower. At these nodes the mass transfer process is reversed (due to the inverse concentration gradient) and the compound is transferred back into the NAPL phase, consequently we have to deal with small scale repartitioning processes in the residual NAPL phase throughout the whole dissolution process. When the length of the mass transfer zone becomes larger than the length of the DNAPL source zone, these compounds will leave the source zone with higher aqueous concentrations according to their local equilibrium concentration at the downstream source zone edge.

The results of the total dissolution time calculations (Zamfirescu, 2000) for different coal tar compositions (B16 and B55) under very simplified field scenario conditions are shown in Figure 2-28 and Figure 2-29 (modified after Zamfirescu, 2000).

It has to be noted, that the simulated duration for complete source zone dissolution (Zamfirescu, 2000) given below (Fig. 2-28, Fig. 2-29) is only valid for the best case conditions, i.e. dissolution takes always place under maximum concentration gradients without any mass transfer limitations. Especially the assumption of permanent, contaminant free water supply from upgradient entering the residual phase source zone is definitely not realistic compared to the actual situation at the 'Testfeld-Süd' field site.

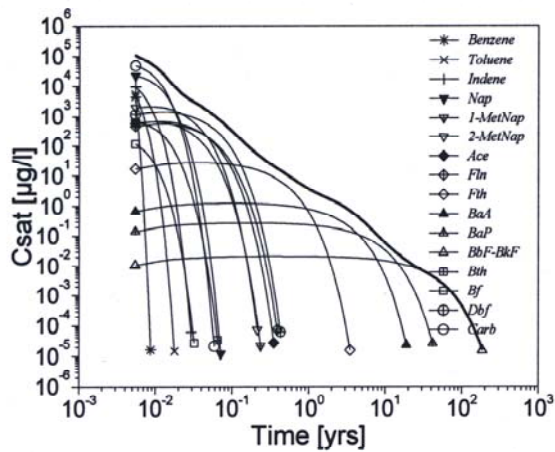


Figure 2-28. Evolution of the saturation concentrations during complete NAPL dissolution of coal tar B16 (modified after Zamfirescu, 2000).

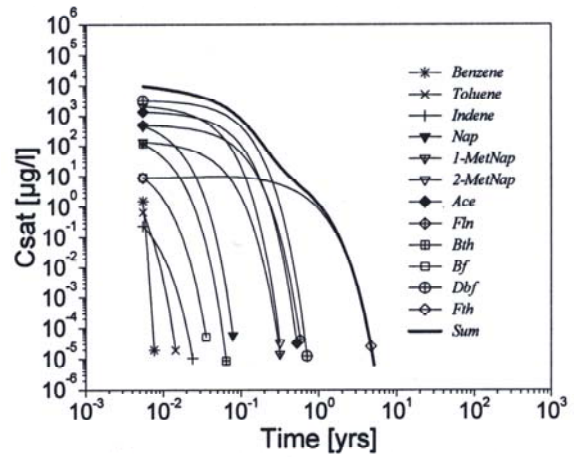


Figure 2-29. Evolution of the saturation concentrations during complete NAPL dissolution of coal tar B55 (modified after Zamfirescu, 2000).

Therefore these kind of calculations can only offer relative comparisons of the individual coal tar dissolution behaviour and they should definitely not be taken as fixed results for future considerations at the 'Testfeld Süd'.

3 Partitioning and Interfacial Tracer Tests

This chapter describes controlled experiments of Partitioning and Interfacial Tracer Tests (PITTs) at laboratory scale, which allow the integral determination of the NAPL (here a multi-component coal tar DNAPL) saturation and its distribution geometry throughout the water saturated subsurface area that is flushed during the experiment.

3.1 Introduction

Contaminant release from residual, non-aqueous phase liquids (NAPLs) into groundwater, depends on the composition of the NAPL (affecting the equilibrium aqueous concentration of the individual compounds according to the Raoult's law), the NAPL volume and the interfacial area between NAPL and groundwater (affecting the length of the mass transfer zone). The determination of these essential source zone parameters with common sampling methods such as core sampling and well logging provides only point scale data at discrete locations, thereby suffering from the principal problem to yield values that are only averages over very small aquifer volumes. Spatially more extensive site characterization methods, such as geophysical techniques, are often difficult or even impossible to be used as means of determining the amount of NAPL present without knowing the initial geophysical properties of the site before it was contaminated.

Partitioning tracer tests (PTTs) as employed in these experiments were initially developed in oil reservoir engineering using both single well tests (Tomich et al., 1973; Sheely, 1978) and interwell tests (Tang, 1992). Here, a typical single well test is carried out by injecting a

certain tracer slug of a dissolved primary partitioning tracer (ethyl acetate) into a formation that is at residual oil saturation. The initial tracer slug is then followed by a slug of tracer free water. Afterwards the well is shut in. During the residence period in the formation (at elevated oil reservoir temperatures and negligible drift due to typically very small background flow velocities) a portion of the primary tracer (ethyl acetate) hydrolyzes to form the secondary non-partitioning tracer (ethyl alcohol). Finally, the well is pumped and the concentrations of both tracers are measured during the extraction phase. Residual crude oil saturation is determined by the delayed arrival of the partitioning tracer (ethyl acetate) breakthrough curve relative to the non-partitioning tracer (ethanol) breakthrough curve and their correlation to the independently obtained distribution coefficients. At potentially NAPL contaminated, typical shallow aquifers the above described single-well setup cannot be realized due to insufficient hydrolyzation rates which are a result of the lower formation temperatures, and due to an excessive drift of the injected tracer body which is a result of the typically higher background flow velocities of ground water. Additionally it should be mentioned that this method may suffer from the limitations (non-uniqueness of interpreted parameters) of single-well push-pull tests (Hall, 1993; Hall, 1996; Haggerty et al., 1998; Schroth et al., 2001; Novakowsky et al., 1998; Kunstmann et al., 1997). The interwell PTTs conducted by Tang (1992) overcome these limitations by injecting tritiated water as non-partitioning tracer and tritiated n-butanol as well as ^{14}C labeled i-amyl alcohol as partitioning tracers in one well and extracting it at the other. The determination of residual crude oil

saturation was again based on distribution coefficients and the relative separation of the two breakthrough curves. However, according to Chen and Knox (1997) the applicable residual crude oil saturation for both kind of oil reservoir engineering tests ranged from 20 to 40%.

As mentioned above the injection of two solutes with different partitioning properties made the method much more robust but it also terminated the potential application as single well tests (at least for the classical arrival-time based evaluation concept). Two tracers with different distribution coefficients will start to separate as soon as they leave the well bore and are transported through a residual oil bearing aquifer. But if the flow direction is subsequently reversed by pumping from the same well, the separation may disappear again as the tracers return to the well bore, i.e. the arrival times of the partitioning and of the non-partitioning tracer at the well may be identical. Therefore a reasonable way to conduct PTTs employing a single well bore (in combination with the classical arrival-time based evaluation) is using a vertical circulation well set-up, for example as presented by Chen and Knox (1997) and Brooks et al. (2002). In their most recent single well push-pull PTT study Istok et al. (2002) used a new approach given by Schroth et al. (2001) to estimate the residual saturation based on an increase in apparent dispersion observed in extraction-phase breakthrough curves. The presence of NAPL is indicated by an increase in apparent dispersion of the partitioning tracer relative to the non-partitioning tracer. However, they had to admit that additional research is needed to verify the ability of this method to quantify NAPL saturations.

The concept of interwell PTTs to detect residual crude oil saturation has been modified and applied for the detection and quantification of residual NAPL phase at contaminated field sites by several researchers (Jin et al., 1995; Wilson and Mackay, 1995; Nelson and Brusseau, 1996; Jin et al., 1997; Annable et al., 1998b; Gierke et al., 1999; Nelson et al., 1999; Young et al.,

1999; Brooks et al., 2002). Concerning the partitioning tracer substances used the aforementioned studies can be subdivided in two groups, the majority that used long chain, often branched, alcohols (e.g. n-pentanol, n-hexanol, 1-hexanol, n-heptanol, 1-heptanol, 3-heptanol, n-octanol, 1-octanol, 2-octanol, 2,3-dimethyl-2-butanol, 3-methyl-3-pentanol, 2,2-dimethyl-3-pentanol, 2,4-dimethyl-3-pentanol, 2-ethyl-1-hexanol, 3,5,5-trimethyl-1-hexanol, 6-methyl-2-heptanol) and the minority that used dissolved gases (e.g. sulfur hexafluoride). Concerning the residual NAPL the studies so far investigated PCE, TCE, jet fuel and PCE in mixture with other chlorinated solvents at residual saturations between 0.06% and 20%. All of them applied the method of moments for the determination of the retardation factor and an analytical solution (Jin et al., 1995), derived from the advection-dispersion equation describing the solute transport in the two phase system water/residual NAPL in porous media, for the subsequent computation of the residual NAPL saturation. These calculations require no numerical simulations and they are independent of the assumptions required by a fluid flow model. Whereas the early studies mainly focused on the establishment and validation of the PTT method the following publications aimed to prove the applicability in the field (Nelson and Brusseau, 1996; Annable et al., 1998; Young et al., 1999; Brooks et al., 2002). Meanwhile PTTs are quite frequently used for the assessment of various in situ clean-up methods (e.g. surfactant and alcohol flushing) applied at field scale (Cain et al. 2000, Young et al., 1999; Brooks et al., 2002, Meinardus et al., 2002; Rao et al., 2000; Rao et al., 1997; Sillan et al., 1998; Jawitz et al., 2000). The theoretical studies of James et al. (1997), James et al. (2000) and Zhang and Graham (2001) focused on the performance optimization of PTTs under non-ideal conditions (e.g. non-uniform flow fields and hydrogeochemically heterogeneous aquifers). Wilson et al. (2000) present a mathematical model for the simulation of PTTs. In contrast to the quite often applied UTCHEM-code (Brown et al., 1994; Delshad et

al., 1996) modeling (Jin et al., 1995; Jin et al., 1997; Young et al. 1999), which assumes local equilibrium conditions and thereby omits the governing mass transfer limitations. The process based model of Wilson et al. (2000) includes the kinetically limited mass transport of the partitioning tracer from and to the NAPL, and is therefore potentially capable to fit the highly asymmetrical breakthrough curves that were obtained in many PTT studies.

The determination of NAPL-water interfacial areas via interfacial tracer tests (ITTs) is a quite recent development (Saripalli et al., 1997; Saripalli et al., 1998; Annable et al., 1998a; Kim et al., 1999). Experiments with subsequent runs of both, PTTs and ITTs were conducted by Annable et al. (1998a) and Dai et al. (2001).

First laboratory experiments with PITTs (combining both: partitioning and interfacial tracers in one run) and a complex multi component NAPL (tar oil) were conducted by Setarge et al. (1999). But these authors faced various problems concerning (1.) the surfactant analysis which was done by an indirect method (TOC and foam height measurements), (2.) the determination of the interfacial adsorption coefficient and the subsequent calculation of the DNAPL-water interfacial area and (3.) the quite contradictory results of the individual partitioning tracers.

Due to the convincing concept, the PTT and ITT methodology originating in the saturated zone branched rapidly and is meanwhile also available for different applications in the vadose zone. Deeds et al. (1999, 2000) used perfluorocarbon gas tracers for the determination of NAPL saturation in an air/water/NAPL system situated in the unsaturated zone. Mariner et al. (1999) investigated a comparable system (air/water/NAPL), but used an additional tracer (difluoromethane) that was suitable for the determination of water saturation. Nelson et al. (1999) conducted gas-phase partitioning tracer experiments for the measurement of soil water content in a well controlled lysimeter study

(air/water). The air/water system at various degrees of saturation was also investigated employing a PTT by Vulava et al. (2002). The effective air-water interfacial area in partially saturated media was the target parameter in the studies of Kim et al. (1997) and Anwar et al. (2000). Both authors used a surfactant as interfacial tracer. While Kim et al. (1997) conducted classical column studies and recorded tracer breakthrough curves, Anwar et al. (2000) had to sacrifice and extract their columns (after the injection of the tracer) to obtain their results.

The same concept but a different tracer philosophy is the background of the PTT experiments performed by Hunkeler et al. (1997) and Semprini et al. (2000). While all aforementioned studies employed artificial tracers these authors used a naturally occurring radioactive isotope, ^{222}Rn , that is found in groundwater as a dissolved gas, as partitioning tracer to detect and quantify residual NAPLs in contaminated aquifers. Due to its non-polarity ^{222}Rn has a high affinity to partition into NAPLs. The field applications rely on observable decreases in ^{222}Rn concentrations in areas with residual NAPL present, compared to its background concentrations in the surrounding uncontaminated areas. Recently, Davis et al. (2002) presented a single well, push-pull tracer test methodology using ^{222}Rn to quantify TCE residual saturations. The computation of the NAPL saturation was based on an increased apparent dispersion of ^{222}Rn relative to the conservative tracer (Bromide) that was recorded during the extraction phase when residual NAPL was present.

A comprehensive overview of conservative and reactive tracer techniques including the aforementioned PITT and ITT as well as other recent developments in tracer testing (e.g. DNA tracers) is given by Ptak et al. (2004).

3.2 Theory

3.2.1 Retardation Factors

The PITT consists of an injection of a suite of partitioning, interfacial and conservative tracers into a well (column inlet) and the recovery of the tracer solution at an extraction well (column outlet). While the conservative tracers will stay unaffected by the presence of NAPL, the reactive compounds (partitioning and interfacial tracers) undergo retardation due to their absorption and adsorption behaviour (see Figure 3-1)

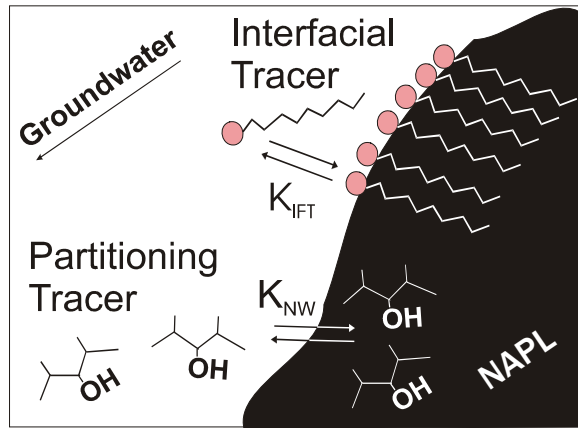


Figure 3-1. Interactions of partitioning and interfacial tracers at the NAPL-water interface during the transport in a NAPL bearing aquifer (modified from Setarge et al. 1999).

The result is a chromatographic separation of the tracers which can be recorded at the extraction well. The higher the affinity to the NAPL phase the better is the separation of the individual breakthrough curves (BTCs). This effect is quantified by the retardation factor R [-] which is defined as:

$$R_{\text{reactive}} = \frac{\mu_{\text{reactive}}}{\mu_{\text{conservative}}} \quad (3-1)$$

where μ is the first normalized temporal moment of the respective tracers at a monitoring location. For a pulse-type experiment this is given by equation 3-2 (according to Valocchi, 1985; Jin et al., 1995):

$$\mu = \frac{\int_0^{\infty} t \frac{C(t)}{C_0} dt}{\int_0^{\infty} \frac{C(t)}{C_0} dt} - \frac{t_p}{2} \quad (3-2)$$

where $C(t)$ is the monitored tracer concentration (either reactive or conservative) that is normalized by its input concentration (C_0), t is the experimental time and $t_p/2$ is the time correction-term for the duration of the tracer-pulse injection (t_p). The actually measured point data BTCs are analysed according to the trapezoidal rule of numerical integration which inserted in equation 3-2 gives:

$$\mu = \frac{\sum_{n=1}^{n=m} \left[\left(t_n + \frac{t_{n+1} - t_n}{2} \right) \left(\frac{C_n/C_0 + C_{n+1}/C_0}{2} \right) (t_{n+1} - t_n) \right]}{\sum_{n=1}^{n=m} \left[\left(\frac{C_n/C_0 + C_{n+1}/C_0}{2} \right) (t_{n+1} - t_n) \right]} - \frac{t_p}{2} \quad (3-3)$$

3.2.2 Retardation of Partitioning Tracers

The dimensionless equilibrium partitioning coefficient K_{NW} [-] is defined as:

$$K_{NW} = \frac{C_N}{C_W} \quad (3-4)$$

where C_N [g/cm³] is the concentration of the tracer in the NAPL and C_W [g/cm³] is the concentration of the tracer in the water phase. Ideal conservative tracers have a partitioning coefficient of zero.

The general equation of partitioning tracer retardation (R_{PART}) can be written as (Nelson and Brusseau, 1996; Setarge et al. 1999):

$$R_{PART} = \frac{\mu_{PART}}{\mu_{\text{conservative}}} = 1 + \frac{K_{NW} S_n}{1 - S_n} + \frac{\rho_d K_d}{n} \quad (3-5)$$

where S_n , ρ_d , K_d , and n denote the average NAPL residual saturation (NAPL volume / pore volume) in the tracer swept volume [-], the bulk density of the aquifer material [g/cm³], the solid-

water distribution coefficient [cm^3/g] and the water filled porosity [-], respectively. If the tracers are not adsorbed by the aquifer material ($K_d = 0$) the last term equals zero and thus the retardation factor depends solely on S_n and K_{NW} , giving:

$$R_{PART} = 1 + \frac{K_{NW} S_n}{1 - S_n} \quad (3-6)$$

which can finally be solved for the only unknown variable (S_n) in the system (Young et al. 1999):

$$S_n = \frac{R_{PART} - 1}{R_{PART} - 1 + K_{NW}} \quad (3-7)$$

It should be noted, that S_n obtained by the method of moments and equations 3-5 to 3-7 represents the average over the tracer flushed pore volume and is not equal to the local residual NAPL saturation.

Since the retardation factor is a function of both the partitioning coefficient of the tracer and the average NAPL residual saturation of the contaminated aquifer, S_n can only be determined by measuring R_{PART} for tracers with a known partitioning coefficient, K_{NW} .

If the average residual NAPL saturation is unknown, which is most likely for all field tests, a whole suite of partitioning tracers with varying partitioning coefficients should be used to ensure, that at least one BTC will have sufficient separation ($R_{PART} > 1.2$; as recommended by Jin et al., 1995) from the conservative tracer BTC, to calculate S_n . Additional BTCs with sufficient separation increase the confidence level of the obtained PITT results.

For PTT column experiments, a first estimate of the anticipated relative partitioning tracer BTC, which means its normalized concentration (C/C_0) over the dimensionless time (t_d) in pore-volumes (PV), can be made by the equilibrium based analytical solution of the one dimensional advection-dispersion equation, given by Dwarakanath et al. (1999):

$$\frac{C}{C_0}(t_d) = \frac{1}{2} \left[\left(\operatorname{erfc} \frac{1 - \frac{t_d}{F_i}}{2\sqrt{\frac{S_w t_d}{Pe F_i}}} \right) + \exp\left(\frac{Pe}{S_w}\right) \left(\operatorname{erfc} \frac{1 + \frac{t_d}{F_i}}{2\sqrt{\frac{S_w t_d}{Pe F_i}}} \right) \right] - \frac{1}{2} \left[\left(\operatorname{erfc} \frac{1 - \frac{(t_d - t_p)}{F_i}}{2\sqrt{\frac{S_w (t_d - t_p)}{Pe F_i}}} \right) + \exp\left(\frac{Pe}{S_w}\right) \left(\operatorname{erfc} \frac{1 + \frac{(t_d - t_p)}{F_i}}{2\sqrt{\frac{S_w (t_d - t_p)}{Pe F_i}}} \right) \right] \quad (3-8)$$

where $S_w = 1 - S_n$ [-] and $F_i = S_w + K_{NW} S_n$ [-]. The dimensionless Peclet number is given as $Pe = v_a d / D_{aq}$ [-] and t_p is the tracer-pulse injection time in dimensionless PVs [-], respectively. Care has to be taken as the computed BTCs are related to the uncontaminated pore volume ($S_w = 1$), which means that in cases where NAPL is present ($S_w < 1$) the breakthrough of an conservative tracer is faster than one PV. To overcome this somehow confusing arrangement, one can replace the ‘PV based time scale’ by the ‘n based time scale’ which is nothing than the ‘PV based time scale’ (initially required for calculation) multiplied by $1/1 - S_n$.

3.2.3 Retardation of Interfacial Tracers

Surface active agents (surfactants) such as Sodium Laurylesulfate (SLES) can be used as interfacial tracers. Their adsorption at an interface can be described by the Gibbs adsorption isotherm (Adamson 1982):

$$\Gamma = -\frac{1}{2RT} \left(\frac{d\gamma}{dC} \right) C \quad (3-9)$$

where Γ , γ , C , R , and T denote the interfacial adsorption [mmol/cm^2], the surface tension [dynes/cm], the concentration of surfactant [mmol/cm^3], the universal gas constant [$\text{dyne cm}/\text{mmol K}$] and the absolute temperature [K].

The equilibrium interfacial adsorption coefficient, K_{IFT} [cm], can be determined by following equation (Saripalli et al. 1998):

$$K_{IFT} = -\frac{1}{2RT} \left(\frac{d\gamma}{dC} \right) \Big|_{C_{IFT}} \quad (3-10)$$

therefore K_{IFT} can be calculated for a given surfactant concentration (C_{IFT}) and varies with the slope of the γ versus C plot which can be obtained by the drop weight method (e.g. Adamson, 1982). When pulse input tracer tests are applied, a constant K_{IFT} value can be estimated in a first approximation by using the maximum interfacial tracer concentration of each BTC (Annable et al. 1998).

The general equation of interfacial tracer retardation (R_{IFT}) can be written as (Saripalli et al. 1998):

$$R_{IFT} = \frac{\mu_{IFT}}{\mu_{conservative}} = 1 + \frac{A_{NW} K_{IFT}}{n} + \frac{\rho_d K_d}{n} \quad (3-11)$$

where A_{NW} , ρ_d , K_d , and n denote the DNAPL-water interfacial area [cm^2/cm^3], the bulk density of the aquifer material [g/cm^3], the solid-water distribution coefficient [cm^3/g] and the water filled porosity [-], respectively. If the interfacial tracer adsorption by the aquifer material is negligibly small ($K_d \approx 0$), the last term equals zero and thus the retardation factor depends only on A_{NW} and K_{IFT} , giving:

$$R_{IFT} = 1 + \frac{A_{NW} K_{IFT}}{n} \quad (3-12)$$

which can finally be solved for the only unknown variable (A_{NW}) in the system (Saripalli et al., 1998):

$$A_{NW} = \frac{(R_{IFT} - 1) n}{K_{IFT}} \quad (3-13)$$

By measuring the retardation factor of the interfacial tracer, the DNAPL-water interfacial area can be estimated if the adsorption isotherm for the interfacial accumulation is known.

3.3 Materials and Methods

3.3.1 Tracer Chemicals

The major chemical and physical properties of the six selected tracer substances: two conservative tracers (sodium chloride, isopropanol), three partitioning tracers (1-hexanol, 4-methyl-2-pentanol, 2,4-dimethyl-3-pentanol) and one interfacial tracer (sodium laurylesulfate) are listed in Table 3-1. The alcohols were purchased as liquids with a purity of >97% (MERCK, Germany). They are characterized by a high water solubility, a density lower than water and low Henry's law constants (H). As their Octanol/water partitioning coefficient (K_{OW}) indicates, these substances will partition into NAPL; the K_{NW} values that were determined for the respective tracers and a tar oil (RÜTGERS, Germany) within this study are already given for comparison.

The anionic surfactant sodium laurylesulfate was directly obtained from the manufacturer (HÜLS, Germany) as a paste with a purity of 70% (aqueous solution). It is highly soluble in water and has a quite high critical micelle concentration (CMC) of 950 mg/L (Setarge et al. 1999). The latter property is especially important for its application as an interfacial tracer, which requires an injection concentration below this limit - otherwise the surfactant may solubilise or even mobilise the NAPL instead of only adsorbing on its interface.

3.3.2 Tar oil DNAPL

The identical industrial tar oil (RÜTGERS, Germany) with a density of $1.2 \text{ g}/\text{cm}^3$ was employed as DNAPL in all types of laboratory experiments (batch, column, large scale tank) as well as for the modelling studies (Chapter 2). The composition of this highly viscous, complex multi-component DNAPL is given in Chapter 2 (Table 2-7).

3.3.3 Aquifer Material

A quartz dominated, well-graded sand (1-2 mm diameter, uniformity coefficient of 1.54) from the River Rhine quaternary alluvium (KIESWERK EUGEN KÜHL UND SÖHNE, Iffezheim, Germany) with a low carbonate

(2.88%) and a very low organic carbon content (0.01%) was used as aquifer material in all the column and the large scale tank experiments. The only exception was column experiment #9d, where a dry sieved aquifer material fraction (0.5-4 mm diameter) from the Testfeld-Süd (borehole B63, 5-6 m depth bgl) was used.

Table 3-1: Physico-chemical properties of (1) conservative tracers: Sodium Chloride (NaCl), Isopropanol (IPA); (2) partitioning tracers: 1-Hexanol (1-HEX), 4-Methyl-2-Pentanol (4M2P) and 2,4-Dimethyl-3-Pentanol (24DM3P); and (3) the interfacial tracer: Sodium Lauryl ethersulfate (SLES), respectively.

Tracer	CAS No.	Formula	MW ^a [g mol ⁻¹]	ρ ^b [g cm ⁻³]	C _w ^c [g L ⁻¹]	BP ^d [°C]	MP ^e [°C]	LogH ^f [atm m ³ mol ⁻¹]	K _{OW} ^g [-]	K _{NW} ^h [-]
NaCl	7647-14-5	NaCl	58.4 ^j	2.17 ^j	358 ^j	1461 ^j	801 ^j	-	-	-
IPA	67-63-0	C ₃ H ₈ O	60.1 ^j	0.78 ^j	++ ^{i,j}	82 ^j	-89 ^j	-5.09 ^m	0.69 ^j	0.8 ^p
4M2P	108-11-2	C ₆ H ₁₄ O	102.2 ^j	0.81 ^j	16.4 ^j	131 ^j	-60 ^j	-4.35 ^m	48 ^m	3.2 ^p
1-HEX	111-27-3	C ₆ H ₁₄ O	102.2 ^j	0.82 ^j	5.8 ^j	157 ^j	-45 ^j	-4.77 ^m	107 ^m	9.6 ^p
24DM3P	600-36-2	C ₇ H ₁₆ O	116.2 ^j	0.83 ^j	7.0 ^m	140 ^j	-70 ^j	-4.15 ^m	245 ⁿ	16 ^p
SLES	68891-38-3	C ₁₂ H ₂₅ (C ₂ H ₄ O) ₂ OSO ₃ ⁻ Na ⁺	382 ^l	1.1 ^k	++ ^{i,k}	- ^k	- ^k	CMC ^o = 950 mg/L ⁿ K _{IFT} = 9.73e-5 -9.24e-4 cm ^p		

^a Molecular weight; ^b Density (20°C); ^c Water solubility; ^d Boiling point; ^e Melting point; ^f Henry's law constant; ^g Octanol/water partitioning coefficient; ^h NAPL/water partitioning coefficient; ⁱ Miscible with water; ^j MSDS, MERCK SCHUCHARDT; ^k MSDS, HÜLS; ^l Product information, CONDEA; ^m EPI Suite Version 3.10 database, U.S. EPA (2000); ⁿ Setarge et al. (1999); ^o Critical micelle concentration, ^p this study.

3.3.4 Analytical Methods

The alcohols 4-Methyl-2-Pentanol (4M2P), 1-Hexanol (1HEX) and 2,4-Dimethyl-3-Pentanol (2,4DM3P) were used as partitioning tracers, they are easily detected by GC-FID analysis even in the presence of high contaminant concentrations in the water. The qualitative as well as quantitative analysis of the above mentioned partitioning tracers (including the conservative tracer IPA) was done by a gas chromatograph equipped with flame ionisation detection under the following conditions: freshly sealed individual samples of 10 ml were contained in 20 ml headspace vials for analysis. Within a automatic headspace-sampling unit (DANI, HSS 3950), the samples were pre-equilibrated at 75°C. When the sampling needle

penetrated the septa of the vials, 1 ml of headspace gas was transferred into a sampling loop and then over a heated transfer line (142°C) into the injector of the GC (CARLO ERBA, HRGC 5160 Mega Series). After separation by the 50m long column, substances were detected by the FID (CARLO ERBA, EL 480). Table 3-2 lists the operating parameters of the GC-FID system.

Recording of peak areas and final quantification was done using the software package Maxima 820 (WATERS). Peak identities and concentrations were established by comparison of peak retention time and area to those of standards. Measured standards covered the range of foreseeable peak areas of the alcohols in order to calibrate each measurement series of samples.

Table 3-2: GC-FID operating parameters.

GC-FID (HRGC 5160 Mega)		
Injector		
Temperature:	180°C	
Carrier:	Nitrogen	
Carrier pressure:	Constant at 1.7bar	
Split ratio:	1:6	
Column		
Type:	WCOT-fused silica CP-Sil-13CB stationary phase	
Film thickness:	1.2µm	
Inner diameter:	0.32mm	
Length:	50m	
Oven (temp. program)		
	$T_0=85^\circ\text{C}$	$t_0=4\text{min}$
$R_1=30^\circ\text{C}/\text{min}$	$T_1=125^\circ\text{C}$	$t_1=4\text{min}$
Detector (FID)		
Temperature:	210°C	

The anionic surfactant, Sodium Lauryl ether Sulfate (SLES), was used as interfacial tracer and is reliably analyzed by a newly developed, IC based method even in the presence of high background ion concentrations (especially sulfate) which are typically found in the gypsum influenced aquifers in southern Germany (e.g. Testfeld-Süd). The qualitative as well as quantitative analysis of SLES was done subsequently after the above described partitioning tracer analysis by an ion chromatograph equipped with an electrical conductivity detector under the following conditions: a 5 ml aliquot of the individual 10 ml samples that were still contained in the 20 ml headspace vials (see previous partitioning tracer analysis) was transferred to special vials (DIONEX, PolyVial, 5 ml) that are required for the auto-sampling unit (DIONEX, AS 40). The auto-sampler pumps an excess-volume of each sample through / into the 100 µl sampling loop of the IC (DIONEX, DX-120). Finally, the sampling loop volume is injected into the separation column (ALLTECH, Hypersil MOS-1, 250 mm length). The isocratic eluent (32% Acetonitrile, 68% Millipore-water, sodium acetate 1 mMol/l) was pumped through the chromatographic column at a flow rate of 1 ml/min. SLES was detected by the standard built in electrical-conductivity-detector (DIONEX, DX-120-CDM-3) without using the built-in suppressor device. Recording of peak

areas and final quantification was done using the software package Peak Net 5.1 (DIONEX). Peak identity and concentrations were established by comparison of peak retention time and area to those of standards. Measurement standards covered the range of foreseeable peak areas of SLES in order to calibrate the analysis for each measurement series of samples.

It should be noted that all previous trials designing an analysis for SLES using a chromatography column especially manufactured for surfactants (ALLTECH, Surfactant-R, 150 mm length) in combination with isocratic eluents (numerous, varying compositions of Millipore-water, Acetonitrile and Methanol) failed, due to an insufficient separation of the target analyte (SLES) from the background ions.

The salt, Sodium Chloride (NaCl), was used as conservative tracer and was measured by the sum parameter of total electrical conductivity (EC). Due to ongoing improvements during the experiments the determination of the NaCl tracer BTC was changed step by step. The following methods were used: (1.) online-monitoring by a separate electrical conductivity cell (materials used and detailed design see Fig. 3-2) made out of a standard conductivity probe (WTW, LA1/T-) that was connected to a stand-alone data-logger (PHYTEC, PRO-DATA junior). This conductivity cell set-up was directly connected to the column-outlet: either in a bypass mode, see column-set-up A (Fig. 3-3); or in in-line mode, see column-set-up B (Fig. 3-4); or to the respective extraction-well in the large scale tank experiment (in-line mode, analogue to column set-up B).

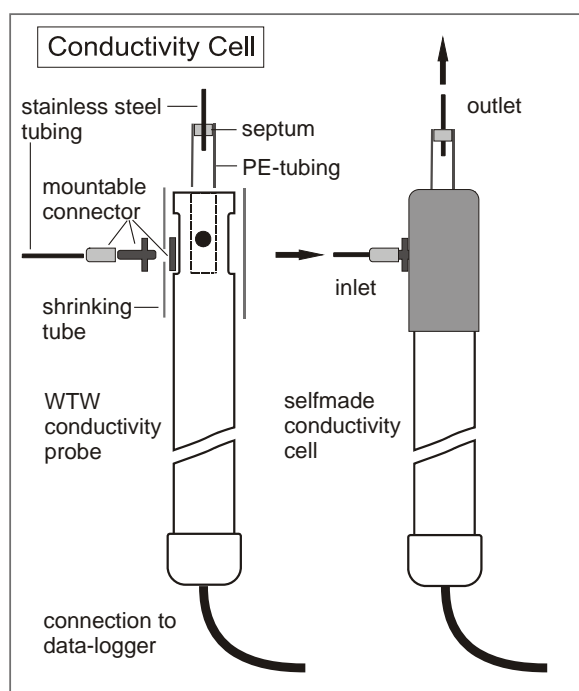


Figure 3-2. *Self-provided electrical conductivity cell: cross-section with indicated design details and materials (left) and sketch of the ready for use flow cell with indicated water flow direction (right).*

(2.) Offline measurements for total electrical conductivity out of separately taken 1.8 ml water samples (see column set-up C, Fig. 3-5) using a HPLC conductivity detector (WATERS, Model 430) and a peristaltic pump (ISMATEC, MC-MS/CA4) for the controlled throughput (flow rate was set to 1ml/min) of each sample through the miniature flow-cell. As its internal cell volume is only about 1.4 μl , stable electrical conductivity readings could be achieved using sample volumes about 1 ml. Both set-ups (1.) and (2.) were externally standardised before and after each measurement sequence using external standards. The conductivity readings were transferred into concentration data via a spreadsheet table calculation software, (MICROSOFT, Excel 2000).

(3.) Offline measurements for discrete ion species (target analytes: Na^+ and Cl^-) via ion chromatography. The qualitative as well as quantitative analysis of Na^+ and Cl^- was done subsequently after the above described partitioning and interfacial tracer analysis by an ion chromatograph equipped with a conductivity detector under the following conditions: the

remaining 5 ml aliquot of the individual samples that was still contained in the 20 ml headspace vials (see previous partitioning and interfacial tracer analysis) was transferred to special vials (DIONEX, Polyvial, 5 ml) that are required for the auto-sampling unit (DIONEX, AS 40). The samples were automatically pumped to two parallel IC units: one for anions and another for cations (both: DIONEX, DX-120). Within the IC devices, the liquid was sent through/into an injection loop (25 μl for the anions and 50 μl for the cations). The ions were separated using the respective separation columns (anions: DIONEX, IonPac CS12A, 150mm length; cations: DIONEX, IonPac AS144, 300mm length). All measurements were made in suppressed conductivity detection mode in order to maintain a stable base conductivity. Recording of peak areas and final quantification was done using the software package Peak Net 5.1 (DIONEX). Peak identity and concentrations were established by comparison of peak retention time and area to those of standards.

3.3.5 Batch Experiments

Combined partitioning isotherm and partitioning kinetic batch tests were carried out in order to determine the dimensionless K_{NW} values for the partitioning tracers and the tar oil used in this study. The complete PITT suite (including conservative, partitioning and interfacial tracers) stock solution was diluted into four different concentrations (C_0 , $C_0/2$, $C_0/4$, $C_0/8$). Headspace vials (nominal volume: 20 ml) were filled with 2 g of tar oil and 20 mL of each concentration level was added. Additional vials were filled with 20 mL of each concentration level solely, to quantify reference concentrations/controls. All samples were prepared in triplicate for each of the six sampling time steps (0.5, 1, 2, 4, 8, and 24 hours). The samples were continuously shaken at constant temperature (20°C) using an overhead shaker. At each sampling time step a 10 ml aliquot of the supernatant tracer solution of each sample of one concentration series (C_0 , $C_0/2$, $C_0/4$, $C_0/8$) was transferred to a fresh 20 ml

head space vial (the rest was discarded) and analysed by the above described GC-FID method.

The drop weight method was used in order to obtain the raw data (liquid-liquid interfacial tension between DNAPL and SLES solution as a function of SLES concentration) required for the subsequent determination of the K_{IFT} [cm] value between the interfacial tracer and the tar oil used in this study. The procedure for the determination of liquid-liquid interfacial tensions consist of a controlled number of drops of the one liquid (here DNAPL) at the end of a pipette tip which is inserted in the second liquid (here SLES solution concentration series), allowing them to gather at the bottom of the container until enough of them have been collected so that the weight per drop can be accurately determined by a precision balance. Further details of this test routine are given by Adamson (1982). The mean volume (V) of the drops can subsequently be determined by the known amount of drops and the known density of the DNAPL. The liquid-liquid interfacial tension (γ) can finally be determined as follows (adapted after Adamson, 1982):

$$\gamma = \frac{\Delta\rho V g}{2\pi r\Phi} \quad (3-14)$$

where γ , $\Delta\rho$, V , g , r and Φ denote the surface tension [N/m], the density difference (between the fluid forming the drop and the fluid that is surrounding the drop) [kg/l], the volume of the falling drop [l], the gravitational constant [m/s²], the radius of the pipette tip [m] and the correction factor [-]. The latter is required as only a portion of the drop actually falls from the tip and is available in tabulated form by Adamson (1982) and Earnshaw et al. (1996). The ITT stock solution containing 0.0027 mMol/cm³ SLES was diluted into 11 different concentrations (100%, 67%, 60%, 50%, 40%, 33%, 27%, 17%, 7%, 3% and 2%), 50 ml of each dilution were put into individual vials and placed onto a precision balance (SATORIUS, BP121S) after that the

approximate amount of 2 g DNAPL was inserted drop-wise via a disposable pipette with an inner tip radius of 0.625 mm (pipette body: SOCOREX SWISS 0.5-5 ml, pipette tip: SOCOREX SWISS Makro 5000) into each vial. The number of drops and their weight were recorded, afterwards the above described routine was used to determine the liquid-liquid interfacial tension between the DNAPL and the respective SLES dilution.

3.3.6 Column Experiments

A total of seven column experiments were run within the laboratory work of this study. It should be noted that the column number is not directly linked to the chronology of the experiments, as the enumeration had already to be fixed (for identification purposes) during the tedious filling/preparation processes of the columns. All column experiments were conducted in glass columns that were customized (FISCHER, approx. net measurements: 15 cm length, 6 cm inner diameter; giving an approx. net volume of 424 ml). Due to the uniqueness of the manual fabrication process (glass blowing) the actual net volume of each column had to be determined gravimetrically before its subsequent filling process. In a first step all columns were packed in saturated layers with aquifer material and the resulting pore volume was determined gravimetrically. Afterwards the content of each column was emptied into an individual stainless steel bowl and the excess water was removed (i.e. that water remained still the first wetting fluid) and then amended with a defined amount of tar oil (DNAPL) of known density to establish the desired residual saturation (S_n). After manual homogenisation the *whole* material was finally re-packed into its respective column (always in saturated layers) resulting in a fully saturated column at defined tar oil saturation.

Throughout the course of the laboratory work the column set-up also underwent stepwise improvement, leading to the following three

slightly different types: Column set-up A (see Fig. 3-3) started with a peristaltic pump (ISMATEC, BVP), which pumped either the tracer solution or Millipore-water through the inlet of the columns at a constant flow rate. Connections to the column and from the column to the water sampling port were made of stainless steel tubing. A Y-connector was used to split a portion of the column effluent to a self-provided conductivity cell (Fig. 3-2) which was used for online monitoring of the NaCl BTC.

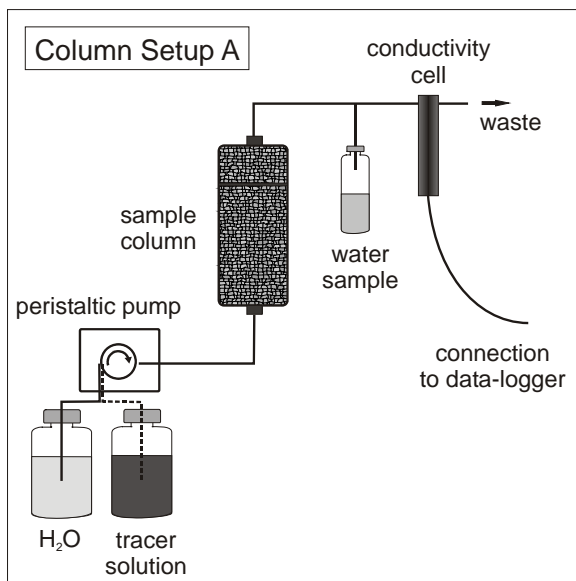


Figure 3-3. Column set-up A: a Y-connector was used to split a portion of the column effluent to (1) the manual water sampling port and (2) to the self-provided conductivity cell which was used for online monitoring of the NaCl BTC.

Due to problems with a controlled splitting of the column effluent at the Y-connector the set-up was changed resulting in column set-up B (see Fig. 3-4), where the whole effluent was directly guided through the self-provided conductivity cell before finally being sampled (almost continuously) at end of the flow path.

Still not being perfect, the above describes set-up was optimised giving column set-up C (see Fig. 3-5), where the online EC measurement was given up and a manually controlled three way valve for the comfortable *continuous* sampling (sampling cycle: take one water sample for tracer analysis (10 ml), switch the valve, take the other water sample for offline electrical conductivity measurement (1.8 ml), switch the

valve back - repeat this cycle until the experiment is finished) of the whole column effluent was installed.

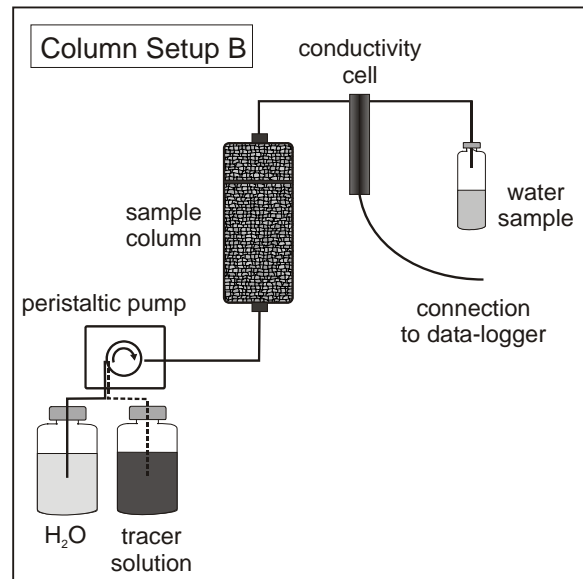


Figure 3-4. Column set-up B: the whole column effluent was directly guided through the self-provided conductivity cell, which was used for online monitoring of the NaCl BTC, before finally being sampled at the manual water sampling port.

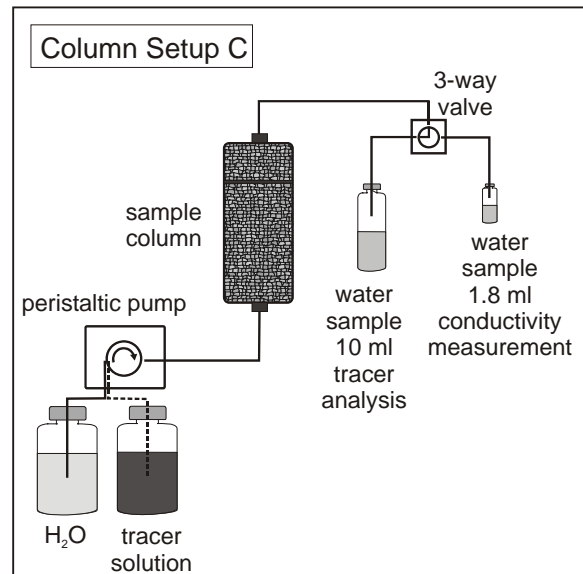


Figure 3-5. Column set-up C: the whole column effluent was guided to a manually controlled three-way valve for the manual sampling (one 10 ml water sample for tracer analysis, the other 1.8 ml water sample for offline electrical conductivity measurement of the NaCl BTC).

All columns were run in an upright position with flow from the bottom to the top and were initially flushed for several hours with Millipore-water to establish a constant flow

regime and a constant background EC (typically around 50 $\mu\text{S}/\text{cm}$). All PITTs were conducted as pulse type injection experiments, i.e. the experiment started with a Millipore-water pre-flush as described above, then the inlet of the pumping tube was manually transferred into a vial with a known volume of the tracer solution, which was pumped into the column until the desired volume was entered at which point the inlet of the pumping tube was manually transferred into a beaker with a known volume of Millipore-water for the rest of the experimental run. At the sampling port, the effluent the flow path ended at a pointed stainless steel capillary, which was able to penetrate through the sealed lids of either 20 ml headspace vials, that were filled to the necessary volume of 10 ml for tracer analysis or 1.8 ml headspace vials, that were filled to their maximum volume for offline EC measurements (for details see analytical methods). After recapping, the 20 ml headspace vials samples could then be used for the sequential analysis techniques described before.

Column #V was packed with Rheinsand containing a controlled 14% residual saturation of tar oil (DNAPL blobs). The experiment was conducted using column set-up A (see Fig. 3-3) under the following conditions: a PITT tracer pulse of 19.33 ml (which equals 12.7% of the water filled porosity, n) was injected over 5 min, subsequently the column was flushed with Millipore-water for 2:31:48 hours, both at the identical linear velocity of 5.6 m/day. During the run-time of this experiment 33 water samples were taken.

Column #IV was packed with Rheinsand containing a controlled 5% residual saturation of tar oil (DNAPL blobs). The experiment was conducted using column set-up B (see Fig. 3-4) under the following conditions: a PITT tracer pulse of 19.00 ml (12.1% of n) was injected over 5:03 min, subsequently the column was flushed with Millipore-water for 2:02:02 hours, both at the identical linear velocity of 5.0 m/day. During

the run-time of this experiment 65 water samples were taken.

The following three columns (column #8b, #8c, #9b) contained the identical coal tar residual saturation (S_n) of exactly 20%, but the linear flow-velocity of the individual experiment was set to different values (6.1 m/day, 3.6 m/day and 1.9 m/day) to evaluate the influence of non-equilibrium transport conditions on PITT results.

Column #8b was packed with Rheinsand containing a controlled 20% residual saturation of tar oil (DNAPL blobs). The experiment was conducted using column set-up C (see Fig. 3-5) under the following conditions: a PITT tracer pulse of 18.02 ml (13.8% of n) was injected over 4:50 min, subsequently the column was flushed with Millipore-water for 3:31:00 hours, both at the identical linear velocity of 6.1 m/day. During the run-time of this experiment 130 water samples were taken.

Column #8c was packed with Rheinsand containing a controlled 20% residual saturation of tar oil (DNAPL blobs). The experiment was conducted using column set-up C (see Fig. 3-5) under the following conditions: a PITT tracer pulse of 22.28 ml (16.4% of n) was injected over 10 min, subsequently the column was flushed with Millipore-water for 8:37:30 hours, both at the identical linear velocity of 3.6 m/day. During the run-time of this experiment 128 water samples were taken.

Column #9b was packed with Rheinsand containing a controlled 20% residual saturation of tar oil (DNAPL coatings, DNAPL being the first wetting fluid). The experiment was conducted using column set-up C (see Fig. 3-5) under the following conditions: a PITT tracer pulse of 18.95 ml (13.5% of n) was injected over 15:20 min, subsequently the column was flushed with Millipore-water for 21:25:00 hours, both at the identical linear velocity of 1.9 m/day. During the run-time of this experiment 102 water samples were taken.

The following three columns (column #9a, #8b, #9b) contained the identical tar oil residual saturation (S_n) of exactly 20%, but the DNAPL distribution geometry and thereby the DNAPL-water interfacial area (A_{NW}) of the individual experiment was set to three different values (DNAPL-pool/ganglia, DNAPL-blobs, DNAPL-coatings) to obtain a qualitative validation of the ITT results.

Column #9a was packed with Rheinsand and a controlled 20% residual saturation of tar oil was injected, creating one large interconnected ganglia, which will be referred as DNAPL pool/ganglia scenario. The experiment was conducted using column set-up C (see Fig. 3-5) under the following conditions: a PITT tracer pulse of 18.99 ml (14.2% of n) was injected over 15:00 min, subsequently the column was flushed with Millipore-water for 15:06:15 hours, both at the identical linear velocity of 2.1 m/day. During the run-time of this experiment 96 water samples were taken.

The last column experiment (column #9d) was a blank column, which contained no residual DNAPL ($S_n = 0\%$), but was filled with aquifer material from the Testfeld-Süd (the anticipated site for field scale application of the PITT) to evaluate any influence of the site specific aquifer material composition on PITT results.

Column #9d was a blank column packed with dry sieved aquifer material (0.5-4 mm diameter fraction) from the Testfeld-Süd (borehole B63, 5-6 m depth bgl) containing no residual DNAPL. The experiment was conducted using column set-up C (see Fig. 3-5) under the following conditions: a PITT tracer pulse of 21.33 ml (14.3% of n) was injected over 15:00 min, subsequently the column was flushed with Millipore-water for 20:18:40 hours, both at the identical linear velocity of 2.1 m/day. During

the run-time of this experiment 96 water samples were taken.

3.3.7 Large scale tank experiments

An additional number of pulse type PITTs were conducted in a large scale tank (8 m length \times 1 m width \times 3 m height) located in the research facility for subsurface remediation at the University of Stuttgart (VEGAS), Figure 3-6 shows a cross-sectional set-up of this experiment including the origin of the x-y-z reference coordinate system for the tank. All parts of the tank are made of inert stainless steel, except for the front wall, which is due to visualisation purposes made out of glass. The quartz-dominated Rheinsand already described before was used to build up the main aquifer (porosity: 0.39, hydraulic conductivity: 5.5e-03 m/s), homogeneous flow conditions within the tank aquifer are achieved by easily controlled in- and outflow mixing chambers. The properties of the two other porous materials (fine sand bottom aquitard and fine gravel high conductivity zone) as well as further details concerning the filling procedure and the properties of the tank can be found in Eberhardt and Grathwohl (2002) and in the technical report LAG 01-01/2051 (2001). Two different tar oil source zones are present within the tank: (1) a rectangular DNAPL blob zone (0.5 m length in flow direction \times 1 m width \times 1 m height) at a residual saturation of 4.86% located in the upper part of the aquifer close to the inflow chamber and (2) a DNAPL pool (2.5 m length in flow direction \times 1 m width \times 0.03 m height; $S_N = 100\%$) at the bottom of the aquifer, both of them were created with the same tar oil (RÜTGERS, Germany) that was already used in the batch and column experiments.

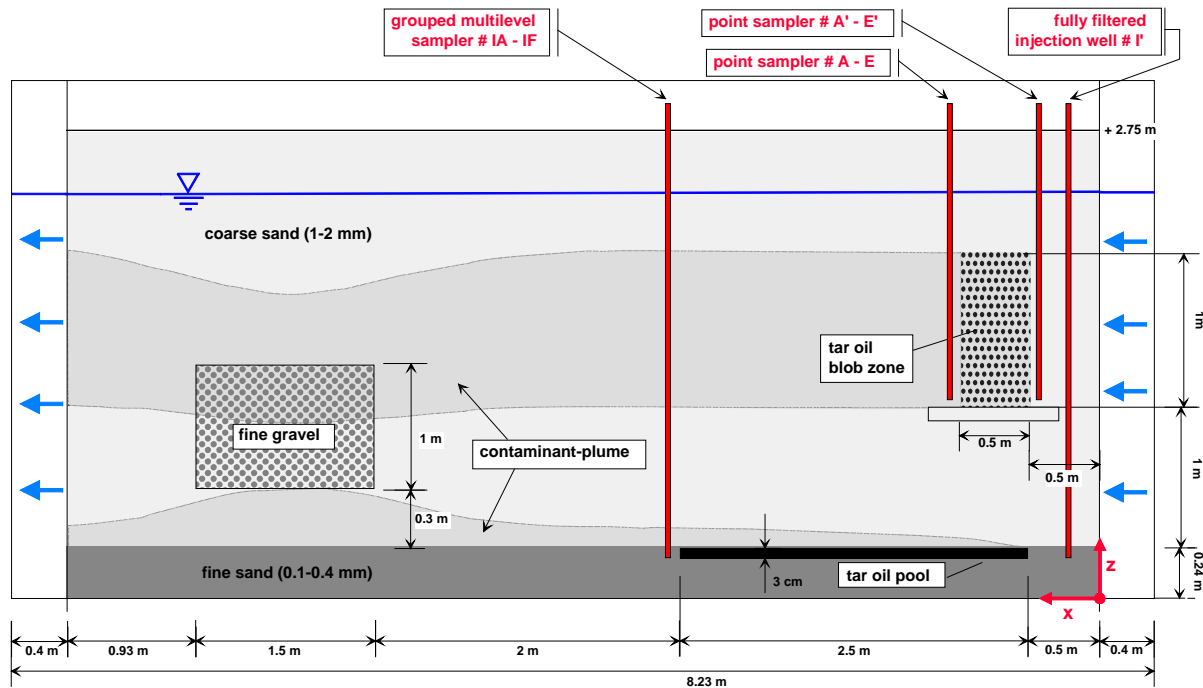


Figure 3-6. Setup of the large scale tank experiment indicating the origin of the tank coordinate system (x,z), the two different source zones (tar oil blob zone, tar oil pool) the major aquifer elements as well as the position of (1) the well pair point samplers (injection: point samplers A'-E'; extraction: point samplers A-E) used for the dipole flow field PITTs, (2) the fully filtered injection well (I') and the grouped multilevel sampler (IA-IF) that were used for the natural gradient PITTs.

PITTs for the assessment of the DNAPL blob zone (after a previous depletion period of approximately 177 days; see experiments by Eberhardt and Grathwohl, 2002) were conducted using five point sampler well-pairs (A-A' – E-E'), see Fig. 3-6 and Fig. 3-7), that were located just at the edge of the tar oil blob zone (the resulting separation distance for each point sampler well-pair in flow direction was 0.6 m). Each point sampler was made of a stainless steel pipe (6 mm OD, 2 mm ID) that was equipped with a fixed (and sealed) drive point at the tip (to enable direct push installation) and was filtered via six holes (1 mm diameter) that were arranged circle wise at equal distances around the pipe at a distance of 2.5 cm measured from the tip of the drive point. The coordinates (x,y,z) [cm] of the respective filter of each point sampler are given in the following description of each experiment. Continuous injection/extraction via peristaltic pumps created a forced gradient dipole flow field which was aligned in the direction of the tank-gradient base flow field (5 m/day). Analogue to the column experiments

all large scale tank PITTs were conducted as pulse type injection experiments, i.e. the experiment started with a Millipore-water pre-flush (to establish the aforementioned dipole flow field), then the inlet of the pumping tube was manually transferred into a vial with a known volume of the tracer solution, which was pumped into the upgradient injection point sampler of the well pair. After the desired tracer volume was injected, the inlet of the pumping tube was manually transferred back into the beaker with Millipore-water for the rest of the experimental run. At the downgradient extraction point sampler of the well pair the whole effluent, that was extracted by a peristaltic pump, was directly guided through a self-provided conductivity cell (see Fig. 3-2) before finally being sampled at a sharpened capillary at the end of the flow path (analogue to column set-up B, see Fig. 3-4). After recapping, the 20 ml headspace vials samples could then be used for the sequential analysis techniques as described before.

The following six individual, forced gradient dipole flow field PITTs at five spatially different located well pair point samplers (A'-A – E'-E) were anticipated for the assessment of the homogeneous DNAPL blob zone ($S_n \leq 4.86\%$). Within this sequence of experiments the extraction/ injection ratio of the individual well pairs was varied stepwise (mostly increased, as overpumping enlarges the catchments area) to overcome unexpected small BTC peaks which might be a result of (a) local, small scale heterogeneities of the source zone / aquifer and (b) the critical coordinate divergence with respect to the base flow streamline (in y and z direction) due to the direct push installation of the well pair point samplers.

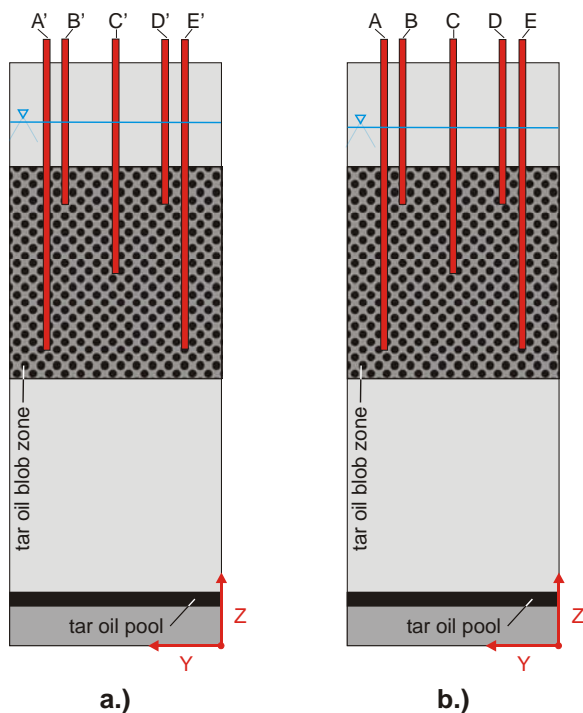


Figure 3-7. Setup of the large scale tank experiment indicating the origin of the tank coordinate system (y,z), the two different source zones (tar oil blob zone, tar oil pool) and the position of the well pair point samplers used for dipole flow field PITTs a.) upgradient injection point samplers A'-E', b.) downgradient extraction point samplers A-E.

The experiment at well pair point sampler A'-A was conducted under the following conditions: a PITT tracer pulse of 120.56 ml was injected over 20 min (flow rate: 6.03 ml/min) at point sampler A' (45,85,144), subsequently the injection was switched to Millipore-water for

8:09:40 hours at the identical flow rate. The withdrawal rate at the downgradient extraction point sampler A (105,85,144) was 5.8 ml/min (i.e. 0.96 times the injection rate at its respective upgradient injection point sampler (A')). During the run-time of this experiment 62 water samples were taken.

The first experiment at well pair point sampler B'-B was conducted under the following conditions: a PITT tracer pulse of 113.40 ml was injected over 20 min (flow rate: 5.67 ml/min) at point sampler B' (45,80,204), subsequently the injection was switched to Millipore-water for 3:27:43 hours at the identical flow rate. The withdrawal rate at the downgradient extraction point sampler B (105,80,204) was 6.1 ml/min and thus 1.08 times higher than the injection rate at its respective upgradient injection point sampler (B'). During the run-time of this experiment 23 water samples were taken.

The second experiment at well pair point sampler B'-B was conducted under the following conditions: a PITT tracer pulse of 141.75 ml was injected over 25 min (flow rate: 5.67 ml/min) at point sampler A' (45,80,204), subsequently the injection was switched to Millipore-water for 4:06:00 hours at the identical flow rate. The withdrawal rate at the downgradient extraction point sampler B (105,80,204) was now set to 21.4 ml/min and thus 3.77 times higher than the injection rate at its respective upgradient injection point sampler (B'). During the run-time of this experiment 34 water samples were taken.

The experiment at well pair point sampler C'-C was conducted under the following conditions: a PITT tracer pulse of 362.44 ml was injected over 26 min (flow rate: 13.94 ml/min) at point sampler C' (45,50,174), subsequently the injection was switched to Millipore-water for 5:12:15 hours at the identical flow rate. The withdrawal rate at the downgradient extraction point sampler C (105,50,174) was 18.96 ml/min and thus 1.36 times higher than the injection rate at its respective upgradient injection point

sampler (C'). During the run-time of this experiment 159 water samples were taken.

The experiment at well pair point sampler D'-D was conducted under the following conditions: a PITT tracer pulse of 273.00 ml was injected over 20 min (flow rate: 13.65 ml/min) at point sampler D' (45,20,204), subsequently the injection was switched to Millipore-water for 3:54:39 hours at the identical flow rate. The withdrawal rate at the downgradient extraction point sampler D (105,20,204) was 18.96 ml/min and thus 1.39 times higher than the injection rate at its respective upgradient injection point sampler (D'). During the run-time of this experiment 43 water samples were taken.

The experiment at well pair point sampler E'-E was conducted under the following conditions: a PITT tracer pulse of 233.60 ml was injected over 20 min (flow rate: 11.69 ml/min) at point sampler E' (45,15,144), subsequently the injection was switched to Millipore-water for 5:45:50 hours at the identical flow rate. The withdrawal rate at the downgradient extraction point sampler E (105,15,144) was 18.85 ml/min and thus 1.61 times higher than the injection rate at its respective upgradient injection point sampler (E'). During the run-time of this experiment 162 water samples were taken.

In order to assess both, the homogeneous DNAPL blob zone ($S_n \leq 4.86\%$) located in the upper part of the aquifer close to the inflow chamber, as well as the DNAPL pool ($S_N = 100\%$) at the bottom of the aquifer in one experiment, an integral, natural gradient flow field PITT was conducted. This test employed one fully filtered, stainless steel injection well I' (13 mm OD, 10 mm ID) that was also installed via direct push, located upgradient of the source zones (x-y-coordinates: (35.5, 50) [cm]; filtered section (z): 22-202 [cm], see Fig. 3-6 and Fig. 3-8a) and a grouped multi-level sampler, made of six point samplers IA-IF (6 mm OD, 2 mm ID, fabrication as described before), which were

arranged perpendicular to the natural gradient flow direction at the downgradient end of the tar oil pool (the resulting flow distance from the injection well to the grouped multi-level sampler was 2.65 m). The coordinates (x,y,z) [cm] of the respective filter of the six individual point samplers forming the grouped multilevel sampler (see Fig. 3-6 and Fig. 3-8b) are given in the following: IA (300, 67.5, 27), IB (300, 60.5, 144), IC (300, 53.5, 204), ID (300, 46.5, 74), IE (300, 39.5, 174), IF (300, 32.5, 29). A miniature submersible pump (COMET, Elegant) was used to inject the dirac-type tracer pulse into the natural-gradient base flow field (5 m/day) of the large scale tank. After the outlet of the aforementioned mini-pump was connected (via a PE-tubing) to the fully filtered injection well (I'), the whole pumping-unit was inserted into a flask containing the desired injection volume of the tracer solution. To start the experiment the pump was connected to the power supply (car battery) until the total (desired) tracer volume was injected, then the pump was disconnected from the power supply. Neither active post-flushing of the well nor further injections were applied until the end of the experiment. The downgradient six point samplers IA-IF of the grouped multi-level sampler, were sampled in parallel at a constant pumping rate via peristaltic pumps (ISMATEC, BVP). The effluent of three selected point samplers (IA, ID, IF) was directly guided through three separate, self-provided conductivity cells (see Fig. 3-2) before finally being sampled at a sharpened capillary at the end of the flow path (analogue to column set-up B, see Fig. 3-4). The effluent of the remaining three point samplers was directly passed to the sampling ports. Analysis of the tracer substances in the obtained water samples was done as described before.

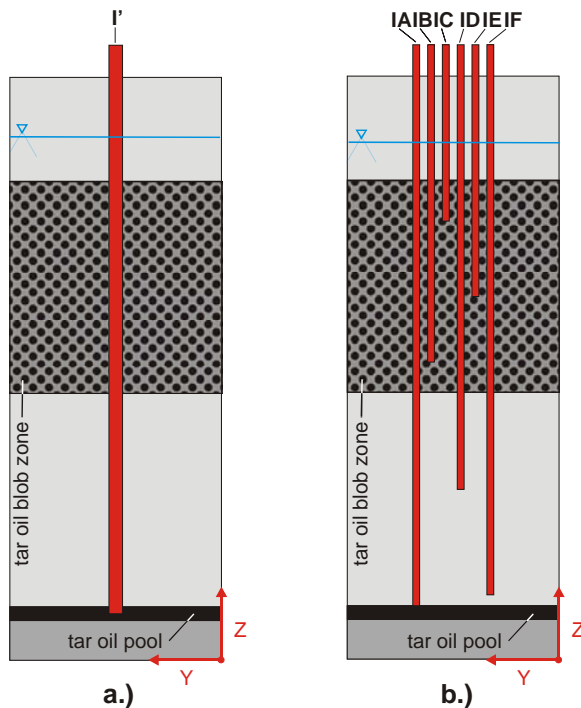


Figure 3-8. Setup of the large scale tank experiment indicating the origin of the tank coordinate system (y,z), the two different source zones (tar oil blob zone, tar oil pool) and the position of the wells employed for the natural gradient flow field PITTs a.) upgradient fully filtered injection well I', b.) downgradient grouped multilevel sampler IA-IF.

The following two individual but almost identical, natural gradient flow field tracer tests were conducted: (1) a preliminary salt tracer test (pre-test) containing only NaCl (integral injection at well I', extraction and online EC-logging at point samplers IA, ID, IF) to check the data logging equipment and to get an idea of the maximum tracer BTC concentrations at the outermost point samplers located close to the tar oil pool and (2) the final PITT containing the whole PIT-suite including NaCl (integral injection at well I', extraction at point samplers IA-IF with online EC-logging at point samplers IA, ID, IF).

The preliminary salt tracer test (pre-test) containing only NaCl was conducted under the following conditions: a NaCl tracer pulse of 1982 ml (density: 1.005 g/l) was injected over 14.5 s (flow rate: 8200 ml/min) at the integral injection well I'. The withdrawal rate at the downgradient extraction point samplers IA, ID, IF was 13 ml/min. During the run-time of this

pre-test only online EC-readings were recorded, no further water samples were taken (i.e. the effluent of all three sampling ports was cumulatively gathered in a container and discarded after the end of the experiment).

The final PITT containing the whole PIT-suite (including NaCl) was conducted under the following conditions: a PIT tracer pulse of 1995 ml (density: 1.001 g/l) was injected over 14.6 s (flow rate: 8200 ml/min) at the integral injection well I'. The withdrawal rate at the downgradient extraction point samplers IA-IF was 13 ml/min. During the run-time of this PITT both online EC-readings (IA, ID, IF) and water samples (IA-IF) were taken.

3.4 Results and Discussion

After the equilibrium partitioning coefficients (K_{NW}) for the alcohols were determined in batch experiments and the interfacial adsorption coefficient (K_{IFT}) for SLES was obtained by the drop weight method, the PITT column experiments were conducted to compare the breakthrough curves of the reactive tracers with the conservative tracer in different column systems (each containing 20% residual tar oil saturation but being differently distributed within the aquifer matrix: grain-coatings, blobs, pools/ganglia) and at different flow velocities. Additional experiments were conducted in a large scale tank setup. An identical tar oil DNAPL (RÜTGERS, Germany) was employed in all experiments. The specific objectives of the experiments were: (1) to check the suitability of the combined PITT for complex, highly viscous, multi-component DNAPLs (here tar oil), (2) to evaluate the PITT based determination of coal tar saturation in dependence of different flow velocities, (3) to validate the PITT based determination of the specific DNAPL/water interfacial areas of three different DNAPL distribution geometries and (4) to check the efficiency of PITTs for the assessment of realistic contaminant scenarios.

3.4.1 Batch Experiments

Batch experiments were performed to determine the equilibrium partitioning coefficients (K_{NW}) of the respective partitioning tracer alcohols and the tar oil (RÜTGERS, Germany) which were used in this study. Representative partitioning kinetics and a partitioning isotherm are shown in Fig. 3-9 and Fig. 3-10, the complete K_{NW} dataset is given in Tab. 3-3. As indicated in Fig. 3-9 the partitioning coefficients show a steep increase between 0.5 and 8 hours, but after 8 hours a plateau establishes, i.e. equilibrium conditions must have been approached. Consequently the dimensionless equilibrium partitioning coefficients (K_{NW}) used for the evaluation of all following PTT experiments were determined by a linear partitioning isotherm based on data of all four dilutions but solely those of the equilibrated 24 hours time step (see Fig. 3-10).

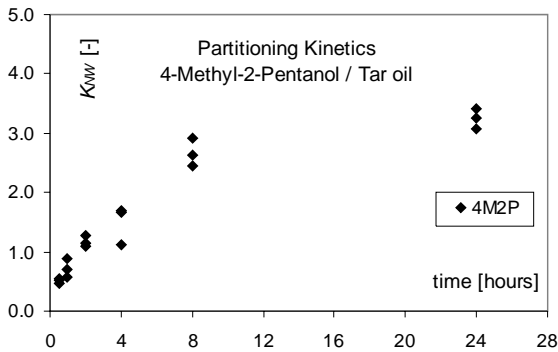


Figure 3-9. Partitioning kinetics of 4-Methyl-2-Pentanol (4M2P) at $C_0/2$.

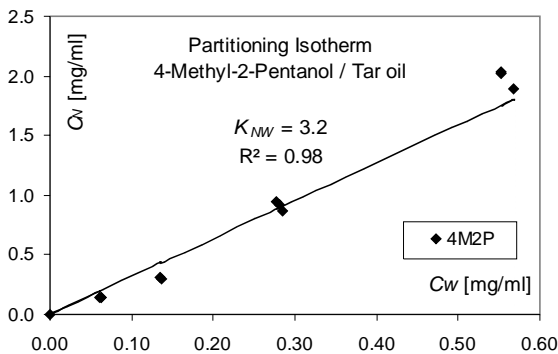


Figure 3-10. Partitioning isotherm of 4-Methyl-2-Pentanol (4M2P) at 24 hours.

The drop-weight method was applied to measure the liquid-liquid interfacial tension between the tar oil and the respective interfacial tracer (SLES) dilution (see Fig. 3-11). These data were

used for the determination of the interfacial adsorption coefficient, K_{IFT} , as follows: the measured data points of liquid-liquid interfacial tensions (γ) were fitted by Eq. 3-15 (Annable et al. 1998):

$$\gamma = \left[1 - \left(\frac{C_{IFT}}{CMC_{FIT}} \right)^\beta \right] (\gamma_{max} - \gamma_{min}) + \gamma_{min} \quad (3-15)$$

where CMC_{FIT} [mmol/cm³] and β [-] are empirical fitting factors; γ_{min} and γ_{max} [dyne/cm] are the minimum and maximum liquid-liquid interfacial tensions that were measured in the experiment. The best fit was obtained using $\gamma_{min} = 10.48$ dyne/cm, $\gamma_{max} = 46.77$ dyne/cm, $CMC_{FIT} = 0.0027$ mmol/cm³ and $\beta = 0.42$ (see Fig. 3-11).

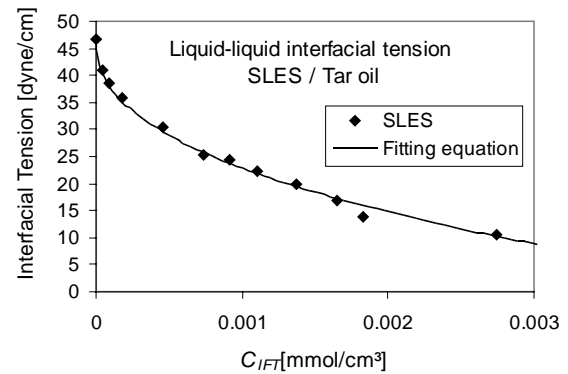


Figure 3-11. Liquid-liquid interfacial tension between the tar oil and various dilutions of Sodium Laurylethersulfate (SLES). The measured data points were fitted by Eq. 3-14.

This fitting function (Eq. 3-15) was now differentiated to obtain the local slope at the desired C_{IFT} concentration. The introduction of this derivative into Eq. 3-10 finally gives the respective interfacial adsorption coefficient:

$$K_{IFT} = \frac{\beta (\gamma_{max} - \gamma_{min})}{2RT(CMC_{FIT})^\beta} C_{IFT}^{\beta-1} \quad (3-16)$$

Using the before derived fitting factors $\gamma_{min} = 10.48$ dyne/cm, $\gamma_{max} = 46.77$ dyne/cm, $CMC_{FIT} = 0.0027$ mmol/cm³ and $\beta = 0.42$ the K_{IFT} values given in Figure 3-12 were determined.

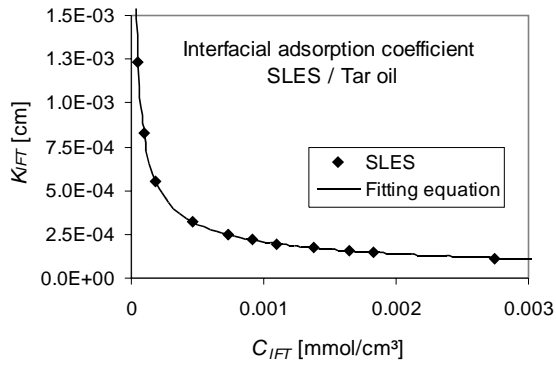


Figure 3-12. Interfacial adsorption coefficient for the tar oil and various dilutions of Sodium Laurylthethersulfate (SLES). The points indicate concentrations were actual measurements were conducted (see Fig. 3-11), the curve gives the complete dataset derived from Eq. 3-15.

For the sake of clarity this relationship was also transformed into the corresponding more classical non-linear interfacial adsorption isotherm (Fig. 3-13).

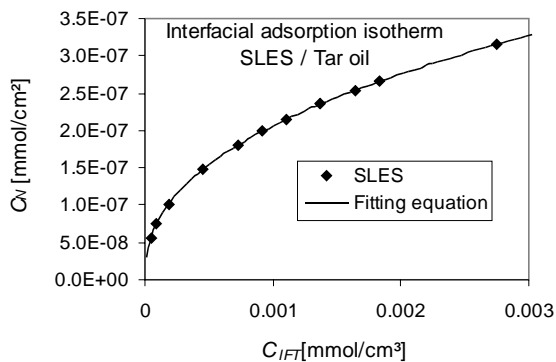


Figure 3-13. Interfacial adsorption isotherm of Sodium Laurylthethersulfate (SLES). The points indicate concentrations were the actual measurements were conducted (see Fig. 3-11), the curve gives the complete dataset being transformed from Eq. 3-15.

3.4.2 Column Experiments

To get an overview of the theoretical detection capabilities of PTTs in column experiments, using the three partitioning tracers (4M2P, 1HEX, 2,4DM2P), their equilibrium retardation factors were calculated according to Eq. 3-6 using the before parameterised K_{NW} values and a bandwidth of tar oil saturations (S_n) between 0 and 50%. The results are given in Figure 3-14.

Sufficient separation from the conservative tracer, i.e. retardation factors of $1.2 < R_{PART} < 4$ as recommend by Jin et al. (1995), is achieved for the whole suite of partitioning tracers at tar oil saturations between 6 and 16%. For the individual tracers 4M2P, 1HEX and 2,4DM2P these conditions are fulfilled at tar oil saturations between 6 and 49%, between 2 and 24% and between 1.2 and 16%, respectively.

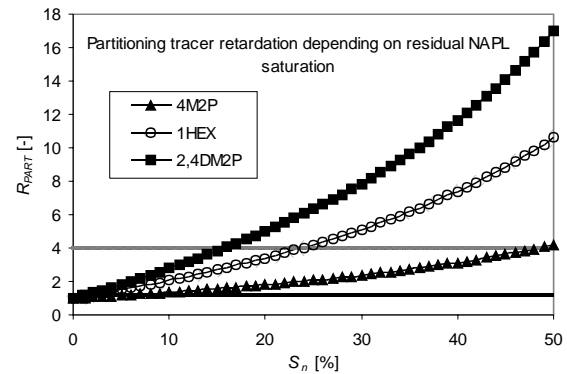


Figure 3-14. Anticipated equilibrium retardation factors (R_{PART}) versus tar oil saturation (S_n). R_{PART} was calculated according to Eq. 3-6 and the respective K_{NW} values determined in the batch experiments. The two horizontal lines indicate the retardation interval ($1.2 < R_{PART} < 4$) recommend by Jin et al. (1995).

Subsequently the anticipated relative partitioning tracer BTCs for one given tar oil saturation (20%), were calculated according to Eq. 3-8, to evaluate the anticipated peak maxima and the separation grade of the individual peaks (see Fig. 3-15 and Fig. 3-16). The parameter settings were chosen close to the column experiments planned in the course of this study, i.e. the before determined K_{NW} values (Tab. 3-3), a Peclet number of 231 ($v_a = 1$ m/day, $d = 0.2$ cm, $D_{aq} = 1.00E-06$ cm²/s) and a tracer pulse injection time of 0.05 pore volumes.

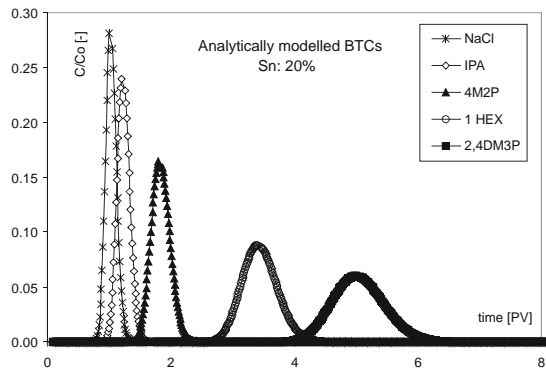


Figure 3-15. Analytically modelled column experiment at 20% tar oil saturation. The BTCs were calculated according to Eq. 3-8 and the respective K_{NW} values determined in the batch experiments. Parameter settings: $Pe = 231$ and $t_p = 0.05$.

As shown in Figure 3-15 the anticipated peak maxima of the partitioning tracers are approximately between 5 and 15% of the input concentrations, the peaks are nearly base-line separated and almost symmetric (including the tailing of the peaks, see Fig. 3-16).

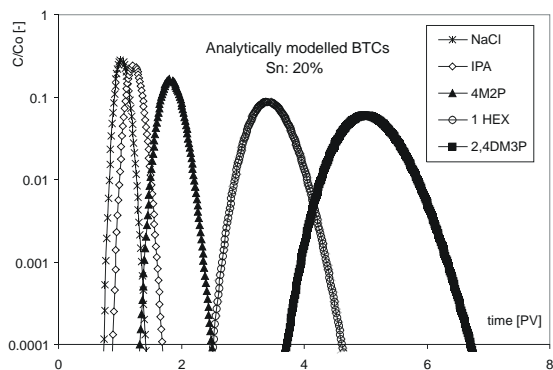


Figure 3-16. Semi-logarithmic plot of the analytically modelled column experiment with 20% tar oil saturation. Parameter settings are identical to Fig. 3-15.

Based on these results (analytical solution Eq. 3-8 under the assumption of equilibrium conditions) no problems such as insufficient separation of the peak maxima or extensive tailings were expected to occur in the following laboratory column experiments.

As the final calculation of the tar oil saturation out of experimental data strongly relies on the accuracy of the determined retardation factors (Eq. 3-1), it was decided to employ two

independent conservative tracers (NaCl and IPA), to increase the confidence level of the obtained results.

The first column experiment conducted throughout the course of the laboratory work was column #V (S_n : 14%), using column setup A, where a Y-connector was used to split a portion of the column effluent to a self-provided conductivity cell (online measurement of the conservative tracer, NaCl, BTC). The measured BTCs of the conservative tracers NaCl and IPA (see Fig. 3-17 and Fig. 3-18) are far from overlaying each other: for NaCl the peak maximum is much smaller and the peak arrival time is delayed, i.e. NaCl is strongly retarded compared to IPA.

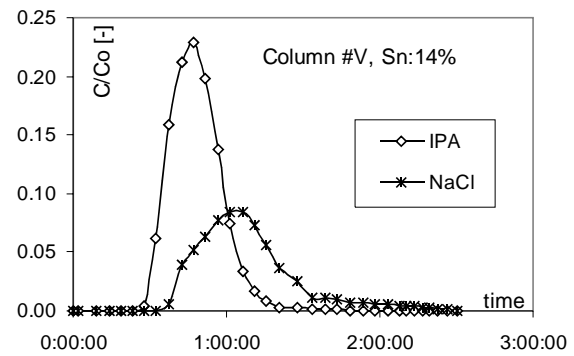


Figure 3-17. BTCs of the two conservative tracers IPA and NaCl passed through column #V (S_n : 14%) using column set-up A.

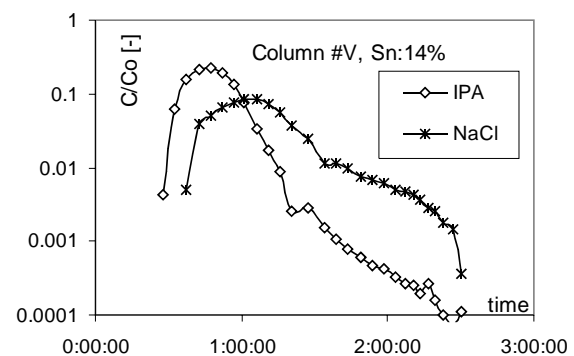


Figure 3-18. Semi-logarithmic BTC-plot of the two conservative tracers IPA and NaCl passed through column #V (S_n : 14%) using column set-up A.

As the determined NaCl mass recovery (Fig. 3-19) is just around 65%, a major problem in the measurement setup of this conservative tracer becomes evident.

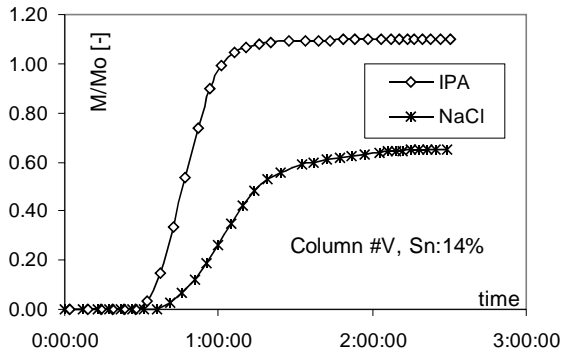


Figure 3-19. Mass recovery of the two conservative tracers IPA and NaCl passed through column #V (Sn: 14%) using column set-up A.

If any retardation of the two conservative tracers is expected, then it should be IPA that is slightly retarded compared to NaCl (see Fig. 3-15) – exhibiting such obvious experimental artefacts this experiment was therefore not further evaluated concerning the tar oil saturation of the column, but solely used for the correction of the experimental bias.

To overcome the obvious problems of the uncontrolled splitting of the column effluent at the Y-connector the experimental setup was changed to column setup B as follows: the whole effluent was now directly guided through the self-provided conductivity cell before finally being sampled at end of the flow path.

The second column experiment conducted throughout the course of the laboratory work was column # IV (S_n : 5%), using column setup B, where the whole column effluent was directly guided through a self-provided conductivity cell (online measurement of NaCl). The measured BTCs of the conservative tracers NaCl and IPA (see Fig. 3-20 and Fig. 3-21) are now almost overlaying each other. The NaCl peak maximum is a little smaller and only the arrival time of the rising peak shoulder and the peak tailing are delayed, i.e. NaCl is still slightly retarded compared to IPA.

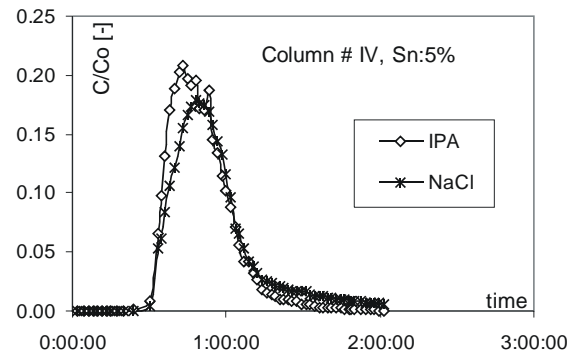


Figure 3-20. BTCs of the two conservative tracers IPA and NaCl passed through column #IV (Sn: 5%) using column set-up B.

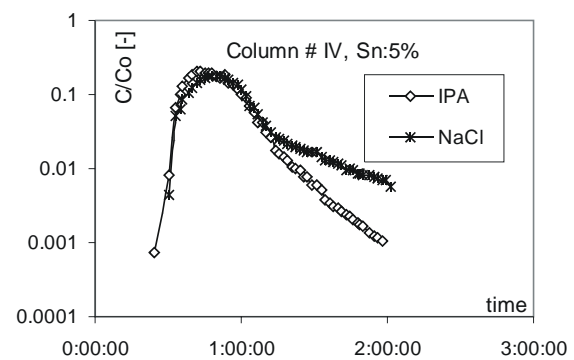


Figure 3-21. Semi-logarithmic BTC-plot of the two conservative tracers IPA and NaCl passed through column #IV (Sn: 5%) using column set-up B.

As the determined NaCl mass recovery is now almost identical to that of IPA (see Fig. 3-22), the major problem in the column set-up seemed to be terminated, but the remaining deviation is still not conform to theory. Thus this experiment was again not further evaluated concerning the tar oil saturation of the column, but solely used for the correction of the experimental set-up.

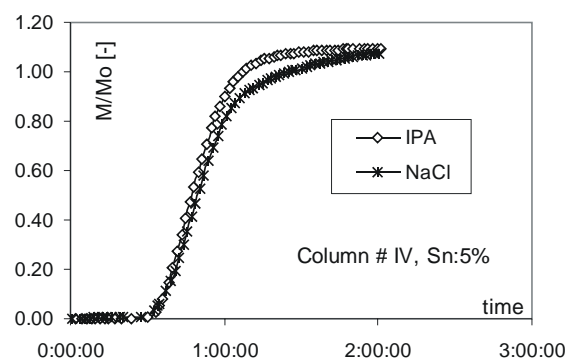


Figure 3-22. Mass recovery of the two conservative tracers IPA and NaCl passed through column #IV (Sn: 5%) using column set-up B.

In the following a conductivity probe breakthrough test was conducted to clarify if the distortion of the NaCl peak is a direct artefact of the self-provided conductivity cell, that was still used in column setup B.

A defined square input pulse was directly (no column was in between the pump and the conductivity cell) passed through the self-provided conductivity cell. The resulting measured BTC of the conservative tracer NaCl was normalized and compared to that of the rectangular NaCl input pulse (see Fig. 3-23).

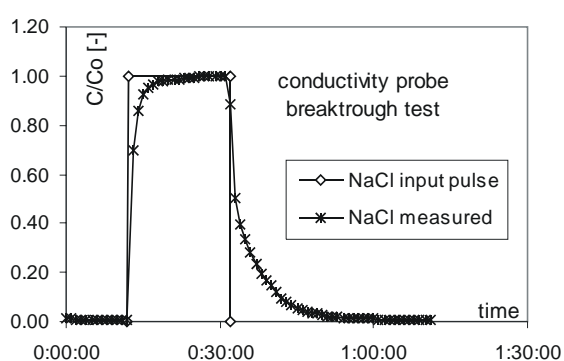


Figure 3-23. Comparison of theoretical NaCl input pulse and resulting, measured NaCl BTC.

The measured NaCl BTC is retarded compared to the theoretical NaCl input pulse and shows the same distortion pattern that was observed in experiment column #IV, i.e. the arrival time of the rising peak shoulder and the peak tailing are delayed. Thus it can be concluded, that the observed retardation is a direct artefact (incomplete water throughput/exchange at low flow velocities) of the self-provided conductivity cell itself.

Consequently the setup was changed again to the final column setup C, where the online EC measurement via the self-provided conductivity cell was terminated and a manually controlled three way valve for the continuous sampling of the whole column effluent was installed. One portion of the samples was now used for offline EC measurements using the miniature flow-cell of a HPLC conductivity detector.

The third column experiment was column #8b (S_n : 20%), using column setup C, where the whole column effluent was sampled at a

manually controlled three way valve (with subsequent offline measurement of NaCl).

The tracer suite was passed through column #8b (S_n : 20%) at two different runs with identical settings (column set-up C); 1st run measuring NaCl and IPA, whereas in the 2nd run only the NaCl was measured. The measured BTCs of the conservative tracers NaCl and IPA (see Fig. 3-24 and Fig. 3-25) are now overlaying each other. Even the NaCl BTC of the 2nd run practically overlays the previous BTCs of the 1st run, indicating a very good reproducibility of the experiment. Just the late peak tailing of both NaCl BTCs is somewhat delayed (only visible in the semi-logarithmic plot Fig. 3-25), i.e. NaCl is still a very little retarded (R_{NaCl} 1st run equals 1.06 and R_{NaCl} 2nd run equals 1.13) compared to IPA ($R_{IPA} = 1$).

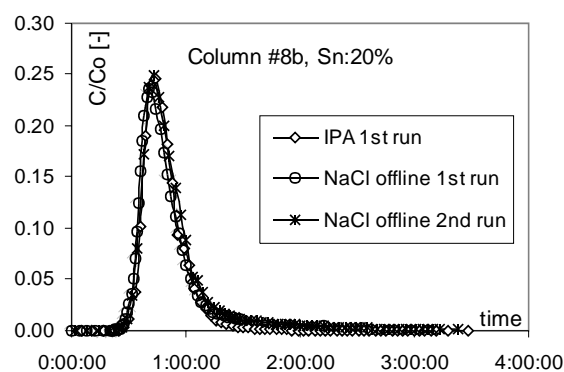


Figure 3-24. BTCs of the conservative tracers NaCl and IPA passed through column #8b (S_n : 20%) at two different runs with identical settings using the offline EC measurement (column set-up C); 1st run measuring NaCl and IPA, whereas in the 2nd run only the NaCl was measured.

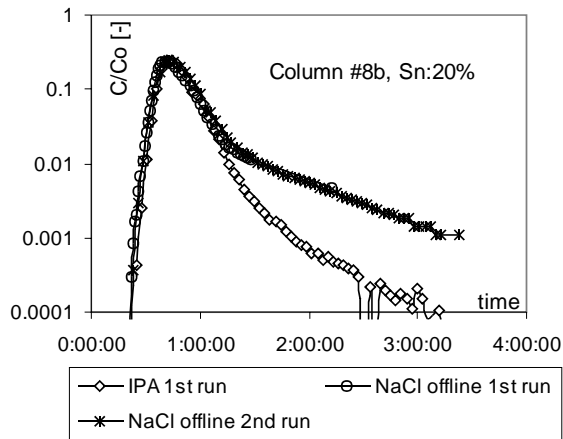


Figure 3-25. Semi-logarithmic BTC plot of the conservative tracers NaCl and IPA passed through column #8b (S_n : 20%) at two different runs with identical settings using the offline EC measurement (column set-up C); 1st run measuring NaCl and IPA, whereas in the 2nd run only the NaCl was measured.

The rising shoulders of the determined NaCl mass recovery BTCs are identical to that of IPA, but Figure 3-26 shows that the remaining deviation in the tailing of the NaCl BTCs (Fig. 3-25) is still sufficient to cause a slight positive error in the final plateau of the mass recovery BTCs, i.e. the mass balance (approximately 110% mass recovery for NaCl 1st run).

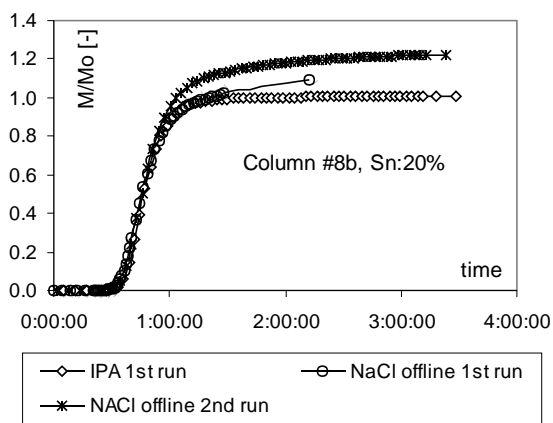


Figure 3-26. Mass recovery of the conservative tracers NaCl and IPA passed through column #8b (S_n : 20%) at two different runs with identical settings using the offline EC measurement (column set-up C); 1st run measuring NaCl and IPA, whereas in the 2nd run only the NaCl was measured.

If this aforementioned deviation of the BTC tailing is coupled with a discrepancy in the peak

maximum (maximum of NaCl 2nd run is a little higher than the two other maxima) the mass recovery is even up to 120%.

Nevertheless, the systematic artificial distortion of the NaCl peak was overcome, the method is well reproducible and the remaining errors are now in the range of the tolerable overall measurement errors of the detection method. Consequently this approved setup was used in all following column experiments.

The following three pulse type PITTs (column #8b, #8c and #9b) were conducted in identical glass columns (6 cm diameter, 15 cm length) filled with identical well graded sand (1-2 mm diameter) containing the identical tar oil residual saturation (S_n) of exactly 20%, but the linear flow-velocity was varied between 6.1 m/day and 1.9 m/day to evaluate the influence of non-equilibrium transport conditions on PITT results.

Column #8b (S_n : 20%, DNAPL blobs), was conducted using column setup C, at a linear flow-velocity of 6.1 m/day. The measured BTCs of the PIT-suite show a significant retardation compared to the conservative tracers NaCl and IPA which are overlaying each other (see Fig. 3-27), just the late peak tailing of the NaCl BTC is somewhat retarded behind the IPA BTC (only visible in the semi-logarithmic plot Fig. 3-28). The partitioning tracers are retarded according to the order of their partitioning coefficients. However, the peaks are far from base-line separation, they are strongly asymmetric and the retardation factor of all partitioning tracers is smaller than expected (see Table 3-3). Consequently the PTT based average tar oil saturation estimate (Eq. 3-7) is only at 7.2% (i.e. 36% of the true S_n value).

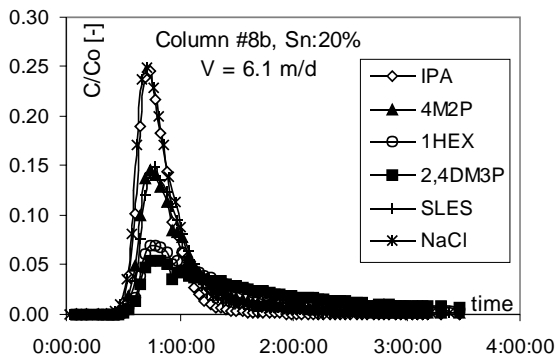


Figure 3-27. BTCs of the conservative tracer NaCl, IPA and the PIT-suite passed at 6.1 m/d through column #8b, $S_n: 20\%$ (DNAPL blobs).

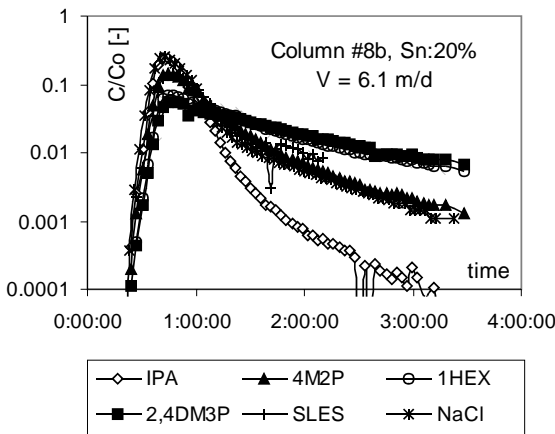


Figure 3-28. Semi-logarithmic BTC-plot of the conservative tracers NaCl, IPA and the PIT-suite passed at 6.1 m/d through column #8b, $S_n: 20\%$ (DNAPL blobs).

The rising shoulders of the determined PIT-suite mass recovery BTCs are significantly retarded compared to the ones of the conservative tracers (NaCl and IPA) again in the correct order of their partitioning coefficients, resulting in the more severe truncation of the more retarded BTCs. Consequently, the mass recovery of the more retarded partitioning tracers is less than that of the conservative tracers (see Fig. 3-29). This leads to the fact that tar oil saturation estimates of partitioning tracers with high partitioning coefficients like 2,4DM3P are generally smaller than that of partitioning tracers with low partitioning coefficients like 4M2P (see Table 3-3).

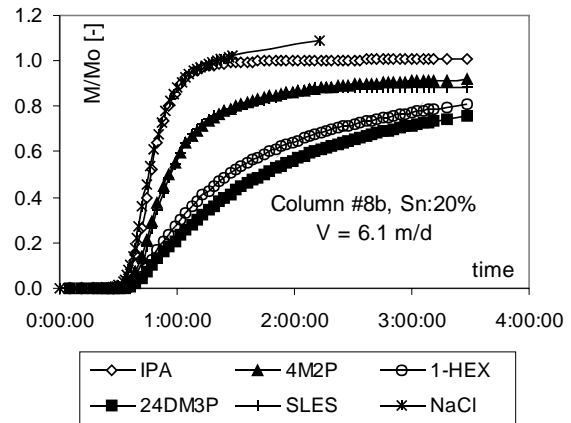


Figure 3-29. Mass recovery of the conservative tracer NaCl and the PIT-suite passed at 6.1 m/d through column #8b, $S_n: 20\%$ (DNAPL blobs).

Column #8c ($S_n: 20\%$, DNAPL blobs), was conducted using column setup C, at a linear flow-velocity of 3.6 m/day. The measured BTCs of the PIT-suite show a higher retardation than in the previous experiment (see Fig. 3-30). The partitioning tracers are again retarded according to the order of their partitioning coefficients. However, the peaks are still not base-line separated, they are strongly asymmetric and the retardation factor of all partitioning tracers is again smaller than expected (see Table 3-3). Consequently the PTT based average tar oil saturation estimate (Eq. 3-7) is only at 10.3% (i.e. 52% of the true S_n value).

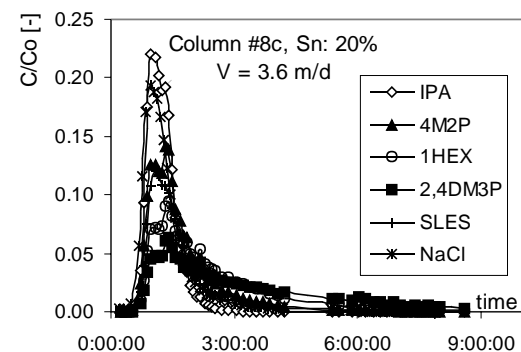


Figure 3-30. BTCs of the conservative tracers NaCl, IPA and the PIT-suite passed at 3.6 m/d through column #8c, $S_n: 20\%$ (DNAPL blobs).

The late tailings of the partitioning tracer BTCs are nicely separated (only visible in the semi-logarithmic plot Fig. 3-31).

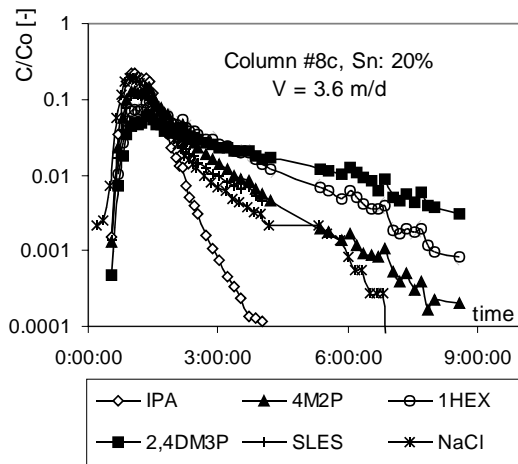


Figure 3-31. Semi-logarithmic BTC-plot of the conservative tracers NaCl, IPA and the PIT-suite passed at 3.6 m/d through column #8c, Sn: 20% (DNAPL blobs).

The mass recovery plots of the PIT-suite show retardation compared to the ones of the conservative tracers (NaCl and IPA) again in the correct order of their partitioning coefficients. Due to the prolonged experimental runtime the truncation of the retarded BTCs is less severe than in the previous experiment. Consequently, the absolute mass recovery (even of the higher retarded partitioning tracers) is also better than that of the previous experiment (see Fig. 3-32). This leads to the fact that the tar oil saturation estimates of the individual partitioning tracers show less deviations from each other (see Table 3-3).

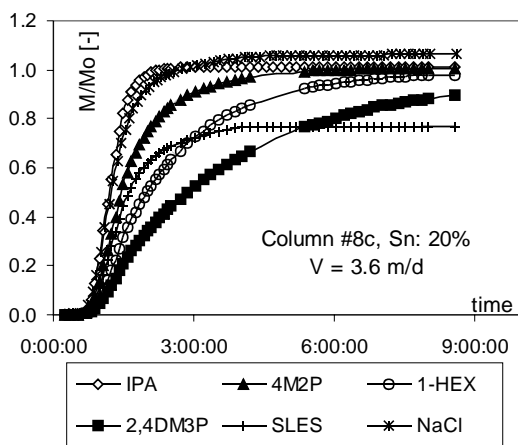


Figure 3-32. Mass recovery of the conservative tracers NaCl, IPA and the PIT-suite passed at 3.6 m/d through column #8c, Sn: 20% (DNAPL blobs).

Column #9b (S_n : 20%, DNAPL coatings), was conducted using column setup C, at a linear flow-velocity of 1.9 m/day. The measured BTCs of the PIT-suite show an even higher retardation than in both previous experiments (see Fig. 3-33). The partitioning tracers are once more retarded according to the order of their partitioning coefficients and the separation of the individual BTCs already starts in the rising shoulders of the peaks. However, the peaks are still not base-line separated, they are still asymmetric and the retardation factor of all partitioning tracers is still smaller than expected (see Table 3-3). Consequently the PTT based average tar oil saturation estimate (Eq. 3-7) is now at 14.7% (i.e. 74% of the true S_n value).

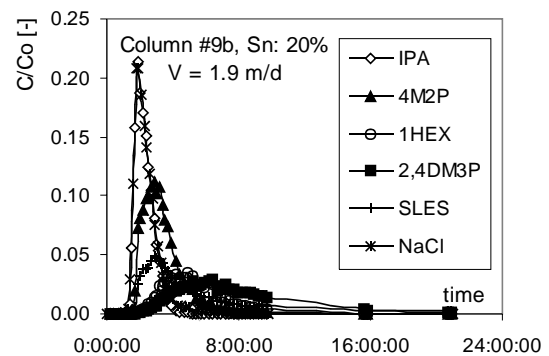


Figure 3-33. BTCs of the conservative tracers NaCl, IPA and the PIT-suite passed at 1.9 m/d through column #9b, Sn: 20% (DNAPL coatings).

The late tailing of some tracer BTCs (IPA, NaCl and 4M2P) is already truncated before the end of the experimental runtime, as their concentration falls beyond the respective detection limit (see Fig. 3-34).

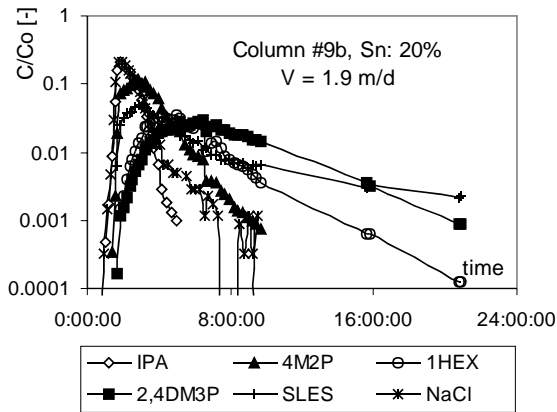


Figure 3-34. Semi-logarithmic BTC-plot of the conservative tracers NaCl, IPA and the PIT-suite passed at 1.9 m/d through column #9b, Sn: 20% (DNAPL coatings).

The rising shoulders of the determined PIT-suite mass recovery BTCs are retarded compared to the ones of the conservative tracers (NaCl and IPA) once more in the correct order of their partitioning coefficients (Fig. 3-35). Due to the prolonged experimental runtime the truncation of the retarded BTCs should be less severe than in both previous experiments. But due to the very low tracer concentrations (which are close to the detection limit and thereby more likely due to measurement errors) over a large portion of the extended tailing the absolute mass recovery (especially of the higher retarded partitioning tracers) is not as good as in the previous experiment.

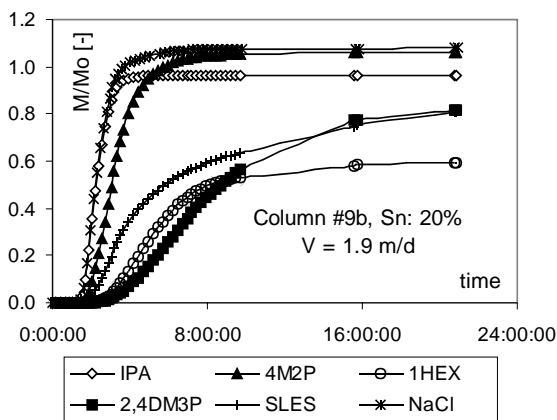


Figure 3-35. Mass recovery of the conservative tracers NaCl, IPA and the PIT-suite passed at 1.9 m/d through column #9b, Sn: 20% (DNAPL coatings).

Despite this fact, the tar oil saturation estimates of the individual partitioning tracers show less deviations from each other than in both previous experiments (see Table 3-3).

The following three pulse type PITTs (column #9a, #8b and #9b) were conducted in identical glass columns (6 cm diameter, 15 cm length) filled with identical well graded sand (1-2 mm diameter) containing the identical tar oil residual saturation (S_n) of exactly 20%, but the DNAPL distribution geometry and thereby the DNAPL-water interfacial area (A_{NW}) was varied between DNAPL-pool/ganglia, DNAPL-blobs and DNAPL-coatings, to obtain a semi-quantitative validation of the ITT results.

Column #9a (S_n : 20%, DNAPL pool/ganglia), was conducted using column setup C. The distribution geometry of the tar oil pool/ganglia within the aquifer matrix can be seen in Figure 3-36.

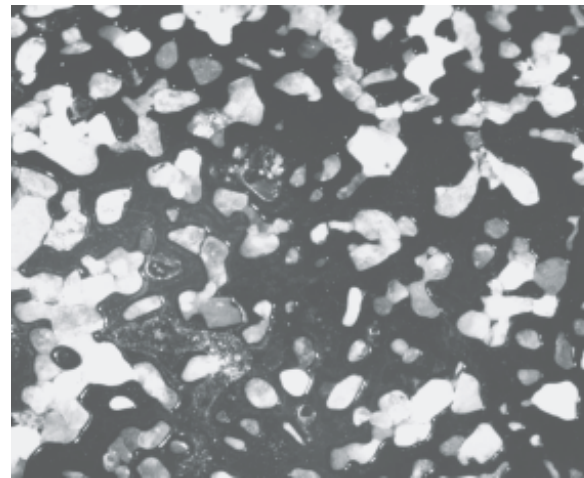


Figure 3-36. Macro photo section of column #9a showing the distribution of the tar oil pool/ganglia (black) within the brighter aquifer matrix material (grainsize: 1-2 mm).

The measured BTC of SLES, the interfacial tracer, shows no retardation compared to the conservative tracer NaCl (see Fig. 3-37). In fact it is even slightly faster transported than the conservative tracer ($R_{IFT} = 0.99$). As suggested by Annable et al. (1998) the constant K_{IFT} value required for the subsequent analytical calculation of A_{NW} (Eq. 3-13) can be determined by using the maximum peak concentration (C_{max}) of the SLES BTC. The parameters

determined are: $C_{max} = 0.13$, $K_{IFT} = 5.74E-04$ cm. As the retardation factor measured for SLES is smaller than one, an ITT based estimation (Eq. 3-13) of the tar oil-water interfacial area is impossible, it can only be stated that it must be negligibly small. This is supported by the small A_{NW} value of $0.2 \text{ cm}^2/\text{cm}^3$ which was estimated by the following geometric relationship: the radius of the assumed spherical DNAPL ganglia (r_g) is given by the volume (V) of the used DNAPL ($r_g = (3V / 4n \pi)^{1/3}$), $A_{NW} = 3S_n / r_g$ and was in a first approximation assumed to equal the effective DNAPL-water interfacial area.

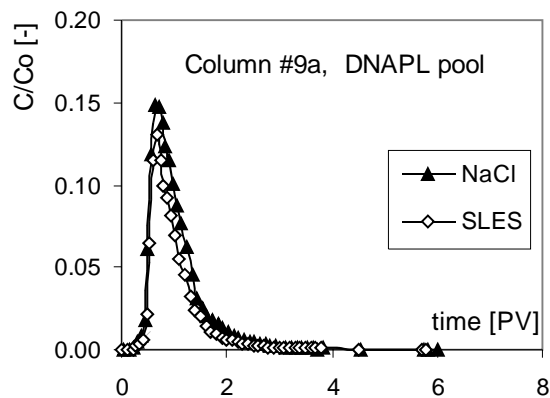


Figure 3-37. BTCs of the conservative tracer NaCl and the interfacial tracer SLES passed through the DNAPL pool/ganglia containing column #9a (S_n : 20%).

This unusual retardation behaviour of the interfacial tracer might either be a measurement error or be explained by the large size of the SLES molecules which may therefore already undergo pore size exclusion effects (Koh et al., 1998). Due to these exclusion effects larger tracer molecules (SLES) are then unable to enter certain domains of the tested column where the smaller tracer molecules (NaCl) can enter without any problems. This will finally result in a shorter residence time (i.e. faster transport velocity) for the larger tracer molecules.

Despite the fact that SLES is more or less transported like a conservative tracer, the determined SLES mass recovery (Fig. 3-38) is just around 80%, this might either be due to the irreversible sorption of the missing tracer mass onto the tar oil-water interface or due to

measurement errors. Despite the fact, that the blank experiment column #9d (see Fig. 3-50) achieved a complete mass recovery (110 %), the first of the before given arguments just seems to be more likely on the first glance, as the mass losses due to irreversible sorption must then consequently increase with an increasing DNAPL-water interfacial area. But this was not observed in the following experiments (Fig. 3-42 and Fig. 3-45).

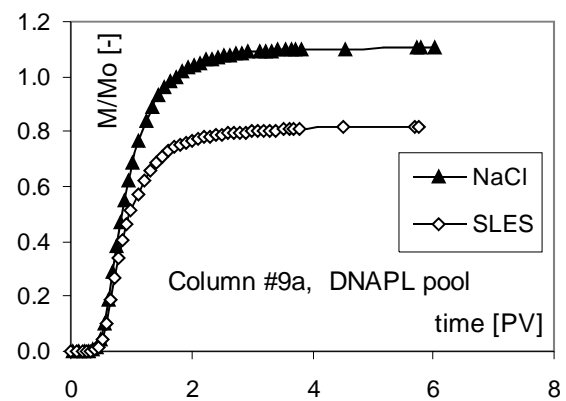


Figure 3-38. Mass recovery of the conservative tracer NaCl and the interfacial tracer SLES passed through the DNAPL pool/ganglia containing column #9a (S_n : 20%).

Column #8b (S_n : 20%, DNAPL blobs), was conducted using column setup C. The distribution geometry of the tar oil blobs within the aquifer matrix can be seen in Figure 3-39.

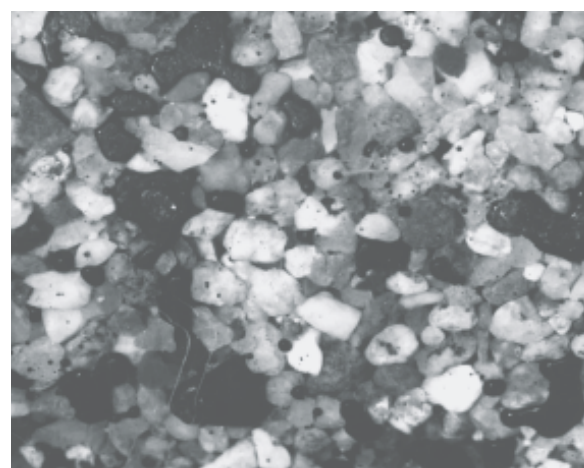


Figure 3-39. Macro photo section of column #8b showing the distribution of the tar oil blobs (black) within the brighter aquifer matrix material (grainsize: 1-2 mm).

The measured BTC of the interfacial tracer (SLES) shows significant retardation compared

to the conservative tracer NaCl (see Fig. 3-40). The separation of the SLES BTC already starts in the rising shoulders of the peaks. However, the two peaks are not base-line separated, both are slightly asymmetric and the retardation factor of the interfacial tracer is 1.16. The determined parameters for the maximum peak concentration and the constant interfacial adsorption coefficient after Annable et al. (1998) are: $C_{max} = 0.148$, $K_{IFT} = 5.33E-04$ cm.

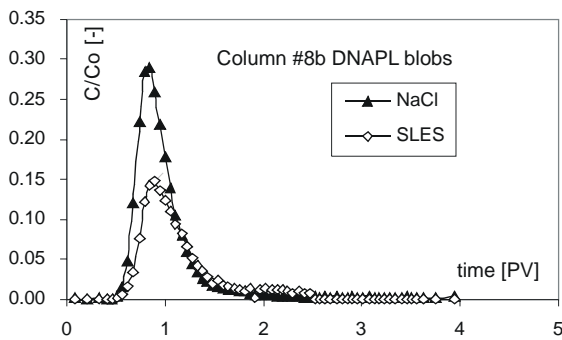


Figure 3-40. BTCs of the conservative tracer NaCl and the interfacial tracer SLES passed through the DNAPL blobs containing column #8b (S_n : 20%).

Consequently the ITT based estimation (Eq. 3-13) of the tar oil-water interfacial area is now at $93 \text{ cm}^2/\text{cm}^3$ (i.e. by a factor of 15 larger than the A_{NW} value of $6.3 \text{ cm}^2/\text{cm}^3$ estimated by the following classical geometric relationship (Grathwohl, 1998): each grain of the aquifer material is assumed to be a sphere (0.75 mm radius), the radius of the DNAPL blobs (r_b) is 1/2 of the radius of the aquifer material grains, $A_{NW} = 3\theta/r_b$ and was in a first approximation assumed to equal the effective DNAPL-water interfacial area).

To investigate the sensitivity of the estimation method suggested by Annabel et al. (1998) on the determination of the constant K_{IFT} finally used for the ITT based estimation of the DNAPL-water interfacial area, the following alternative methods were used. The constant K_{IFT} value was determined by using: (1) the arithmetic mean of the maximum peak concentration (C_{max}) and the minimum peak concentration (C_{min}), (2) the harmonic mean of C_{max} and C_{min} as well as (3) the geometric mean

of C_{max} and C_{min} of the SLES BTC, respectively (see Fig. 3-41).

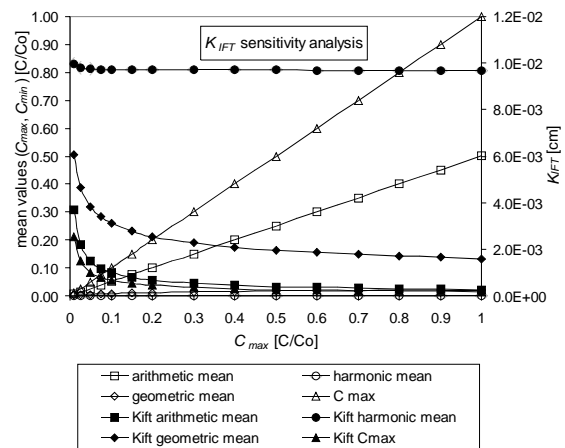


Figure 3-41. Sensitivity analysis of the constant K_{IFT} value depending on the different methods: C_{max} as suggested by Annable et al. (1998) compared to the arithmetic mean, the harmonic mean, and the geometric mean of C_{max} and C_{min} , respectively.

While the harmonic mean values are strongly dominated by C_{min} and are thus practically linear over the whole concentration range, the other mean values show effects due to the changing C_{max} and the non-linearity of the interfacial adsorption isotherm, i.e. the determined parameters for the constant interfacial adsorption coefficient vary up to one order of magnitude over the whole concentration range.

In the following the calculations for column #8b were repeated under the aforementioned varying conditions: (1) arithmetic mean ($C_{mean} = 0.07$, $K_{IFT} = 7.95E-04$ cm, the resulting A_{NW} is $62 \text{ cm}^2/\text{cm}^3$), (2) geometric mean ($C_{mean} = 0.009$, $K_{IFT} = 2.78E-03$ cm the resulting A_{NW} is $18 \text{ cm}^2/\text{cm}^3$), (3) harmonic mean ($C_{mean} = 0.001$, $K_{IFT} = 9.71E-03$ cm the resulting A_{NW} is $5 \text{ cm}^2/\text{cm}^3$). These considerations show, that the determined tar oil-water interfacial areas using these alternative methods (especially the harmonic mean) are much closer to the A_{NW} value given by the geometrical considerations ($6.3 \text{ cm}^2/\text{cm}^3$).

The determined SLES mass recovery (Fig. 3-42) is now closer to 100%, the remaining difference is within the overall measurement error of the detection method.

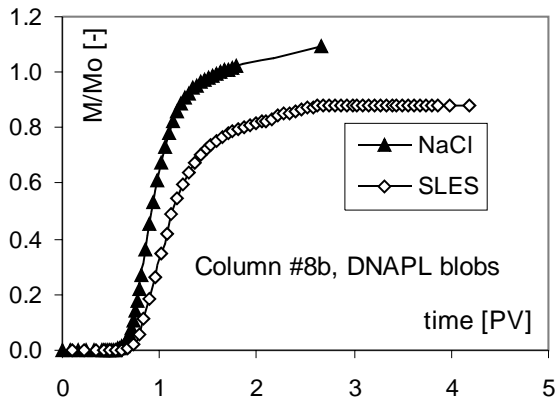


Figure 3-42. Mass recovery of the conservative tracer NaCl and the interfacial tracer SLES passed through the DNAPL blobs containing column #8b (S_n : 20%).

Column #9b (S_n : 20%, DNAPL coatings), was conducted using column setup C. The distribution geometry of the tar oil coatings within the aquifer matrix can be seen in Figure 3-43.

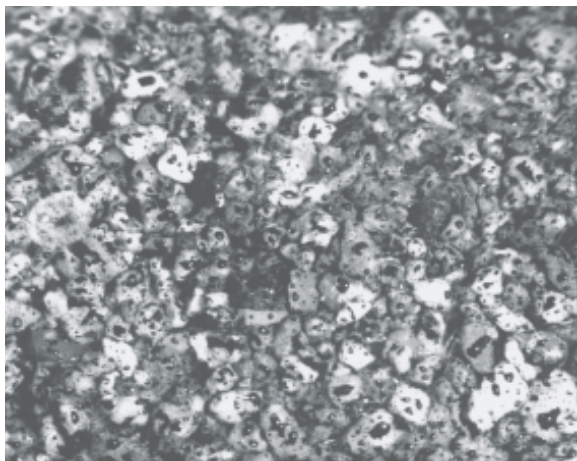


Figure 3-43. Macro photo section of column #9b showing the distribution of the tar oil coatings (black) onto the brighter aquifer matrix material (grainsize: 1-2 mm).

The measured BTC of the interfacial tracer (SLES) shows very significant retardation compared to the conservative tracer NaCl (see Fig. 3-44). The separation of the SLES BTC is already clearly visible in the rising shoulders of the two peaks. However, both peaks are still not base-line separated and the SLES BTC is now

strongly asymmetric, the retardation factor of the interfacial tracer is 2.69. The determined parameters for the maximum peak concentration and the constant interfacial adsorption coefficient after Annable et al. (1998) are: $C_{max} = 0.048$, $K_{IFT} = 1.02E-03$ cm.

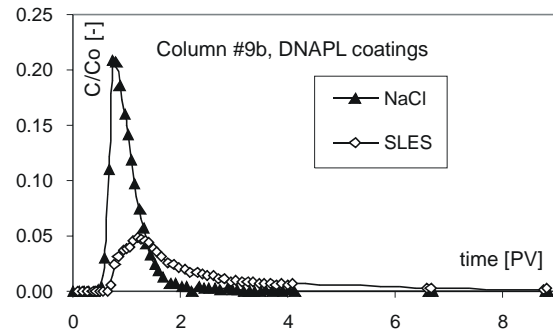


Figure 3-44. BTCs of the conservative tracer NaCl and the interfacial tracer SLES passed through the DNAPL coatings containing column #9b (S_n : 20%).

The ITT based estimation (Eq. 3-13) of the tar oil-water interfacial area is at $531 \text{ cm}^2/\text{cm}^3$ (i.e. by a factor of 22 larger than the A_{NW} value of $23.8 \text{ cm}^2/\text{cm}^3$ estimated by the following geometric relationship: each grain of the aquifer material is assumed to be a sphere of 0.75 mm radius which is completely covered by a thin DNAPL coating, the radius of the DNAPL coatings (r_c) thus equals approximately the radius of the aquifer material grains, $A_{NW} = 3(1-n)/r_c$ and was in a first approximation assumed to equal the effective DNAPL-water interfacial area). It must be admitted that the starting point of this assumption, the ideal DNAPL coating around each aquifer material grain was actually not fulfilled (see Fig. 3-43), but each aquifer material grain was covered by many tiny DNAPL droplets. The visual analysis and comparison of both macro photo sections (Fig. 3-39 and Fig. 3-43) lead to the assumption, that the average droplet diameter in column #9b is approximately 1/10 of the blob diameter of column #8b. But even under these new boundary conditions, the ITT based estimation of the tar oil-water interfacial area ($531 \text{ cm}^2/\text{cm}^3$) is still by a factor of 8 larger than the A_{NW} value of $63 \text{ cm}^2/\text{cm}^3$ estimated by the corrected geometrical A_{NW} estimation.

In the following the calculations for column #9b were repeated using the before described alternative methods for the constant K_{IFT} determination: (1) arithmetic mean ($C_{mean} = 0.02$, $K_{IFT} = 1.51E-03$ cm, the resulting A_{NW} is $358 \text{ cm}^2/\text{cm}^3$), (2) geometric mean ($C_{mean} = 0.005$, $K_{IFT} = 3.84E-03$ cm the resulting A_{NW} is $141 \text{ cm}^2/\text{cm}^3$), (3) harmonic mean ($C_{mean} = 0.001$, $K_{IFT} = 9.71E-03$ cm the resulting A_{NW} is $55 \text{ cm}^2/\text{cm}^3$). These considerations show, that the estimated tar oil-water interfacial areas using these alternative methods are again much closer to the A_{NW} value given by the geometrical considerations ($63 \text{ cm}^2/\text{cm}^3$).

The determined SLES mass recovery (Fig. 3-45) is only around 80%, the remaining difference is likely due to measurement errors associated with the truncation of the BTC tailing.

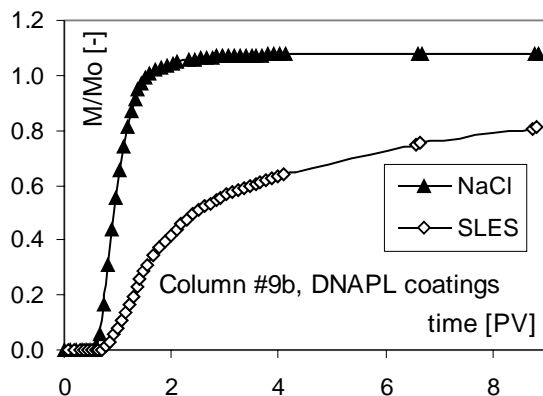


Figure 3-45. Mass recovery of the conservative tracer NaCl and the interfacial tracer SLES passed through the DNAPL coatings containing column #9b (S_n : 20%).

The last column experiment (column #9d) was a blank column, which contained no residual tar oil, but was filled with aquifer material from the Testfeld-Süd (TFS), the anticipated site for field scale application of the PITT, to evaluate any influence of the site specific aquifer material composition on PITT results.

Column #9d (S_n : 0%) was conducted at a linear velocity of 2.1 m/day using column set-up C. The measured BTCs of the PT-suite (4M2P, 1-HEX) show no significant retardation compared to the conservative tracer IPA, which means they are almost overlaying each other

(see Fig. 3-46). Only the late peak tailing of the 1-HEX BTC decreases somewhat faster than the BTCs of IPA and 4M2P (only visible in the semi-logarithmic plot Fig. 3-47), which is likely due to measurement errors close to the detection limit. The retardation factor of all partitioning tracers practically equals 1, what is anticipated for this blank column experiment (see Table 3-3). Consequently the PTT based average tar oil saturation estimate meets the true S_n value (0%).

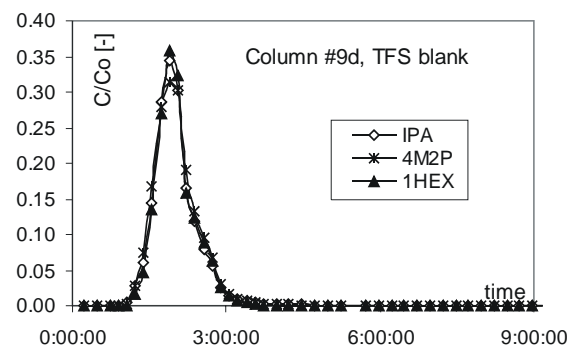


Figure 3-46. BTCs of the PT-suite passed through TFS blank column #9d (S_n : 0%).

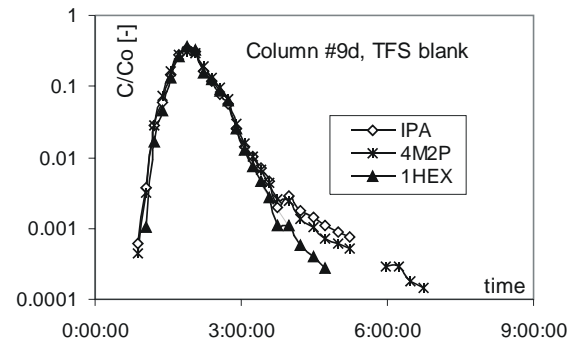


Figure 3-47. Semi-logarithmic BTC-plot of the PT-suite passed through TFS blank column #9d (S_n : 0%).

The rising shoulders of the determined 4M2P and 1-HEX mass recovery BTCs are steep and practically identical to that of IPA (see Fig. 3-48). The remaining positive error in the final plateau height of the all three mass recovery BTCs, i.e. the final deviation from the mass balance is very small and within the overall measurement error of the detection method.

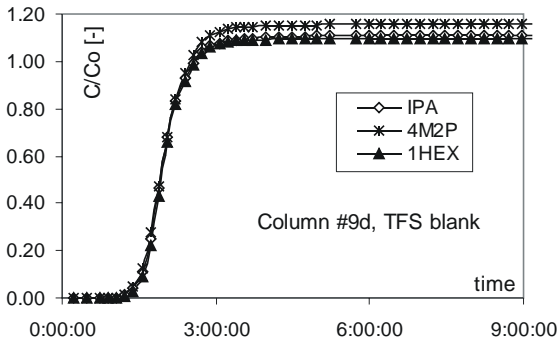


Figure 3-48. Mass recovery of the PT-suite passed through TFS blank column #9d (S_n : 0%).

The measured BTC of the interfacial tracer (SLES) shows a significant shift of the main peak compared to the conservative tracer NaCl (see Fig. 3-49). The separation of the SLES BTC already starts in the rising shoulders of the two peaks. However, both peaks approach more or less the same peak maximum, but astonishingly the tailing of the conservative tracer is even much more extended and more asymmetric than that of the interfacial tracer. Thus, the actually resulting retardation factor of the interfacial tracer is 0.96. The determined parameters for the maximum peak concentration and the constant interfacial adsorption coefficient are: $C_{max} = 0.24$, $K_{IFT} = 4.03E-04$ cm. As the determined retardation factor of SLES is smaller than one, an ITT based estimation (Eq. 3-13) of A_{NW} is impossible.

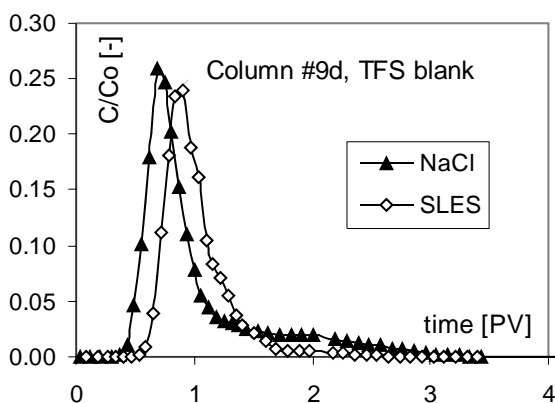


Figure 3-49. BTCs of the conservative tracer NaCl and the interfacial tracer SLES passed through the TFS blank column #9d (S_n : 0%).

Ignoring the extraordinary tailing of the NaCl BTC or using a truly conservative tracer, the ITT based estimation (Eq. 3-13) of the tar oil-water interfacial area would definitely lead to a

false positive value, which means that the evaluation has to be made according to Eq. 3-11 which takes the adsorption onto the aquifer material into account.

Knowing that the column #9d contains no DNAPL at all, but the SLES is shifted on the time axis (the SLES peak maximum is not significantly smaller than NaCl maximum, the opposite of which was observed in all other column experiments containing tar oil distribution geometries which retarded the IFT, see Fig. 3-40 and Fig. 3-44) it must be concluded, that fast if not equilibrated but completely reversible surface-adsorption processes onto the aquifer material are responsible for this effect. This behaviour would be typical for ion exchange effects, which are likely to happen in this natural aquifer material.

The rising shoulders of the determined SLES mass recovery BTC shows the identical slope but is clearly retarded to that of that IPA (see Fig. 3-50). While the remaining positive error in the final plateau height of the SLES mass recovery BTC is small and within the overall measurement error of the detection method, the positive error of the NaCl mass recovery starts to exceed these limits.

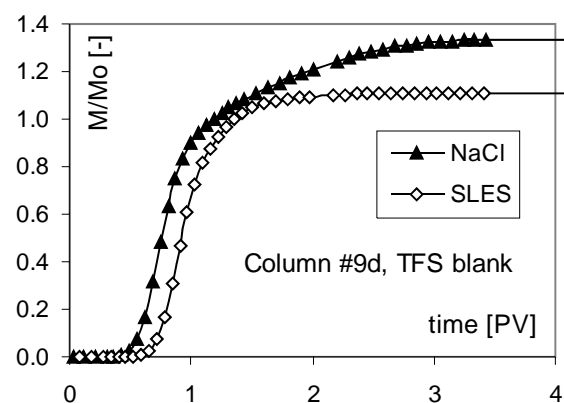


Figure 3-50. Mass recovery of the conservative tracer NaCl and the interfacial tracer SLES passed through the TFS blank column #9d (S_n : 0%).

To investigate the cause for this unexpected, extensive tailing of the NaCl BTC and the resulting positive error of the mass balance, all samples of column #9d were subsequently transferred to offline measurements for discrete

ion species (target analytes: Na^+ and Cl^-) via ion chromatography (IC).

The measured BTCs of the conservative tracers Cl^- (via IC measurements) and IPA (see Fig. 3-51) are now overlaying each other even in the extended parts of the tailing. The measured BTC of Na^+ (via IC measurements) is strongly retarded behind all other BTCs, its peak maximum is much smaller than all other peak maxima but the peak tailing is quite similar to the NaCl BTC (determined via total electrical conductivity measurements).

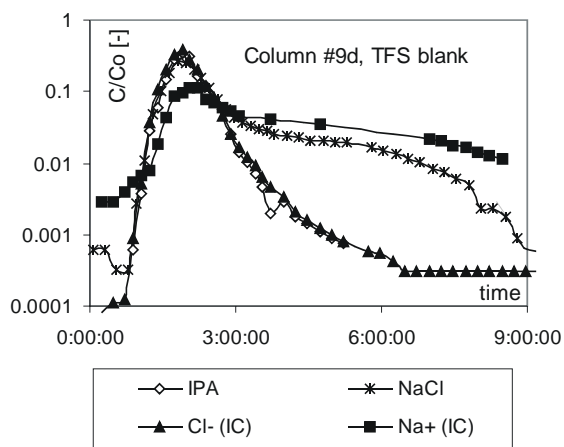


Figure 3-51. BTCs of the two conservative tracers IPA and NaCl passed through TFS blank column #9d (Sn: 0%) using two different methods for NaCl determination: 1. NaCl measured by electrical conductivity (as applied in all previous experiments) 2. ion species (Na^+ , Cl^-) measured separately by IC.

The rising shoulder of the determined Cl^- mass recovery BTC shows the same shape (steep rise and early plateau) like that of IPA (see Fig. 3-52), but reaches a higher value in the final plateau height (which is likely due to amplified measurement errors resulting from the required dilution of the samples around to the peak maximum for the IC measurement). The rising shoulder of the determined Na^+ mass recovery BTC is clearly retarded behind all other mass recovery BTCs but shows a comparable shape (gentle rise and late plateau) like that of NaCl.

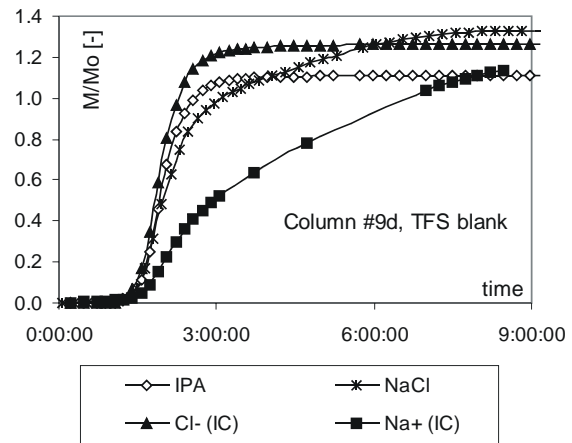


Figure 3-52. Mass recovery of the two conservative tracers IPA and NaCl passed through TFS blank column #9d (Sn: 0%) using two different methods for NaCl determination: 1. NaCl measured by electrical conductivity (as applied in all previous experiments) 2. ion species (Na^+ , Cl^-) measured separately by IC.

Due to the obligatory neutrality of the charge balance the separation of Na^+ from Cl^- must have been compensated by the release of other positively charged ions from the aquifer material (e.g. Ca^{2+}). This also explains why the NaCl (measured via total electrical conductivity) exhibits the most extensive positive error in the final plateau of the mass recovery, as all other additionally released ions are also detected by this method.

Lessons learned during the column experiments: (1) besides IPA only Cl^- itself behaves as an ideal conservative tracer and shall therefore be measured as discrete ion, (2) the tailing in the late part of all previously measured NaCl BTCs (via total electrical conductivity) is due to the masked retardation of Na^+ , (3) this effect is now amplified due to the presence of silt and clay minerals onto the natural aquifer material of the Testfeld-Süd which was used in column #9d.

3.4.3 Large scale Tank experiments

Additional pulse type PITTs were conducted in a large scale tank ($8\text{ m} \times 3\text{ m} \times 1\text{ m}$) at the VEGAS facilities. The following six individual, forced gradient dipole flow field PITTs at five spatially different located well pair point samplers (A'-A – E'-E) were anticipated for the direct assessment of the homogeneous tar oil blob zone ($0.5\text{ m} \times 1\text{ m} \times 1\text{ m}$, $S_n \leq 4.86\%$) and thus were located just at the upgradient and downgradient edges of the above mentioned DNAPL blob zone. The injection and extraction point samplers were only partially penetrating, separated by 0.6 m and aligned in the direction of the tank-gradient base flow field (5 m/day). The extraction/ injection ratio of the individual well pairs was varied between 0.96 up to 3.77 , to enlarge the catchments area and thereby optimise the mass recovery. Three out of the six conducted experiments failed (A'-A, B'-B 1st and D'-D) i.e. no tracers arrived at the corresponding extraction point samplers. This gave the first evidence, that (1) the synthetic aquifer of the tank experiment is not perfectly homogeneous and/or (2) the direct push installation of the well pair point samplers is not as accurate as anticipated. The three successfully conducted experiments (B'-B 2nd, C'-C and E'-E) are listed in the following.

The second experiment at well pair point sampler B'-B ($S_n \leq 4.86\%$) was conducted at an extraction/ injection ratio of 3.77 . The measured BTC of the partitioning tracer (4M2P) shows no significant retardation compared to the conservative tracers IPA and NaCl, which means all three are practically overlaying each other (see Fig. 3-53 and Fig. 3-54). Even the late peak tailing of 4M2P shows no retardation at all, thus resulting in a retardation factor of 1. Consequently the PTT based average tar oil saturation estimate (Eq. 3-7) gives a false negative S_n value of 0% . The measured BTC of SLES, the interfacial tracer, also shows (see Fig. 3-53 and Fig. 3-54) no retardation compared to the conservative tracer NaCl ($R_{IFT} = 1$). Consequently the ITT based estimation (Eq. 3-

13) of the tar oil-water interfacial area gives a false negative A_{NW} value of $0\text{ cm}^2/\text{cm}^3$, too.

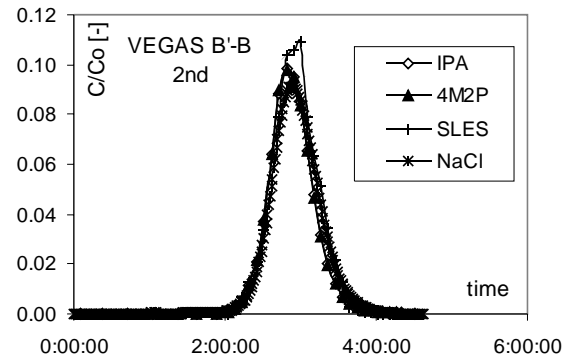


Figure 3-53. BTCs of the conservative tracer NaCl and the PIT-suite passed through the DNAPL blob zone of the large scale tank experiment (injection at well #B', extraction at well #B; $S_n \leq 4.86\%$).

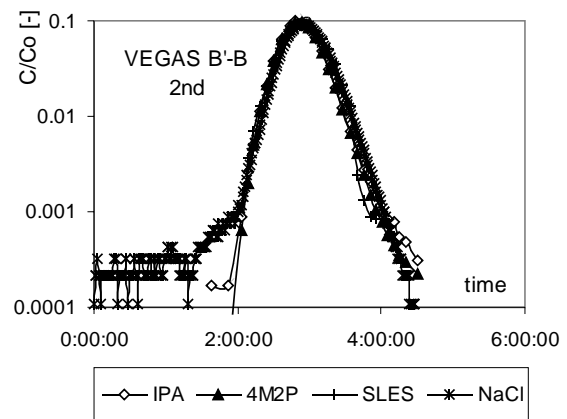


Figure 3-54. Semi-logarithmic BTC-plot of the conservative tracer NaCl and the PIT-suite passed through the DNAPL blob zone of the large scale tank experiment (injection at well #B', extraction at well #B; $S_n \leq 4.86\%$).

The rising shoulder of the determined 4M2P mass recovery BTC is steep and practically identical to that of IPA and NaCl (see Fig. 3-55). The slight positive relative deviation in the final plateau height of SLES mass recovery BTC compared to the three other BTCs is very small and within the overall measurement error of the detection method. However, the absolute deviation of all four BTCs from the theoretically anticipated mass recovery (a forced gradient dipole flow field at a extraction/ injection ratio of 3.77 , aligned in the direction of the tank-gradient base flow field has theoretical a lower peak maximum due to dilution effects but a mass recovery of 100% as the drawdown zone

of the extraction well is larger than that of the injection well) is quite large and gives further evidence of the heterogeneity of the synthetic aquifer. In this case the inaccuracy of the direct push installation of the well pair point samplers becomes negligible as the range of influence created by overpumping of the extraction well can be assumed to be much larger than the average positioning error of the point samplers.

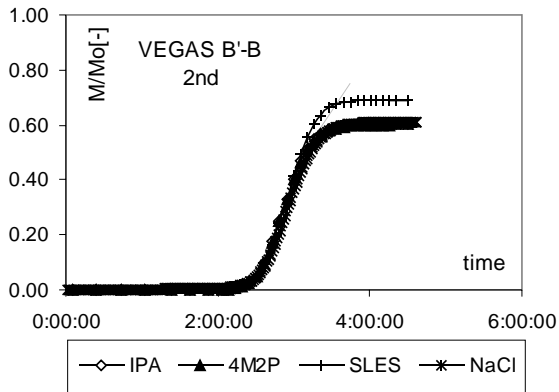


Figure 3-55. Mass recovery of the conservative tracer NaCl and the PIT-suite passed through the DNAPL blob zone of the large scale tank experiment (injection at well #B', extraction at well #B; $S_n \leq 4.86\%$).

The experiment at well pair point sampler C'-C ($S_n \leq 4.86\%$) was conducted at a extraction/injection ratio of 1.36. Once more the measured BTC of the partitioning tracer (4M2P) shows no significant retardation compared to the conservative tracers IPA and NaCl, which means all three are practically overlaying each other (see Fig. 3-56 and Fig. 3-57). Even the late peak tailing of the 4M2P shows no retardation at all, thus resulting in a retardation factor of 1. Consequently the PTT based average tar oil saturation estimate (Eq. 3-7) gives again a false negative S_n value of 0%. The measured BTC of SLES, the interfacial tracer, shows no retardation compared to the conservative tracer NaCl (see Fig. 3-56 and Fig. 3-57). In fact it is even slightly faster transported than the conservative tracer ($R_{IFT} = 0.97$). Consequently an ITT based estimation (Eq. 3-13) of the tar oil-water interfacial area is impossible, it can only

be stated that it must be negligibly small (i.e. it is again a false negative value).

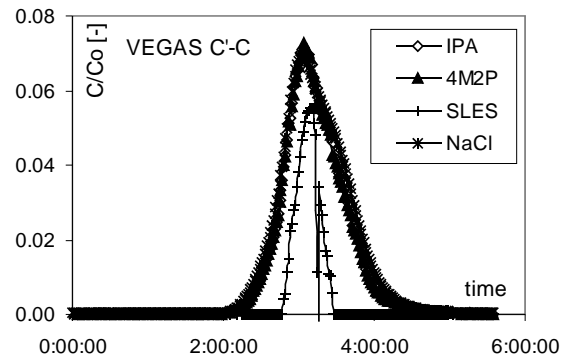


Figure 3-56. BTCs of the conservative tracer NaCl and the PIT-suite passed through the DNAPL blob zone of the large scale tank experiment (injection at well #C', extraction at well #C; $S_n \leq 4.86\%$).

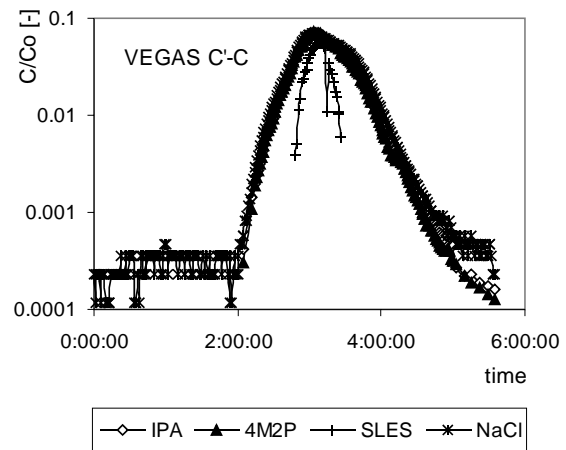


Figure 3-57. Semi-logarithmic BTC-plot of the conservative tracer NaCl and the PIT-suite passed through the DNAPL blob zone of the large scale tank experiment (injection at well #C', extraction at well #C; $S_n \leq 4.86\%$).

The rising shoulder of the determined 4M2P mass recovery BTC is steep and practically identical to that of IPA and NaCl (see Fig. 3-58). The slight positive relative deviation in the final plateau height of NaCl mass recovery BTC compared to the two other BTCs of IPA and 4M2P is very small and within the overall measurement error of the detection method. However, the relative deviation of SLES from the three other BTCs is quite severe and can not be explained by the overall measurement error of the detection method. The applied flow field

shall theoretically achieve a higher peak maximum but a lower mass recovery compared to the previous experiment (B'-B 2nd), but actually the peak maximum is even smaller and only the mass recovery behaves as expected. So obviously the extraction point sampler must be located in the outer fringe of the injected tracer cloud. The combination of this special spatial location of the point sampler with a smaller aqueous diffusion coefficient of SLES (due to its large molecular size) which finally leads to a smaller transversal dispersion might be an explanation for the extraordinary shape of the SLES BTC which is totally enclosed by all other BTCs.

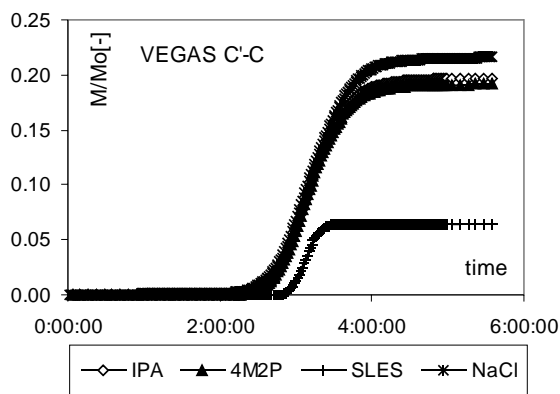


Figure 3-58. Mass recovery of the conservative tracer NaCl and the PIT-suite passed through the DNAPL blob zone of the large scale tank experiment (injection at well #C', extraction at well #C; $S_n \leq 4.86\%$).

The experiment at well pair point sampler E'-E ($S_n \leq 4.86\%$) was conducted at a extraction/injection ratio of 1.61. The measured BTCs of the PIT-suite show a very slight retardation compared to the conservative tracers NaCl and IPA which are almost overlaying each other (see Fig. 3-59). The late peak tailing of 2,4DM3P is visible in the semi-logarithmic plot (Fig. 3-60). The partitioning tracers are retarded according to the order of their partitioning coefficients. However, the retardation factor of all partitioning tracers is much smaller than expected (see Table 3-3). Consequently the PTT based average tar oil saturation estimate (Eq. 3-

7) is only at 0.48% (i.e. 10% of the true S_n value).

The measured BTC of SLES, the interfacial tracer, also shows a very slight retardation compared to the conservative tracer NaCl (see Fig. 3-56 and Fig. 3-57). The resulting retardation factor of the interfacial tracer is 1.05. The determined parameters for the maximum peak concentration and the constant interfacial adsorption coefficient after Annable et al. (1998) are: $C_{max} = 0.054$, $K_{IFT} = 9.53E-04$ cm.

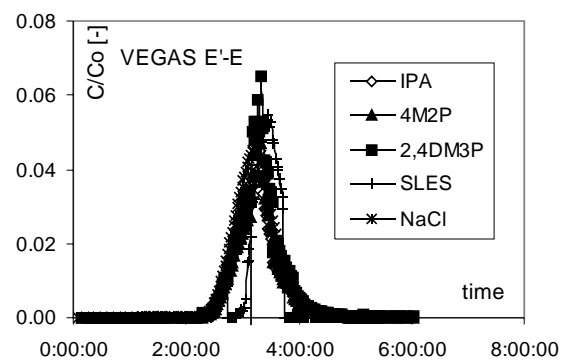


Figure 3-59. BTCs of the conservative tracer NaCl and the PIT-suite passed through the DNAPL blob zone of the large scale tank experiment (injection at well #E', extraction at well #E; $S_n \leq 4.86\%$).

Consequently the ITT based estimation (Eq. 3-13) of the tar oil-water interfacial area is now at $19 \text{ cm}^2/\text{cm}^3$ (i.e. by a factor of 13 larger than the A_{NW} value of $1.5 \text{ cm}^2/\text{cm}^3$ estimated by the following classical geometric relationship (Grathwohl, 1998): each grain of the aquifer material is assumed to be a sphere (0.75 mm radius), the radius of the DNAPL blobs (r_b) is $1/2$ of the radius of the aquifer material grains, $A_{NW} = 3\theta/r_b$ and was in a first approximation assumed to equal the effective DNAPL-water interfacial area).

Using the alternative method which gave the best fit in the column experiments (harmonic mean of C_{max} and C_{min} , and its parameters $C_{mean} = 0.001$, $K_{IFT} = 9.74E-03$ cm), the ITT based estimation (Eq. 3-13) of the tar oil-water interfacial area is at $2 \text{ cm}^2/\text{cm}^3$ (i.e. just by a factor of 1.3 larger than the A_{NW} value of

1.5 cm²/cm³ estimated by the aforementioned geometric relationship.

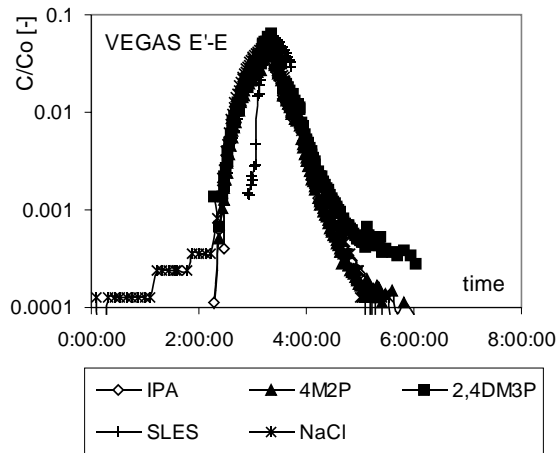


Figure 3-60. Semi-logarithmic BTC-plot of the conservative tracer NaCl and the PIT-suite passed through the DNAPL blob zone of the large scale tank experiment (injection at well #E', extraction at well #E; $S_n \leq 4.86\%$).

The rising shoulder of the determined mass recovery BTCs are steep and practically identical to that of IPA and NaCl (see Fig. 3-61). The positive relative deviation in the final plateau height of NaCl and 2,4DM3P mass recovery BTCs (19%) compared to the three other BTCs (14%) of IPA, 4M2P and SLES is due to the more extended tailing of both substances.

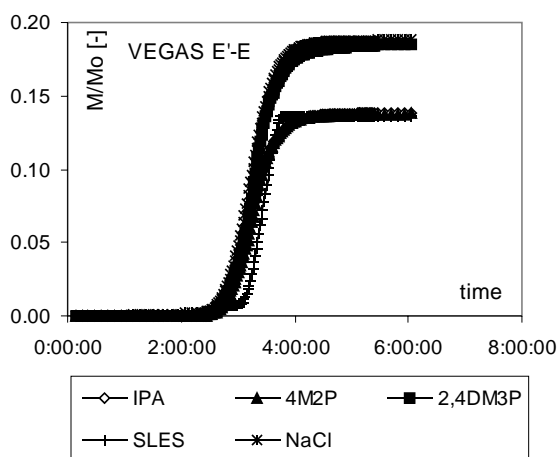


Figure 3-61. Mass recovery of the conservative tracer NaCl and the PIT-suite passed through the DNAPL blob zone of the large scale tank experiment (injection at well #E', extraction at well #E; $S_n \leq 4.86\%$).

In order to assess both, the homogeneous DNAPL blob zone ($S_n \leq 4.86\%$) located in the

upper part of the large scale tank close to the inflow chamber, as well as the DNAPL pool ($S_n = 100\%$) at the bottom of the large scale tank the following experiment, an integral, natural gradient flow field PITT was conducted. This test employed one fully filtered, stainless steel injection well (I') located upgradient of the source zones (DNAPL blob zone and DNAPL pool) and a grouped multi-level sampler, made of six point samplers (IA-IF) which were arranged perpendicular to the natural gradient flow direction at the downgradient end of the DNAPL pool. The resulting flow distance from the injection well to the grouped multi-level sampler was 2.65 m.

To get an first overview of the anticipated relative conservative tracer peaks at the above given settings, the BTCs at the individual multi-level samplers (IA-IF), were calculated according to the analytical solution for a slug injection via line source into a 2D flow field (De Josselin De Jong, 1958), to evaluate the anticipated peak maxima (see Fig. 3-62). The parameter settings were chosen close to the integral tank experiment planned in the course of this study, i.e. $v_a = 5$ m/day, length of the line source = 180 cm, injected tracer mass = 10,000 mg (2 litres at 5,000 mg/l), $\alpha_L = 0.2$ cm, $\alpha_T = 0.08$ cm (this exaggerated value was chosen to account for the actual spreading of the tracer cloud during the injection) and the three different positions of the six point samplers (transport distance [cm]/distance perpendicular to plume centreline [cm]): IC, ID (265/3.5); IB, IE (265/10.5) and IA, IF (265/17.5).

As expected, the concentration of the respective peak maximum decreases with increasing distance from the plume centreline. While the predicted peak concentrations at both inner point samplers are within the bandwidth of previous experiments, the concentrations at the outermost point samplers (IA, IF) might fall beyond the detection limits. Therefore it was decided to conduct a preliminary salt tracer test (pre-test) containing solely NaCl to quantify the transport

of a conservative tracer at the two outermost point samplers (IA, IF) located in the close vicinity of to the DNAPL pool (at the bottom of the aquifer) and at one of the innermost point sampler (ID) located in the DNAPL free zone.

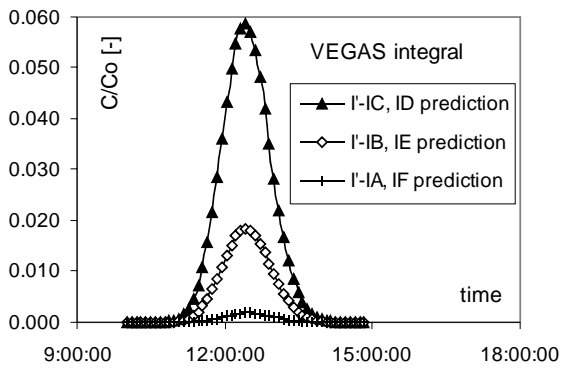


Figure 3-62. Analytical modelling of a conservative tracer using integral injection into a natural gradient flow field at well I' and extraction at the multi-level point samplers IA-IF. The BTCs at the respective point samplers (IA-IF) were calculated according to De Josselin De Jong (1958) using the parameter settings given in the text.

The preliminary salt tracer test (pre-test) containing solely NaCl was conducted under the following conditions: integral injection at well I', extraction and online EC-logging at point samplers IA, ID, IF. During the run-time of this pre-test only online EC-readings were recorded. Surprisingly, the measured BTCs of the conservative tracer NaCl show the complete opposite of the expected behaviour: the BTCs of the outermost point samplers (IA, IF) do not only arrive earlier but they also exhibit the higher peak maxima (see Fig. 3-63).

Based on these data it was concluded, that the initial spreading of the tracer cloud was much more pronounced than expected (causing concentrations higher than anticipated) and that point sampler ID is obviously badly connected to the surrounding aquifer (causing concentrations lower than anticipated and at a later arrival time).

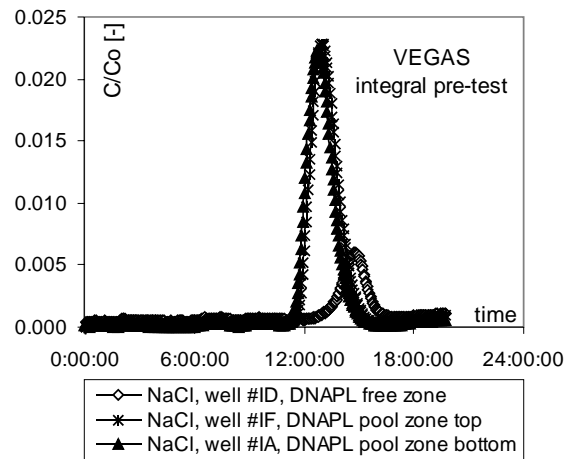


Figure 3-63. BTCs of the conservative tracer NaCl passed through the large scale tank set-up during the preliminary salt tracer test (pre-test) containing only NaCl (integral injection at well I', extraction at point samplers #ID, #IF and #IA).

As point sampler ID is located in the DNAPL free zone and was thus not in the major focus of interest and the concentrations at the outermost point samplers were within the detection bandwidth, it was decided to conduct the final integral PITT at exactly identical settings but injecting the whole PIT-suite (including NaCl). During the run-time of this PITT both, online EC-readings (IA, ID, IF) and water samples (IA-IF) were taken. Before the collected water samples were transferred to analysis, the online EC-recordings were evaluated. Astonishingly, the measured BTCs of the conservative tracer NaCl at the outermost point samplers (IA, IF) do now not show any measurable peaks, while the BTC at the innermost point sampler (ID) stays unaffected (see Fig. 3-64). This means, that the measurement result changed dramatically and is now conform to the behaviour predicted by the above given analytical solution.

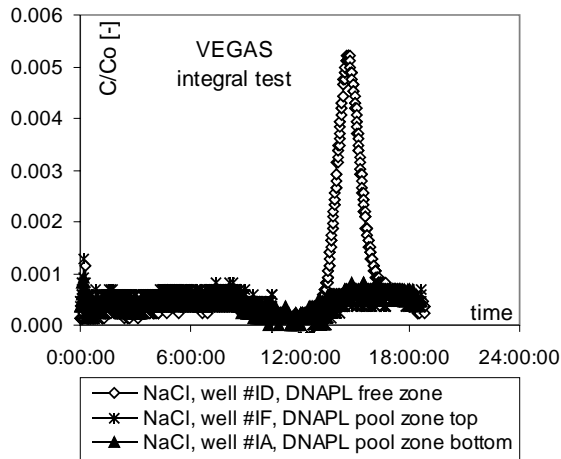


Figure 3-64. BTCs of the conservative tracer NaCl passed through the large scale tank set-up during the final PITT containing the whole PIT-suite including NaCl (integral injection at well #I', extraction at point samplers #ID, #IF and #IA).

As neither the flow field nor the injection nor extraction conditions were changed between the preliminary integral salt tracer test (pre-test) and the final integral PITT (integral test), the significant changes (see Fig. 3-65) must be due to a difference in the tracer solutions. Both tracer solutions contained the identical NaCl concentrations but due to the presence of the partitioning tracers (alcohols) in the PITT solution its density is significantly lower (1.001 g/l) than that of the pure salt tracer solution (1.005 g/l). Based on both data sets it finally must be concluded, that density effects (parts of the uniformly injected tracer cloud were sinking down to form a tracer cloud which then looks like an upside down mushroom) are responsible for (1) the extended spreading of the salt tracer solution perpendicular to the flow direction (i.e. the density driven tracer cloud could approach the outermost point samplers at the bottom of the aquifer) as well as for (2) the extended spreading of the salt tracer solution in flow direction (i.e. the density driven tracer cloud arrives earlier at the point samplers at the bottom of the aquifer). Both effects were restricted to the very bottom of the aquifer, as point sampler ID which is located in the DNAPL free zone between the bottom of the aquifer and the blob zone is not influenced at all,

i.e. the BTCs of both experiments are practically overlaying each other (see Fig. 3-65).

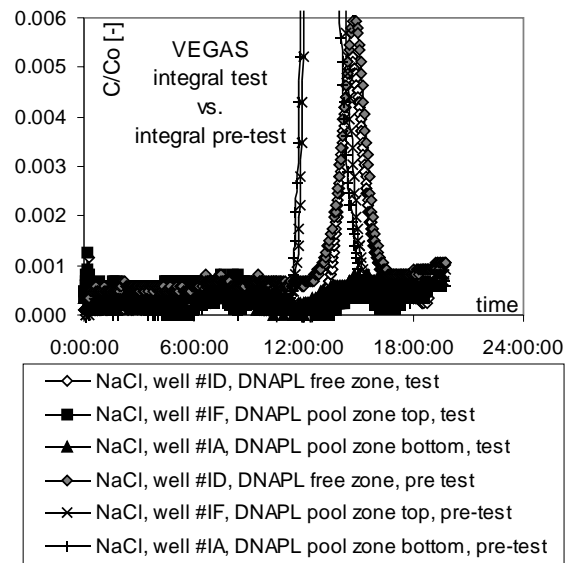


Figure 3-65. Comparison of the NaCl BTCs of the preliminary salt tracer test (pre-test) containing only NaCl versus the real PITT containing the whole PIT-suite including NaCl (integral injection at well #I', extraction at point samplers #ID, #IF and #IA; density PIT-solution: 1.001 g/l, density NaCl tracer solution: 1.005 g/l).

Lessons learned in the large scale tank experiments are:

- (1) density differences as small as 5 permille can already cause a severe bias of tracer test results
- (2) alcohols can be used to compensate the density effects of salt tracer solutions.

During the final integral natural gradient flow field PITT two out of the six experiments failed (I'-IA, I'-IF) i.e. no tracers arrived at the corresponding extraction point samplers. Due to very time consuming and tedious sample preparations two further experiments (I'-IC, I'-IE) were not selected for subsequent partitioning tracer measurement. The two remaining, successfully conducted experiments (I'-IB, I'-ID) were fully analysed and are listed in the following.

The BTCs of the PIT-suite measured at point sampler IB (the tracers were passing through a 2.65 m long domain of the large scale tank experiment including the DNAPL blob zone, overall $S_n \leq 0.9\%$) show no significant retardation compared to the conservative tracer

IPA, which means all five BTCs are practically overlaying each other (see Fig. 3-66). Only in the very late peak tailing of NaCl and 2,4DM3P some slight retardation is observed (see Fig. 3-67), but the resulting retardation factor determined by the method of moments is still 1.00. Consequently the PTT based average tar oil saturation estimate (Eq. 3-7) of the tracer swept volume gives a false negative S_n value of 0%.

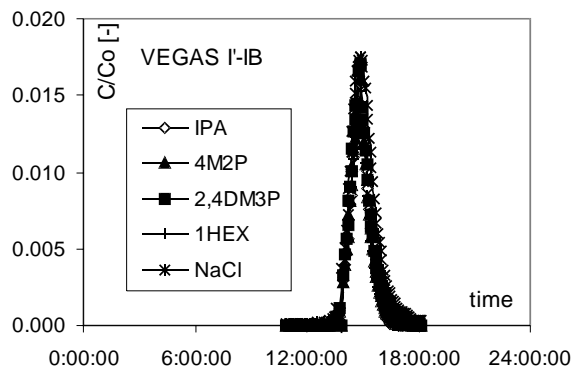


Figure 3-66. BTCs of the conservative tracer NaCl and the PIT-suite passed through a 2.65 m long domain of the large scale tank experiment including the DNAPL blob zone (integral injection at well #I', extraction at point sampler #IB, overall $S_n \leq 0.9\%$).

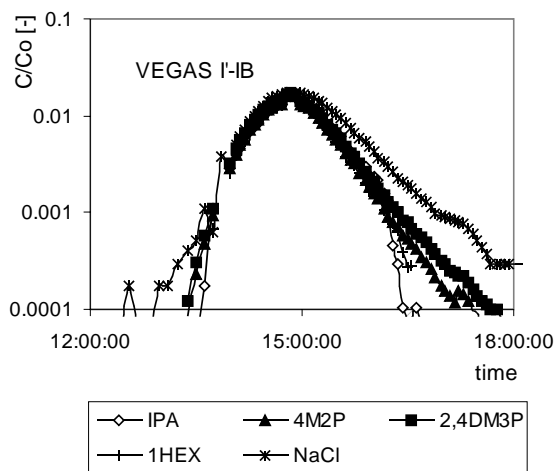


Figure 3-67. Semi-logarithmic BTC plot of the conservative tracer NaCl and the PIT-suite passed through a 2.65 m long domain of the large scale tank experiment including the DNAPL blob zone (integral injection at well #I', extraction at point sampler #IB, overall $S_n \leq 0.9\%$).

The rising shoulder of the determined mass recovery BTCs are quite steep and practically identical to that of IPA (see Fig. 3-68). The positive relative deviation in the final plateau

height of NaCl mass recovery BTC compared to the four other BTCs is due to its more extended tailing. However, the absolute mass recovery is just around 1%, but such small numbers were anticipated for a natural gradient flow field PITT using integral injection over the whole aquifer thickness and BTC monitoring by point samplers.

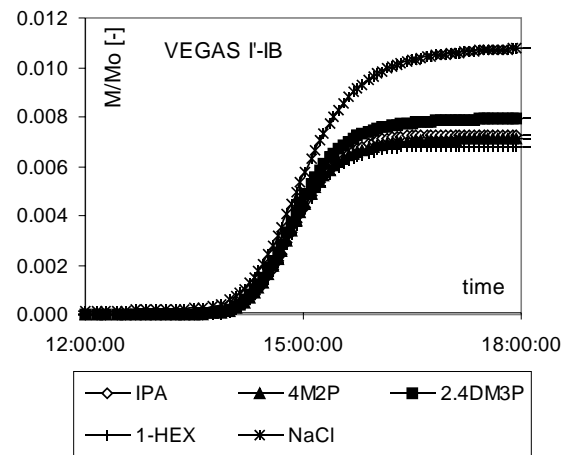


Figure 3-68. Mass recovery of the conservative tracer NaCl and the PIT-suite passed through a 2.65 m long domain of the large scale tank experiment including the DNAPL blob zone (integral injection at well #I', extraction at point sampler #IB, overall $S_n \leq 0.9\%$).

The BTCs of the PIT-suite measured at point sampler ID (the tracers were passing through a 2.65 m long DNAPL free domain of the large scale tank experiment, overall $S_n = 0\%$) show no significant retardation compared to the conservative tracer IPA, which means all five BTCs are almost overlaying each other (see Fig. 3-69). Just the very late peak tailing of NaCl 4M2P and 2,4DM3P show optically some slight retardation (see Fig. 3-70), but this time even the resulting retardation factors determined by the method of moments are larger than 1.00 (see Table 3-3). Consequently the PTT based average tar oil saturation estimate (Eq. 3-7) of the tracer swept volume gives a false positive S_n value of %.

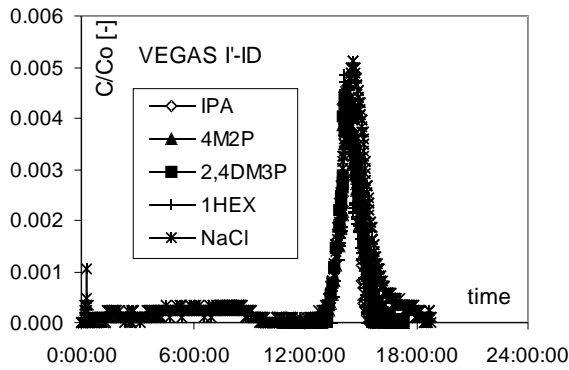


Figure 3-69. BTCs of the conservative tracer NaCl and the PIT-suite passed through a 2.65 m long DNAPL free domain of the large scale tank experiment (integral injection at well #I', extraction at point sampler #ID, overall $S_n = 0\%$).

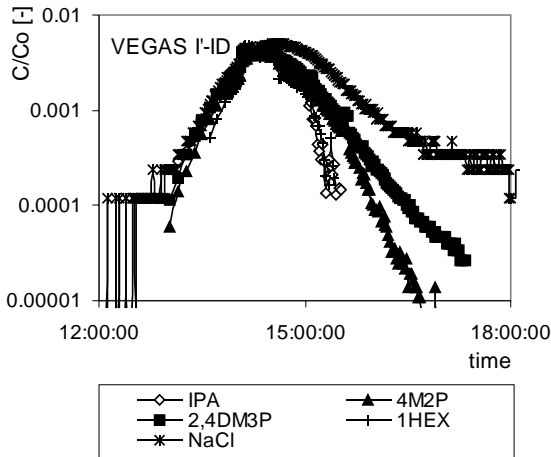


Figure 3-70. Semi-logarithmic BTC plot BTCs of the conservative tracer NaCl and the PIT-suite passed through a 2.65 m long DNAPL free domain of the large scale tank experiment (integral injection at well #I', extraction at point sampler #ID, overall $S_n = 0\%$).

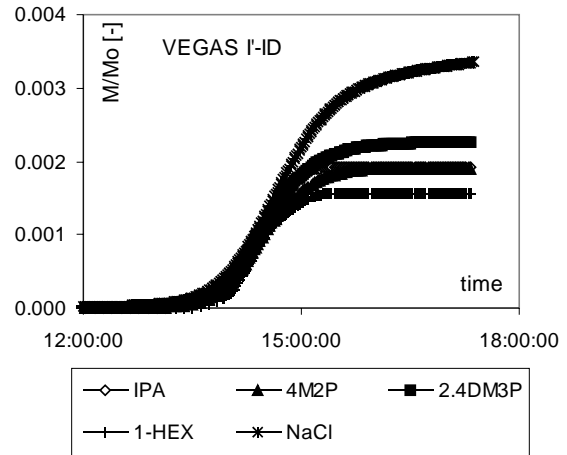


Figure 3-71. Mass recovery BTCs of the conservative tracer NaCl and the PIT-suite passed through a 2.65 m long DNAPL free domain of the large scale tank experiment (integral injection at well #I', extraction at point sampler #ID, overall $S_n = 0\%$).

3.5 Summarized Results of the PITT Experiments

The results of the PITTs were in general agreement with the current understanding of partitioning and interfacial tracer behavior.

Suitability of the PITT was proven for the complex multi-component mixtures (coal tar/tar oil) which can be found at former coal gasification plants.

The combination of interfacial and partitioning tracers during the PITT studies not only determined the DNAPL saturation, it also clearly distinguished between major different DNAPL distribution geometries (tar oil coatings vs. blob zone), which are important parameters concerning 1) the prediction of the long-time behaviour of the source zone and 2) the feasibility of in-situ remediation techniques.

Table 3-3. Summarized results of the batch, column and large scale tank experiments

Experiment ↓ / Tracer →	NaCl	IPA	4M2P	1HEX	2,4DM3P	SLES
Batch Experiments						
$K_{NW}[-]$	0	0.8	3.2	9.6	16	-
$K_{IFT}[cm]$	-	-	-	-	-	Fig. 3-12
Column Experiments						
<i>Column #8b, S_n: 20%, DNAPL blobs, v_a: 6.1 m/day</i>						
$R_d [-]$ expected	1	1.2	1.8	3.4	5.0	n.d.
$R_d [-]$ measured	1.11	1.00	1.30	1.79	1.94	1.09
S_n [%] calculated	0	0	8.6	7.6	5.5	-
$A_{NW} [cm^2/cm^3]calc.$	-	-	-	-	-	93 (5*)
<i>Column #8c, S_n: 20%, DNAPL blobs, v_a: 3.6 m/day</i>						
$R_d [-]$ expected	1	1.2	1.8	3.4	5.0	n.d.
$R_d [-]$ measured	1.16	1.00	1.45	2.03	2.59	1.09
S_n [%] calculated	0	0	12.3	9.7	9.0	-
$A_{NW} [cm^2/cm^3]calc.$	-	-	-	-	-	-
<i>Column #9b, S_n: 20%, DNAPL coatings, v_a: 1.9 m/day</i>						
$R_d [-]$ expected	1	1.2	1.8	3.4	5.0	n.d.
$R_d [-]$ measured	1.08	1.00	1.52	2.69	3.85	2.69
S_n [%] calculated	0	0	14.2	15.0	14.9	-
$A_{NW} [cm^2/cm^3]calc.$	-	-	-	-	-	531 (55*)
Large scale tank Experiments						
<i>E'-E, $S_n \leq 4.86\%$, DNAPL blobs, v_a: 5 m/day</i>						
$R_d [-]$ expected	1	1.04	1.16	-	1.84	n.d.
$R_d [-]$ measured	1	1.006	1.014	-	1.028	1.04
S_n [%] calculated	0	0.7	0.4	-	0.17	-
$A_{NW} [cm^2/cm^3]calc.$	-	-	-	-	-	19 (2*)

However, the PITT-determined tar oil residual saturation of each experiment conducted during this study was smaller than the actually existing DNAPL-volume. This is believed to be a coupled effect of non-equilibrium tracer transport (resulting in strong asymmetric BTCs) which affects seriously the interpretation of pulse-type tests using the method of temporal moments. Despite the theoretical independence of the first moment from mass transfer limitations, spreading and asymmetry (the second and third moments) will increase with increasing mass transfer limitations (Valocchi, 1985; Brooks et al. 2002, Imhoff et al., 2003) – both is likely to increase truncation errors which consequently result in underestimation of the NAPL saturation. It should be noted, that all column experiments conducted in this study showed strongly asymmetric BTCs which are a clear indicator for mass transfer limitations of

partitioning tracers into the quite viscous coal tar. As a consequence of slow kinetics a reduced tracer retardation, and consequently a smaller calculated saturation compared to the actual one, finally results from the unavoidable truncation of the BTC tailing by the detection limit of the tracer substances.

The following two facts strongly support the hypothesis that the underestimation of tar oil residual saturation in the column experiments conducted within this study is due to mass transfer limitations: a) the decrease in flow velocity from 6.1 m/day to 3.6 m/day increases the average NAPL residual saturation estimate from 0.072 to 0.103 (i.e. 36% and 52% of the true S_n value, 0.20), further improvement is obtained in the NAPL coatings experiment at a flow velocity of 1.9 m/day which gives an average NAPL residual saturation estimate of

14.7% (i.e. 74% of the true S_n value, 0.20) b) the tracers with the smaller partitioning coefficients (K_{NW}) in general tend to predict higher residual NAPL saturations compared to the tracers with the higher K_{NW} (as indicated by the summarized results in Tab.3-3). The latter ones have a higher absorption affinity towards the NAPL and are therefore subject to an increased rate limited sorption/desorption compared to the low K_{NW} tracers.

To overcome these limitations and to improve the estimated residual NAPL saturation Annable et al. (1998) proposed the following exponential extrapolation method: the tailing of each BTC (last 5-10 data points) was fit by a log-linear regression, which was then used to extrapolate the data to very low concentrations (far beyond the detection limit) until the first normalized temporal moment of the respective BTC converged to a constant value. Young et al. 1999 even went further, as they first fitted a 'smooth curve' to the whole measured tracer BTCs before calculating the respective first normalized temporal moment. As both methods ignore the relevant mass transfer process and use subjectively biased curve fitting, they were not applied within this study – the experience of Brooks et al. (2002) support this standpoint, as these authors had to admit that even employing these 'data improvements methods' they were unable to correctly determine an overall residual NAPL saturation (PCE) of 0.3% that was established in a controlled release blind test, while Young et al. (1999) claimed to determine an overall residual NAPL saturation (TCE) of 0.06%.

Meanwhile a number of factors have been identified which may negatively effect the accuracy of residual NAPL saturation determination via PTTs, such as mass transfer limitations (Willson et al., 2000; Imhoff et al.,

2003), nonlinear partitioning behaviour (Wise et al., 1999; Wise, 1999), variable NAPL composition (Lee et al., 1998), background tracer retardation and heterogeneous NAPL distributions (Zahng et al., 2001).

These effects may cause limitations of the applicability of PTTs at coal tar contaminated field sites. Therefore, overall residual coal tar saturation should exceed 5% to obtain significant retardation of the tracers used in this study. The approximate location and extension of the zone of residual DNAPL saturation should be known in advance, and the flow velocity should be smaller than 5 m/day to approach conditions closer to equilibrium. Also, improved evaluation approaches, based for example on fitting of solutions from process-based formulations of the partitioning tracer transport (e.g. based on the model of Wilson et al., 2000), should be developed to account for the truncation of the BTCs.

A general conclusion that can be drawn from the experimental results is, that the PTTs, under the conditions of this study, provided a reliable qualitative confirmation of the presence of DNAPL within the swept zone. The quantitative estimates of DNAPL saturation were subject to varying degrees of underestimation due to mass transfer limitations. The reliability of the PTT method is likely to be better for cases where the investigated DNAPL is less viscous (e.g. creosote), the average grainsize of the aquifer material is smaller than 1.5 mm (which consequently leads to a smaller DNAPL blobs diameter) and the flow velocity ranges beyond the lower end of the investigated bandwidth (i.e. less than 1.9 m/day).

Nevertheless, NAPL saturation measurements obtained with PTTs must be considered as underestimates of actual volumes.

4 Ketone Partitioning Tracer Tests at Borden

This chapter describes the introduction and first-time application of ketones as a new class of highly oxidation resistant partitioning tracers and their controlled use at laboratory scale as well as their final employment as a characterisation tool before oxidizer remedial activities at a manmade source zone at the Borden field site, in the latter case allowing the pre-remedial integral determination of the NAPL (here a multi-component creosote DNAPL) saturation altered by ongoing dissolution/depletion of more than one decade.

4.1 Introduction

The planning of natural gradient field-scale PITTs at 'Testfeld-Süd', i.e. the selection of suitable wells and the design of the input pulse was done with respect to the multi-tracer test results of Bösel et al. (2000). After the final written application for the permission to conduct PITTs at 'Testfeld -Süd' was launched to the concerning authorities (AfU, LGRB) in September 2000, and after additional information was given in a long-lasting further correspondence, the decision making of the authorities was not yet finished in May 2002. Despite the fact that these substances were already used in a field pilot-project in Kehl (Germany), it seems that the absence of regulations on how to handle these new tracer substances completely paralyzed the permission process of the authorities being responsible for the 'Testfeld-Süd'.

Due to this fact, field activities were shifted to overseas, where PITTs are meanwhile sporadic used in the field. In 1991 a known volume of creosote was emplaced at a field research site at

Canadian Forces Base (CFB) Borden, Canada (King and Barker, 1999, King et al., 1999). After ten years of ongoing experiments delineating plume formation, the source zone will now be remediated. Researchers at the University of Waterloo (Prof. J. Barker) intend to oxidise the source by flushing it with potassium permanganate, KMnO_4 . In order to compare its remediation efficiency to other more established procedures it is necessary to monitor the progress and efficiency of this innovative remediation technique. Partitioning tracer tests (PTTs) can be used as a characterisation tool before remedial efforts in order to determine the volume and spatial distribution of NAPL within the subsurface, and afterwards as a performance assessment tool to quantify the remediation results and to determine the quantity of NAPL that still remains in the aquifer (Jin et al., 1995; Cain et al., 2000; Noordman et al., 2000; Jawitz et al., 2000). Due to the experience with PTTs and complex multi component mixtures (coal tar oil) already gained in the previous experiments (Chapter 3) the University of Waterloo was offered the possibility to conduct a PTT in conjunction with the KMnO_4 remediation method at Borden as a joint venture field experiment by scientists of both Universities.

So far a suite of alcohols injected simultaneously with a conservative tracer has been typically used for a PTT; however, due to the highly oxidative nature of the remediation technique proposed, it was realized that tracers with high resistance to oxidation will be needed. Molecules with the carbonyl group rather than the hydroxyl group show a higher persistence in oxidative environment (e.g. Forsey, 2004), but little was known how they might partition into NAPL phases. Using the little data that were available on ketone octanol/water partitioning

coefficients (K_{ow}), some preliminary estimations set the stage for the choice of specific ketones and their subsequent laboratory classification as partitioning tracers.

4.2 Theory

The theoretical background for these tests is almost completely identical to the partitioning tracer test theory described in chapter 3.2 and is therefore not entirely repeated. However, for 3D field site PTTs (especially concerning the manmade Borden source zone with well controlled initial NAPL saturation conditions) it is not only relevant to obtain the average residual saturation (S_n) of the a priori unknown tracer flushed pore volume, but also to get an estimate of the absolute NAPL phase volume (V_n) still being present in the tracer flushed subsurface.

The absolute NAPL phase volume (V_n) determination is based on the first normalized temporal moment of the conservative tracer ($\mu_{conservative}$) and the applied pumping rate (Q) at the respective extraction well during the forced gradient PTT, giving the effective pore volume (V_{eff}) flushed by the tracer test at the respective extraction well (e.g. Annable et al., 1998):

$$V_{eff} = Q \mu_{conservative} \quad (4-1)$$

After the calculation of the average residual saturation (S_n) of the tracer flushed pore volume according to equation 3-7 (see chapter 3.2), the absolute NAPL phase volume (V_n) in the swept zone of the respective well is given by (Annable et al., 1998):

$$V_n = \frac{S_n V_{eff}}{1 - S_n} \quad (4-2)$$

To increase the confidence level of the obtained V_n values it is recommended to base the estimates on the BTC data of multiple partitioning tracers.

4.3 Materials and Methods

Previous PTTs applied in the lab and the field have predominantly used alcohols. Such substances as Isopropanol, 2,3-Dimethyl-2-Butanol, 4- and 6-Methyl-2-Pentanol, 2,4- and 2,2-Dimethyl-3-Pentanol, 1-Hexanol, *n*-Heptanol, and *n*-Octanol have been used with varying success (Piepenbrink et al., 2001; Setarge et al., 1999; Annable et al., 1998; Gierke et al., 1999; Cain et al., 2000).

Due to the highly oxidative nature of the remediation technique (KMnO₄-flushing), it was required to develop a method to use ketones as a new class of partitioning tracers. Due to the double bond located between oxygen and a carbon atom these are in general more resistant to oxidation than alcohols (Forsey, 2004).

4.3.1 Tracer Chemicals

The major chemical and physical properties of the seven selected tracer substances: two conservative tracers (Sodium Chloride, Acetone) and five partitioning tracers (2,4-Dimethyl-3-Pentanone, 2-Heptanone, 5-Methyl-3-Heptanone, 2-Octanone, 3-Methyl-2-Butanone) are listed in Table 4-1. The ketones were purchased as liquids with a purity of >97% (MERCK, Germany). They are characterized by a moderate water solubility, a density lower than water and low Henry's law constants (H). As their Octanol/water partitioning coefficient (K_{ow}) indicates, these substances will partition into NAPL; the K_{NW} values that were determined for the respective tracers and a creosote DNAPL (CARBOCHEM, Mississauga, Ontario, Canada) within this study are already given for comparison (see Tab. 4-1).

Isobutanol was used as a fixed internal standard (ISTD), i.e. it was added to each sample just prior to analysis to further increase the quality of the measurements.

Table 4-1: Physico-chemical properties of (1) conservative tracers: Sodium Chloride (NaCl), Acetone (ACN); (2) partitioning tracers: 2,4-Dimethyl-3-Pentanone (2,4DM3PN) 2-Heptanone (2HPN), 5-Methyl-3-Heptanone (5M3HPN), 2-Octanone (2OCN) and 3-Methyl-2-Butanone (3M2BN) the latter was only used in the field test at Borden; and (3) the fixed internal standard: Isobutanol (IBA), respectively.

Tracer	CAS No.	Formula	MW ^a [g mol ⁻¹]	ρ ^{b 1} [g cm ⁻³]	C _w ^{c 1/2/3} [g L ⁻¹]	LogH ^{d 2} [atm m ³ mol ⁻¹]	K _{OW} ^{e 2/3} [-]	K _{NW} ^f [-]
NaCl	7647-14-5	NaCl	58.4	2.17	358 ^j	-	-	-
ACN	67-64-1	C ₃ H ₆ O	58.1	0.79	++ / 1000 / 219	- 4.40 ^m	0.58 / 0.58	0.38
2,4DM3PN	565-80-0	C ₇ H ₁₄ O	114.2	0.81	insol. / 5.7 / 2.7	- 3.45 ^m	72.4 / 38	117
2HPN	110-43-0	C ₇ H ₁₄ O	114.2	0.82	4.3 / 4.3 / 214	- 3.77 ^m	95.5 / 53.7	202
5M3HPN	541-85-5	C ₈ H ₁₆ O	128.2	0.82	3 / -- / 1.37	- 3.37 ^m	-- / 141.3	567
2OCN	111-13-7	C ₈ H ₁₆ O	128.2	0.82	insol. / 0.90 / 0.88	- 3.72 ^m	234 / 166	894
3M2BN	563-80-4	C ₅ H ₁₀ O	88.2	0.82	-- / -- / 71.87	- 4.01 ^m	6.9 / 4.7	--
IBA	78-83-1	C ₄ H ₁₀ O	74.12	0.80	10.2 / 85.0 / 10.5	- 5.01 ^m	5.8 / 5.8	-

^a Molecular weight; ^b Density (20°C); ^c Water solubility; ^d Henry's law constant; ^e Octanol/water partitioning coefficient; ^f NAPL/water partitioning coefficient determined in this study; ¹ MSDS, MERCK SCHUCHARDT, ² EPI Suite Version 3.12, U.S. EPA (2000) Experimental Data Base, ³ estimated data using EPI Suite Version 3.12, U.S. EPA (2000), ++ miscible with water in any proportions, -- no data available.

4.3.2 Creosote DNAPL

The residual phase used for the emplaced source at Borden is an industrial wood preservative, creosote. As it, like coal tar, has a greater density than water and is composed mainly of hydrophobic compounds, it is classified as a dense nonaqueous phase liquid (DNAPL). It is a complex mixture of many substances and contains by mass approximately 85% PAHs, 10% phenolic compounds and 5% oxygen-, sulphur-, and nitrogen-heteroaromatic compounds (King and Barker, 1999). The material used in this experiment was obtained from Carbochem in Mississauga, Ontario, Canada. In order to monitor the behaviour of additional chemicals, the creosote was amended with certain additional phenolic, heterocyclic and aromatic compounds (King and Barker, 1999).

4.3.3 Analytical Methods

The qualitative as well as quantitative analysis of all organic tracer substances (ketones) was

done by gas chromatography followed by flame ionisation detection.

Freshly sealed individual samples of 10 ml were contained in 20 ml headspace vials for analysis. Within a DANI-HSS3950 automatic sampling unit, the samples were pre-equilibrated at 50°C.

When the sampling needle penetrated the vials, 1ml of headspace gas was transferred into a sampling loop and then over a heated transfer line (142°C) into a GC-FID (Carlo Erba HRGC 5160 Mega Series). After separation, substances were quantified with a Carlo Erba EL 480 FID-detector. Table 4.2 lists the main operating parameters for the GC-FID.

Measurement standards covered the range of foreseeable peak areas of the ketones in order to calibrate the analysis for each measurement series of samples. Also, as a fixed internal standard (ISTD), 1µl of Isobutanol was injected into each sample or standard prior to measurement. Recording of peak areas and final quantification was done using the software package *Chromeleon 6.10 Build 474* by DIONEX.

Table 4-2: GC-FID operating parameters.

GC-FID (HRGC 5160 Mega)	
Injector	
Temperature:	180°C
Carrier:	Nitrogen
Carrier pressure:	Constant at 1.7bar
Split ratio:	1:6
Column	
Type:	WCOT-fused silica CP-Sil-13CB stationary phase
Film thickness:	1.2µm
Internal diameter:	0.32mm
Length:	50m
Oven (temp. program)	
	T ₀ =85°C t ₀ =4min
R ₁ =30°C/min	T ₁ =125°C t ₁ =4min
Detector (FID)	
Temperature:	240°C

The salt, Sodium Chloride (NaCl), was used as additional conservative tracer and was measured (1) by the sum parameter of total electrical conductivity (EC) and (2) as discrete ion species (target analytes: Na⁺ and Cl⁻) via ion chromatography. Detailed descriptions of the employed analytical methods are already given in Chapter 3.3.4.

4.3.4 Batch Experiments

Batch tests were carried out in order to obtain the dimensionless partitioning coefficients (K_{NW}) of the tracers into the DNAPL substance (amended CARBOCHEM industrial creosote) for the following five ketones: Acetone (ACN), 2,4-Dimethyl-3-Pentanone (2,4DM3PN), 2-Heptanone (2HPN), 5-Methyl-3-Heptanone (5M3HPN), and 2-Octanone (2OCN).

The K_{NW} determination batch experiments were done in 20 ml headspace vials, filled with 2 g of amended CARBOCHEM creosote and 20 ml of ketone tracer stock solution (ACN = 1.61 g/l, 2,4DM3PN = 1.00g/l, 2HPN = 1.00g/l, 5M3HPN = 0.20g/l and 2OCN = 0.20g/l). The tracer stock solution was used in dilutions of 5, 40, 70 and 100%. All samples were run in duplicate. The batch test vials were shaken in an overhead shaker at one rotation per second for 72 hours. From experience with the Rüttgers

coal tar oil, this time period was known to be sufficient to allow for equilibrium partitioning conditions to be established. For the final quantification an aqueous phase aliquot of 10 ml from each sample was transferred to a fresh 20 ml headspace vial (the rest was discarded) and analysed by the above described GC-FID method.

4.3.5 Column Experiments

The columns used for these experiments were made of stainless steel and had a length of 12.2 cm, an inner diameter of 4.0 cm and therefore a volume of 153 cm³. Columns were filled in saturated layers with the experiment specific material. A thin layer of Quartz filter gravel was packed on both ends to minimise dead volume and to establish a homogeneous hydraulic head over the entire inlet and outlet areas. All BTCs were dead volume corrected by accounting for the stagnant volume of the tubing used in the set-up and for the remaining volume within the quartz gravel. Brass lid fittings on both ends were used to close the columns and to establish the connection to the rest of the experimental set-up.

All columns were run in an upright position with flow from the bottom to the top and were initially flushed with 1-5 pore volumes (PVs) of Millipore water to establish a constant flow regime and stable background conditions.

As the ketones (in contrast to the previously used alcohols) showed strong sorptive losses when being transferred through the peristaltic pumping tube (Bromley, 2002) the experimental set-up had to be changed again, resulting in column set-up D (see Fig. 4-1). It started with a peristaltic pump (ISMATEC, BVP), which delivered a constant flow rate of Millipore water through a three-way valve to the inlet of the columns. But the tracer injection was now controlled by a syringe pump (TSE SYSTEMS, 540101), connected to the same three-way valve and set to the identical flow rate as the peristaltic pump. Within an experiment the syringe pump

was first used to inject the tracer pulse, after which the three-way valve between the syringe pump, the peristaltic pump and the respective column was manually switched over to allow water flow to be maintained by the peristaltic pump. All connections in contact with the tracer pulse were made of stainless steel or PTFE tubing.

At the column outlet, the effluent flowed to a computer controlled robotic sampler (GILSON ABIMED, Liquid Handler 222 XL), which allowed for continuous sampling. The flow path ended at the needle of the robotic device, which penetrated through the sealed lids of 20 ml headspace vials and filled them to the necessary volume of 10 ml for analysis (for details see individual column specifics). The total tubing dead space of this set-up was 4.01 ml. After recapping, these samples were directly transferred to analysis.

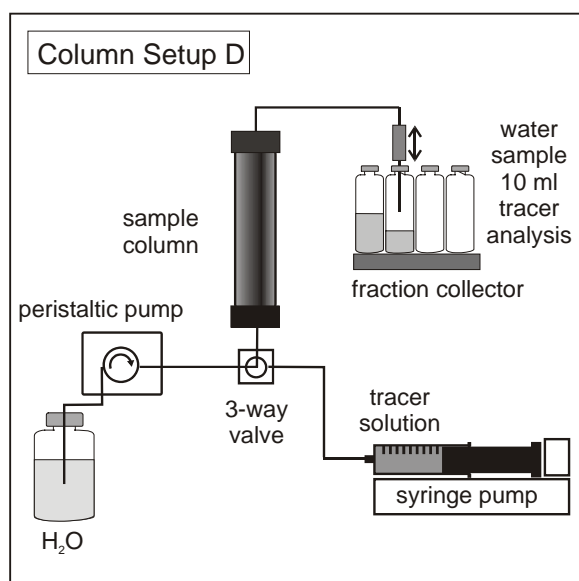


Figure 4-1. Column set-up D: a manually controlled three-way valve was used to switch between the water base flow delivered by the peristaltic pump and the tracer pulse injected by the syringe pump. The whole column effluent was guided to a fraction collector for automatic sampling.

The properties of the individual column tests were according to the settings given in the following:

Column #BSCIV was a blank column packed with the clean aquifer material originating from

the Borden field site ('sand pit'). A constant flow rate of 0.5 m/day was established during the whole experiment: a 10.3 ml (20% PV) tracer pulse was injected with the syringe pump and was then flushed by 200 ml of water (3.9 PVs). In total 84 samples were taken (70x2ml, 14x5ml).

Column #BSCVI was a test with a controlled creosote residual saturation ($S_n = 7\%$). The column was packed with a homogeneous mixture of clean Borden sand and amended CARBOCHEM creosote. A constant flow rate of 0.5 m/day was established, then a 10.4 ml (20% PV) tracer pulse was injected into the column at a flow rate of 0.5 m/day, after which 2250 ml (44 PVs) of water were pumped through the column producing 331 samples.

4.3.6 Field Tests

The DNAPL source zone composed of amended CARBOCHEM creosote was emplaced in the Borden aquifer on August 28, 1991 as shown schematically in Fig. 4-2. The emplacement of 74 kg of Creosote material (at a density of 1.03 g cm^{-3} , giving an absolute NAPL phase volume (V_n) of 71.84 l) resulted in an approximate residual saturation of 7% in the rectangular shaped elements of the source zone, see Fig. 4-2 (King and Barker, 1999). To maintain a similar overall porosity as that of the uncontaminated Borden sand, the addition of the creosote was into a coarse, gravel-like material. This was expected to allow for groundwater flow through the source to be similar to that of undisturbed conditions (King and Barker, 1999). Due to more than 10 years of ongoing dissolution/depletion the recent residual saturation of the emplaced source zone is unknown and had to be determined via PTTs before the planned remediation activities. As the natural gradient flow velocity at the Borden field site is very slow (0.1 m/day) the tests had to be carried out under forced gradient conditions.

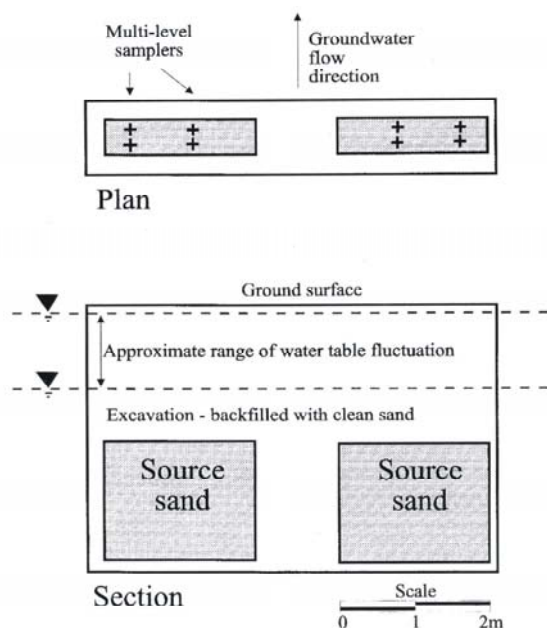


Figure 4-2. The Borden emplaced source: (top) plan view showing multilevel samplers installed through source and (bottom) view of section perpendicular to the direction of groundwater flow (taken from King and Barker, 1999)

The well set-up (4 injection and 4 extraction wells, each operated at a cumulative pumping rate of 3 l/min) and the model predicted flow field during the forced gradient PTT carried out at the Borden emplaced source is shown in Figure 4-3.

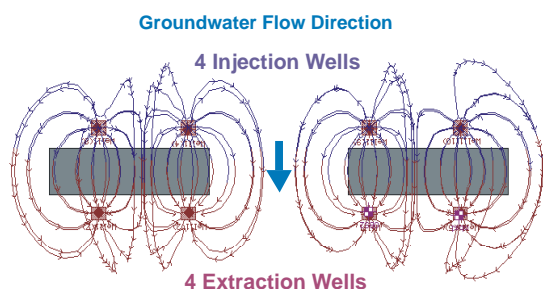


Figure 4-3. The Borden emplaced source: plan view showing the well set-up and modelled flow field during the forced gradient partitioning tracer test (Courtesy of C. Lamarche).

For the pre-remediation PTT the tracer stock solution containing Acetone (1.2 g/l), 3-Methyl-2-Butanone (1 g/l), 2,4-Dimethyl-3-Pentanone (1 g/l), 2-Heptanone (1 g/l) and Sodium-Bromide (1.5 g/l) was injected at a cumulative rate of 3 l/min for 3.9 hours. The cumulative extraction rate (Q) equalled the cumulative injection rate. This flow field was maintained throughout the whole

sampling period which lasted more than 9 days, all samples were taken at a port which cumulated the total outflow of the four extraction wells.

Due to a massive aquifer clogging during and after the KMnO_4 remediation trials, the post-remediation PTTs were not carried out up to now.

4.4 Results and Discussion

After the equilibrium partitioning coefficients (K_{NW}) for the ketones were determined in batch experiments, the PTT column experiments were conducted to compare the breakthrough curves of the reactive tracers with the conservative tracer in different column systems (blank column, column at controlled residual saturation). After the proof of the suitability for the ketones as partitioning tracers was given in the column experiments the subsequent field test was conducted at the emplaced source zone at the Borden field site. The identical creosote DNAPL (amended CARBOCHEM creosote) was employed in all experiments. The specific objectives of the experiments were: (1) to check the suitability of the newly introduced ketone PTTs for complex, multi-component DNAPLs (here creosote), (2) to evaluate the PTT based determination of creosote saturation in presence of natural aquifer material, (3) to check the efficiency of PITTs for the assessment of realistic contaminant scenarios in the field.

4.4.1 Batch Experiments

Batch experiments were performed to determine the linear equilibrium partitioning coefficients (K_{NW}) of the respective partitioning tracer ketones and the amended CARBOCHEM creosote DNAPL which were used in this study. After being shaken for 72 hours (to assure equilibrium conditions) at 5, 40, 70 and 100% of the initial tracer concentration, the linear partitioning coefficients were finally obtained. A representative partitioning isotherm is shown in

Fig. 4-4, the complete K_{NW} dataset is given in Tab. 4-3.

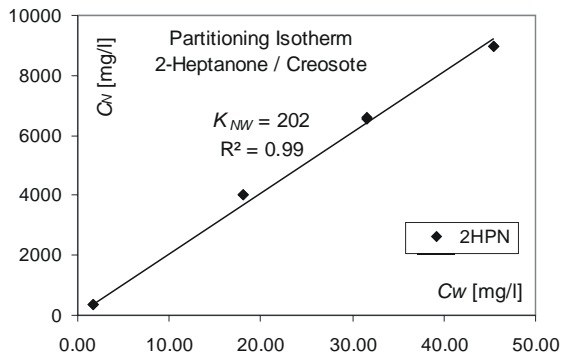


Figure 4-4. Partitioning isotherm of 2-Heptanone (2HPN) at 72 hours.

4.4.2 Column Experiments

Column #BSCIV (S_n : 0%) was conducted at a linear velocity of 0.5 m/day using column set-up D. The measured BTCs of the PT-suite (2,4DM3PN, 2HPN, 5M3HPN, 2OCN) show no significant retardation compared to the conservative tracers IPA and Cl^- , which means all BTCs are almost overlaying each other (see Fig. 4-5). Only the Na^+ and thus also the NaCl (measured via total EC) BTCs display some retardation respectively tailing (most likely due to ion exchange effects). The late peak tailing of the 5M3HPN and 2OCN BTCs decreases somewhat later than the other BTCs (only visible in the semi-logarithmic plot Fig. 4-6), which is likely due to small sorption effects on the Borden aquifer material. The retardation factor of all partitioning tracers are close to 1, what is anticipated for this blank column experiment (see Table 4-3). Consequently the PTT based average tar oil DNAPL saturation estimate is close to the true S_n value (0%). Only the value given by the second conservative tracer, Acetone, is out of reasonable range, but this is due to its very small partitioning coefficient that relates even the smallest retardation (also slight measurement errors) to a high residual saturation. From the overall performance of this experiment it could be concluded that the selected tracers are suitable for being used in the Borden aquifer.

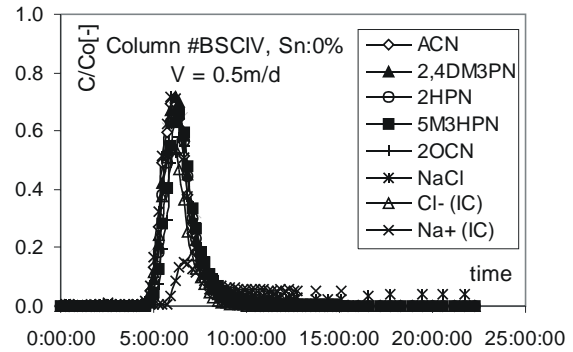


Figure 4-5. BTCs of the conservative tracer NaCl, ACN and the PT-suite passed at 0.5 m/d through blank column #BSCIV (S_n : 0%).

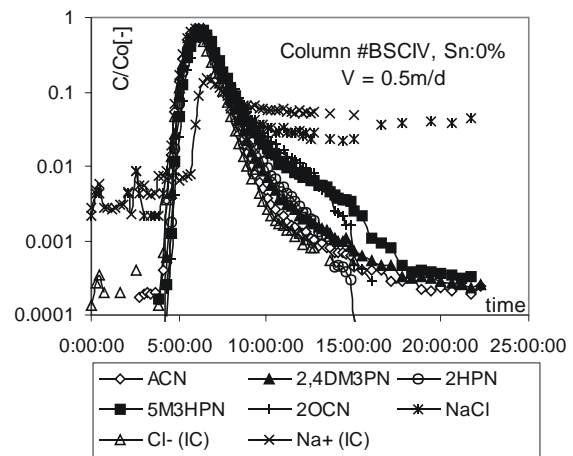


Figure 4-6. Semi-logarithmic BTC-plot of the conservative tracer NaCl, ACN and the PT-suite passed at 0.5 m/d through blank column #BSCIV (S_n : 0%).

The rising shoulders of the determined mass recovery BTCs are steep and almost overlaying each other (see Fig. 4-7), exceptions are NaCl (measured via total EC) which shows the typical positive error in the final plateau height of the mass recovery BTCs, all other deviations from the mass balance are very small and within the overall measurement error of the detection method.

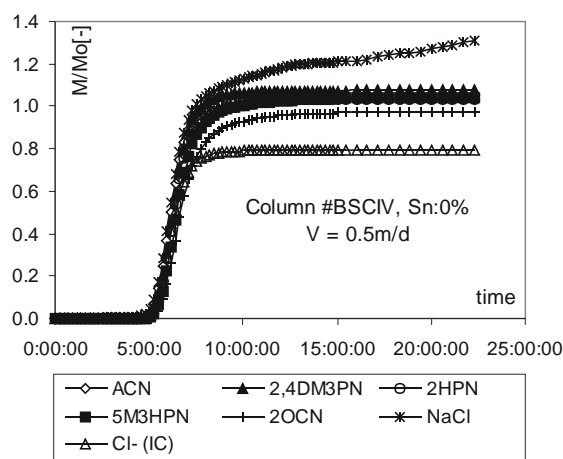


Figure 4-7. Mass recovery of the PT-suite passed through blank column #BSCIV (Sn: 0%).

Column #BSCVI (S_n : 7%, this equals the former initial saturation of the source zone emplaced at Borden), was conducted using column set-up D, at a linear flow-velocity of 0.5 m/day. The measured BTCs of the PT-suite (see Fig. 4-8) show a much higher retardation than in the previous blank experiment. The partitioning tracers are retarded according to the order of their partitioning coefficients and the separation of the individual BTCs starts not only in the rising shoulders of the peaks, but the peaks are almost base-line separated and almost symmetric. However, the retardation factor of all partitioning tracers is still smaller than expected (see Table 4-3). Consequently the PTT based average creosote DNAPL saturation estimate (Eq. 3-7) is only at 4.4% (i.e. 62% of the true S_n value).

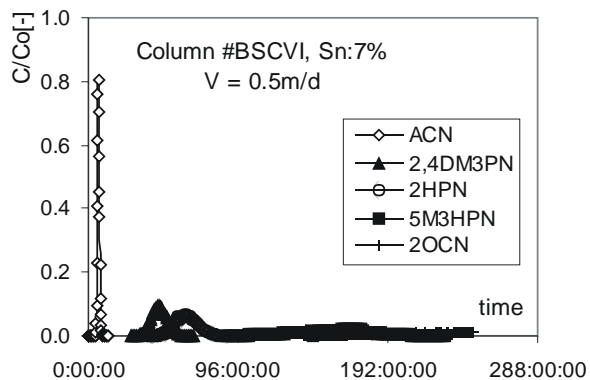


Figure 4-8. BTCs of the conservative tracer ACN and the PT-suite passed at 0.5 m/d through column #BSCVI (Sn: 7%).

The peak of the 2OCN tracer BTC shows a very extreme retardation and was unfortunately truncated by the end of the experimental runtime, i.e. before its concentration actually falls beyond the respective detection limit (see Fig. 4-9).

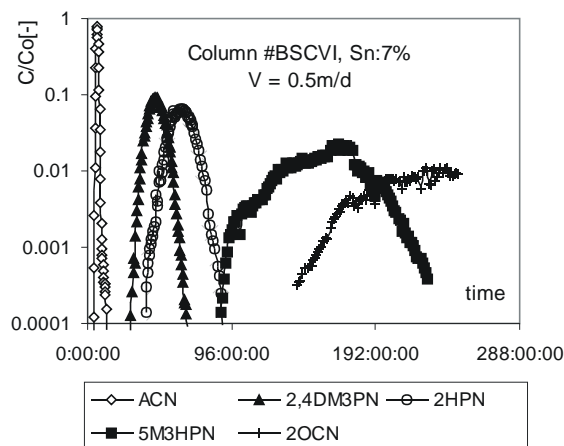


Figure 4-9. Semi-logarithmic BTC-plot of the conservative tracer ACN and the PT-suite passed at 0.5 m/d through column #BSCVI (Sn: 7%).

These results show that the PTT determined residual saturations are smaller than the actually present residual saturation of 7%, but they are quite constant compared to each other (only the saturation of > 3.4% calculated by 2-Octanone (2OCN), is out of range as its BTC is truncated). This underestimation is either due to non-equilibrium conditions within the column experiment (as it was observed for all previous coal tar experiments) or due to some losses of (a) highly volatile creosote compounds during the manual homogenisation procedure of the column material respectively (b) highly soluble creosote compounds during the flushing of the column throughout the experiment. As the chromatographic separation of the individual BTCs is excellent and the shape is quite symmetric, the latter scenario is more realistic. Therefore it can be concluded that 2,4DM3PN and 2HEPN are suitable partitioning tracers for the small residual saturation that is expected for the depleted source zone present at the Borden aquifer. The retardation of 5M3HPN and 2OCN might be too high to be measurable under field conditions, therefore they were cancelled out of the final field tracer suite and replaced by one

potentially less retarding substance (3-Methyl-2-Butanone).

The rising shoulders of the determined PT-suite mass recovery BTCs are strongly retarded compared to the one of the conservative tracer (ACN) once more in the correct order of their partitioning coefficients (Fig. 4-10). Due to the prolonged experimental runtime there is no truncation of the retarded BTCs (except for 2OCN, which is severely truncated) thus the absolute mass recovery is excellent. Due to this fact, the creosote DNAPL saturation estimates of the individual partitioning tracers show only minor deviations from each other (see Table 4-3).

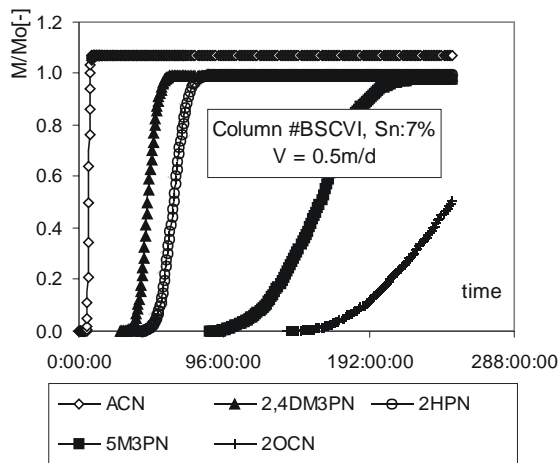


Figure 4-10. Mass recovery of the PT-suite passed through column #BSCVI (Sn: 7%).

4.4.3 Field Experiment

The BTCs of the forced gradient pre-remediation PTT, that were measured at the cumulative output port integrating over the four extraction wells at the emplaced source zone field test in Borden at unknown residual saturation (< 7%, which equals the former initial saturation) are given in Figure 4-11. The measured BTCs of the newly introduced class of ketone PTTs show a significant retardation compared to the conservative tracers (see Fig. 4-11, Tab. 4-3). The partitioning tracers are again retarded according to the order of their partitioning coefficients. However, the peaks are

not base-line separated and they are strongly asymmetric.

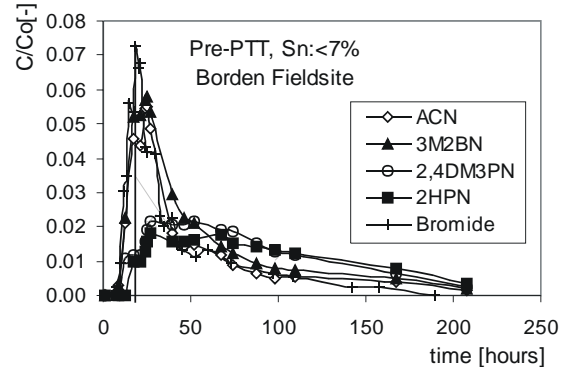


Figure 4-11. BTCs of the forced gradient pre-remediation PTT passed through the source zone at the Borden field site; residual NAPL saturation is unknown, but must be smaller than the initial saturation (Sn: 7%).

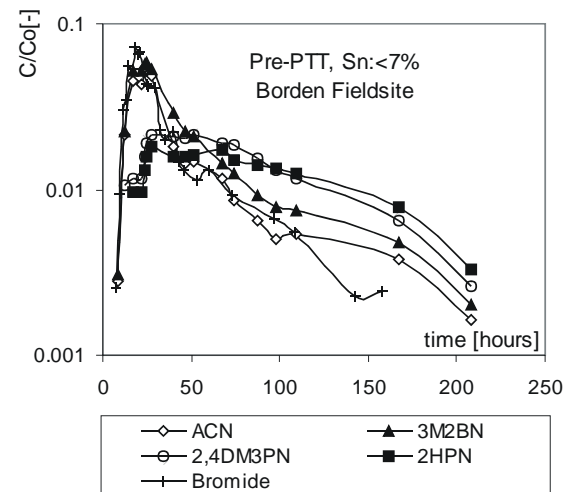


Figure 4-12. Semi-logarithmic BTC-plot of the forced gradient pre-remediation PTT passed through the source zone at the Borden field site; residual NAPL saturation is unknown, but must be smaller than the initial saturation (Sn: 7%).

Once again the saturation determined by the second conservative tracer, Acetone, is out of reasonable range, due to the known fact that its very small partitioning coefficient correlates small measured retardation to a high residual saturation. The deviation of the Acetone BTC from the Bromide BTC seems to be more than the standard measurement artefact and may be caused by biodegradation (either during the experiment or sample storage). Therefore all retardation factor calculations were done with respect to the first conservative tracer, Bromide.

The PTT (2,4DM3PN and 2HPN) based average creosote DNAPL saturation estimate of the whole tracer flushed aquifer volume (Eq. 3-7) is at 0.55%. This value seems pretty low compared to the initial saturation of 7%. However, it has to be recognised that this test was a 3D PTT field experiment under forced gradient conditions, flushing a much larger aquifer volume than just the rectangular source zone itself. Thus the results obtained so far are not directly comparable.

The PTT based average creosote DNAPL saturation estimate of the absolute NAPL phase volume (V_n) still being present in the tracer flushed subsurface has to be based on the first normalized temporal moment of the conservative tracer ($\mu_{conservative} = 2817$ min) and the applied pumping rate ($Q = 3$ l min⁻¹) at the extraction well, giving the effective pore volume ($V_{eff} = 8451$ l) flushed by the tracer test. Using the values of the average residual saturation (S_n) of the tracer flushed pore volume (Eq. 3-7), the average absolute NAPL phase volume estimate (Eq. 4-2) in the swept zone of the respective well is at 46.7 l (i.e. 65% of the initial V_n value of 71.84 l).

With respect to the ageing of the source zone this value seems to be quite reasonable, but further evidence might only be given by the average value of several coring samples that were taken by the University of Waterloo (C. Lamarche) prior to the remediation activities. Unfortunately these cores are not evaluated yet.

The rising shoulders of the determined PT (2,4DM3PN and 2HPN) mass recovery BTCs are significantly retarded compared to the ones of the conservative tracers (Bromide and ACN) again in the correct order of their partitioning coefficients (see Fig. 4-13). The incomplete mass recovery of all tracers shows that the experiment was stopped too early resulting in a truncation of the still rising mass recovery BTCs. However, the overall mass recovery is quite good for a field experiment under 3D forced gradient conditions, where the applied

divergent–convergent flow field with its theoretically infinite flow lines automatically produces a quite considerable tailing of the BTCs.

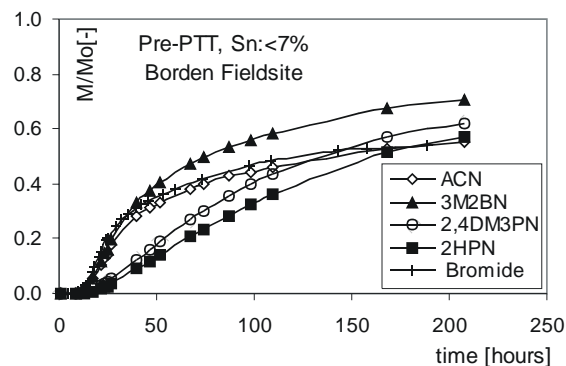


Figure 4-13. Mass recovery of the forced gradient pre-remediation PTT passed through the source zone at the Borden field site.

4.5 Summarized results of the Ketone PTTs

The suitability of the ketones as PTs for complex, multi-component DNAPLs (here creosote) was proven in batch experiments revealing relatively high partitioning coefficient being potentially able to detect low residual creosote saturations. Despite these relatively high K_{NW} values the PTs showed no significant retardation when being passed through a blank column containing natural aquifer material (clean Borden sand), which demonstrated their suitability to be used in field experiments at Borden without detecting false positive saturation values. The PTT based average creosote DNAPL saturation estimate in the column experiment at controlled creosote saturation in presence of natural aquifer material was at 62% of the true S_n value, i.e. the DNAPL saturation was underestimated but clearly positive. The efficiency of the ketone PTTs for the assessment of realistic contaminant scenarios in the field was clearly given by the reasonable average absolute NAPL phase volume estimate in the PTT swept zone (65% of the initial V_n value).

Table 4-3. Summarized results of the batch, column and field experiments

Experiment ↓ / Tracer →	Cl ⁻ / Br ⁻	ACN	2,4DM3PN	2HEPN	5M3HPN	2OCN
Batch Experiments						
$K_{NW}[-]$	0	0.38	117	202	567	894
Column Experiments						
<i>Column #BSCIV, Sn: 0%, and v_a: 0.5 m/day</i>						
$R_d [-]$ expected	1	1	1	1	1	1
$R_d [-]$ measured	1	1.02	1.05	1.05	1.10	1.13
S_n [%] calculated	0	5.0	0.04	0.02	0.01	0.01
<i>Column #BSCVI, Sn: 7%, and v_a: 0.5 m/day</i>						
$R_d [-]$ expected	1	1.02	9.8	16.2	43.6	68.3
$R_d [-]$ measured	-	1	7.1	9.8	24.3	>32.8
S_n [%] calculated	0	0	5.0	4.2	4.0	>3.4
Field Experiment						
<i>Pre-PTT, at Borden Fieldsite, $S_n < 7\%$</i>						
$R_d [-]$ expected	1	<1.02	<9.8	<16.2	-	-
$R_d [-]$ measured	1	1.23	1.76	1.94	-	-
S_n [%] calculated	0	37.6	0.6	0.5	-	-

So it can be concluded, that the selected ketones were not only successfully implemented in the PTT methodology but were also successfully used in their first-time pre-remediation PTT field test at the CFB Borden field site in Canada.

A general conclusion that can be drawn from the experimental results is, that the ketone PTTs, under the conditions of this study, provided a reliable qualitative confirmation of the presence of creosote DNAPL within the tracer swept zone. The quantitative estimates of DNAPL saturation were once again subject to a certain degree of underestimation but this is now more likely due to losses of (a) highly volatile creosote compounds during the manual homogenisation procedure of the column material respectively or (b) highly soluble creosote compounds during the flushing of the column throughout the experiment. As it should be noted, that the column experiment conducted in this study showed highly symmetric PTT BTCs which are an indicator for equilibrium

mass transfer conditions of partitioning tracers into the less viscous creosote. However, in comparison to the alcohols and the quite viscous tar oil DNAPL used in Chapter 3, the absolute reliability of the newly introduced ketone PTT method was not really improving; despite the fact, that the investigated DNAPL (creosote) is less viscous than tar oil, the average grain size of the Borden aquifer material is much smaller than 1.5 mm (which consequently leads to a smaller DNAPL blobs diameter) and the flow velocity was only at 0.5 m/day.

Nevertheless, due to the higher partitioning coefficients of the ketones the limitations of the applicability of PTTs at DNAPL contaminated field sites stated in Chapter 3 were clearly overcome: an overall residual creosote saturation as low as 0.55% was sufficient to obtain significant retardation of the ketone tracers used in the Borden field experiment, i.e. the lower detection limit of the PTT method was improved by a factor of ten.

5 Summary and Conclusions

The application of sophisticated analysis techniques, lab- and field-scale experiments in combination with new developed and refined PTT, PITT and different NAPL dissolution simulation methods throughout the research of this thesis allowed the investigation of the governing contaminant release processes within DNAPL source zones.

The application of a numerical model for multi-component NAPL dissolution in porous media (BIONAPL3/D) gave further insight into equilibrium and non-equilibrium processes during NAPL dissolution. After completion of the calibration the code was used in forward modelling runs of multi-component NAPL dissolution. The validation via measured data revealed a convincing performance. Furthermore the hypothesis of re-partitioning, which leads to an enrichment of former depleted residual NAPL phase with soluble compounds delivered in the aqueous phase from upgradient, was confirmed in numerical experiments.

A suite of alcohols and an anionic surfactant were combined in PITT experiments to determine the NAPL saturation and the interfacial area between NAPL and water phase. Besides the NAPL composition these two variables are the governing parameters for the long-term dissolution behaviour of the source zone and are therefore important prerequisites for the detailed numerical modelling of NAPL dissolution time scales. The PITTs in conjunction with coal tar NAPL were successfully tested in extended lab studies at various scales (batch, column, large scale tank). As the local authorities are obviously unable to make their decision about the application of these new tracer substances, the permission

process for the final field application at the 'Testfeld-Süd' is still in progress.

Due to this fact the field activities were shifted to overseas, to the emplaced source zone at the field research site Canadian Forces Base (CFB) Borden, Canada. The field tests were performed in a joint venture with researchers from the University of Waterloo (Prof. J. Barker), who investigated the use of an oxidative source remediation technique. The tracer technique was intended for a remediation efficiency assessment by pre- and post-remediation PTTs. With regard to the highly oxidative nature of the proposed remediation technique, a new tracer group with more resistance to oxidation had to be introduced. The selected ketones were successfully implemented in the PTT methodology (batch and column experiments with original creosote and Borden aquifer material) and finally used in an efficient pre-remediation field test at CFB Borden, Canada.

The results of this research significantly improved the understanding of source zone characterization via partitioning and interfacial tracer tests, the contaminant release processes involving residual NAPL at field scale and enhanced the insight of the long-term attenuation processes of multi-component NAPL source zones.

References

- Adamson, A. W. (1982): *Physical Chemistry of Surfaces*. 'The drop weight method' S 21-23 and 'The nature and thermodynamics of liquid interfaces' S. 53-105
- Annable, M. D., Jawitz, J. W., Rao, P. S. C., Dai, D. P., Kim, H. K., Wood, A. L. (1998): Field evaluation of interfacial and partitioning tracers for characterization of effective NAPL-water contact areas. *Ground Water*. 36(3), 495-502
- Annable, M. D., Rao, P. S. C., Hatfield, K., Graham, W. D., Wood, A. L., Enfield, C. G. (1998): Partitioning tracers for measuring residual NAPL: field-scale test results.- *Journal of Environmental Engineering* 124 (6), 498-503
- Annable, M.D., Rao, P.S.C., Kim, H., Saripalli, K.P.(1998): Response to comment on "estimation of nonaqueous phase liquid-water interfacial areas in porous media following mobilisation by chemical flooding" .- *Environ. Sci. Technol.* 32(23), 3838-3839
- Anwar, A. H. M. F., Bettahar, M., Madzubayashi, U. (2000): A method for determining air/water interfacial area in variably saturated porous media.- *J. Contam. Hydrol.* 43, 129-146
- Bear, J., *Dynamics of Fluids in Porous Media*, American Elsevier Pub. Co., New York, 1972.
- Bösel, D., Herfort, M., Ptak, Th., Teitsch, G. (2000): Design, performance, evaluation and modelling of a natural gradient multitracer transport experiment in a contaminated heterogeneous porous aquifer. In: Dassargues, A. (Ed.), *Tracers and Modelling in Hydrogeology. Proceedings of TraM'2000, the international Conference on Tracers and Modelling in Hydrogeology*. Liège, Belgium, May 2000. IAHS Publ., Vol. 262, 45-51
- Bradford, S. A., Phelan, Th. J., Abriola, L. M. (2000): Dissolution of residual tetrachloroethylene in fractional wettability porous media: Correlation development and application.- *J. Contam. Hydr.* 45, 35-61
- Bromley, S. (2001): Ketones as partitioning tracers: Laboratory experiments and quantitative modelling. M. Sc. Thesis, Center for Applied Geoscience, University of Tübingen
- Brooks, M.c., Annable, M.D., Rao, P.S.C., Hatfield, K., Jawitz, J.W., Wise, W.R., Wood, A.J., Enfield, C.G.(2002): Controlled release, blind tests of DNAPL characterization using partitioning tracers.- *J. Contam. Hydrol.* 59, 187-210.
- Brown, C.L., Pope, G.A., Abriola, L.M., Sepehrnoori, K. (1994): Simulation of surfactant-enhanced aquifer remediation.- *Water Resour. Res.* 30, (2), 2959-2977
- Cain, R. B., Johnson, G. R., McCray, J. E., Blanford, W. J., Brusseau, M. L.(2000): Partitioning Tracer tests for evaluating remediation performance .- *Ground Water*. 38(5), 752-761
- Chen, L., Knox, R.C. (1997): Using vertical circulation wells for partitioning tracer tests and remediation of DNAPLs. *Ground Water Monit. Remediat.* 17(3):161-168., 1069-3629
- Dai, D., Barranco JR., F. T., Illangasekare, T. H. (2001): Partitioning and interfacial tracers for differentiating NAPL entrapment configuration: column-scale investigation.- *Environ. Sci. Technol.* 35 (24), 4894-4899
- Davis, B.M., Istok, J.D., Semprini, L.(2002): Push-pull partitioning tracer tests using radon-222 to quantify non-aqueous phase liquid contamination.- *J. Contam. Hydrol.* 58, 129-146

- Deeds, N. E., McKinney, D. C., Pope, G.A. (2000): Laboratory characterization of non-aqueous phase liquid/tracer interaction in support of a vadose zone partitioning interwell tracer test.- J. Contam. Hydr. 41, 193-204
- Deeds, N., Pope, G.A., McKinney, G.C. (1999): Vadose Zone characterisation at a contaminated field site using partitioning interwell tracer technology .- Environ. Sci. Technol. 33 (16), 2745-2751
- Delshad, M., Pope, G.A., Sepehrnoori, M. (1996): A compositional simulator for modelling surfactant-enhanced aquifer remediation.- J. Contam. Hydrol. 23, 303-327
- Dwarakanath, V., Deeds, N., Pope, G.A. (1999): Analysis of partitioning interwell tracer test.- Environ. Sci. Technol. 33 (21), 3829-3836
- Eberhardt, C., Grathwohl, P. 2002. „Time scales of organic contaminant dissolution from complex source zones: coal tar pools vs. blobs”. J. Contam. Hydr. 59, 45-66
- Ferreira-Reckhorn, S. B., Zuquette, L. V., Grathwohl, P. (2001): Experimental investigations of oxygenated gasoline dissolution. – Journal of Environmental Engineering. 127 (3), 208-216
- Field, J.A., Istok, J.D.(1998): Comment on “estimation of nonaqueous phase liquid-water interfacial areas in porous media following mobilisation by chemical flooding” .- Environ. Sci. Technol. 32(23), 3836-3837
- Finkel, M., Eberhardt, C., Teutsch, G., Grathwohl, P., Liedl, R. 2001. „Langzeitentwicklung der Schadstoffkonzentrationen aus Schadensherden“. LAG 01-01/2051 FKZ 02WT9714/0
- Frind, E. O., Molson, J. W., Schirmer, M. Guiguer, N. (1999): Dissolution and mass transfer of multiple organics und field conditions: the Borden emplaced source. Water. Resour.Research 35 (3), 683-694
- Gierke, J. S., Sanders, D. L., Perram, D. L.(1999): Laboratory studies of aqueous partitioning tracer tests for measuring nonaqueous phase liquid volumes.- Water Environment Research. 71(4), 465-474
- Grathwohl, P. (1998): Diffusion in natural porous media: Contaminant transport, Sorption / Desorption and Dissolution Kinetics. Kluwer academic publishers, Boston. 207pp.
- Haggerty, R., Schroth, M. H., Istok, J. D.(1998): Simplified method of ‘push-pull’ test data analysis for determining in situ reaction rate coefficients.- Ground Water 36(2) 314-324
- Hall, S. H. (1993): Single well tracer tests in aquifer characterisation. –Groundwater Monitoring and Remediation Spring 1993 118-124
- Hall, S. H. (1996): Practical single well tracer methods for aquifer testing. Workshop at the Tenth National Outdoor Action Conference and Exposition, May 13-15, 1996, Las Vegas. 13S.
- Hunkeler, D., Hoehn, E., Höhener, P., Zeyer, J. (1997): 222Rn as a Partitioning Tracer to detect diesel fuel Contaminatio in Aquifers: Laboratory study and field observations. .- Environ. Sci. Technol. 31(11), 3180-3187
- Imhoff, P. T, Miller, C. T.(1996): Dissolution fingering during the solubilisation of nonaqueous pahse liquids in saturated porous media 1. Model predictions. Water Res. Research 32 (7) 1919-1928
- Imhoff, P. T., Arthur, M. H., Miller, C. T. (1998): Complete dissolution of trichloroethylene in saturated porous media.- Environ. Sci. Technol. 32(16), 2417-2424
- Imhoff, P. T., Thyrum, G. P., Miller, C. T.(1996): Dissolution fingering during the solubilisation of nonaqueous pahse liquids in saturated porous media 2. Experimental observations Water Res. Research 32 (7) 1929-1942

- Imhoff, P.T., Pirestani, K., Jafapour, Y., Spivey, K.M. (2003): Tracer interaction effects during partitioning tracer tests for NAPL detection.- *Environ. Sci. Technol.* 37(7), 1441-1447
- Istok, J.D., Field, J.A., Schroth, M.H., Davis, B.M., Dwarakanath, V. (2002): Single-well Push-pull partitioning tracer tests for NAPL detection in the subsurface.- *Environ. Sci. Technol.* 36(12), 2708-2716
- James, A. I., Graham, W. D., Hatfield, K., Rao, P.S. C., Annable, M. D.(2000): Estimation of spatially variable residual nonaqueous phase liquid saturation in nonuniform flow fields using partitioning tracer data. *Water Resources Research.* 36 (4) 999-1012
- James, A.I., Graham, W.D., Hatfield, K., Rao, P.S.C. (1997): Optimal estimation of residual non-aqueous phase liquid saturations using partitioning tracer concentration data.- *Water Resour. Res.* 33, (12), 2621-2636.
- Jawitz, J. W., Sillan, R. K., Annable, M. D., Rao, P. S. C., Warner, K. (2000): In situ alcohol flushing of a DNAPL source zone at a dry cleaner site.- *Environ. Sci. Technol.* 34(17), 3722-3729
- Jin, M., Butler, G.W., Jackson, R.E., Mariner, P.E., Pickens, J.F., Pope, G.A., Brown, C.L., McKinney, D.C. (1997): Sensitivity models and design protocol for partitioning tracer tests in alluvial aquifers. *Ground.Water.* 35(6), 964-972
- Jin, M., Delshad, M., Dwarakanath, V., McKinney, D. C., Pope, G. A., Sepehrnoori, K., Tilburg, C., E., Jachson, R. E. (1995): Partitioning tracer test for detection, estimation and remediation performance assessment of subsurface nonaqueous phase liquids.- *Water Resources Research* 31 (5), 1201-1211
- Khachikian, C., Harmon, T. C. (2000): Nonaqueous phase Liquid dissolution in porous media: current state of knowledge and research needs. *Transport in Porous Media* 38, 3-28
- Kim, H., Rao, P. S. C., Annable, M. D.(1997): Determination of effective air-water interfacial area in partially saturated porous media using surfactant adsorption. *Water Res. Research* 33 (12) 2705-2711
- Kim, H., Rao, P.S.C., Annable, M.D. (1999): Consistency of the interfacial tracer technique: experimental evaluation.- *J. Contam. Hydrol.* 40, 79-94.
- King, M. W. G., Barker, J. F. (1999): Migration and natural fate of a coal tar creosote plume 1. Overview and plume development.- *J. Contam. Hydr.* 39, 249-279
- King, M. W. G., Barker, J. F., Devlin, J. F., Butler, B. J. (1999): Migration and natural fate of a coal tar creosote plume 2. Mass balance and biodegradation indicators.- *J. Contam. Hydr.* 39, 281-307
- Kunstmann, H., Kinzelbach, W., Marschall, P., Li, G. (1997): Joint inversion of tracer tests using reversed flow fields.- *J. Contam. Hydr.* 26, 215-226
- Lane, W.F.; Loehr, R.C. (1992): Estimating the Equilibrium Aqueous Concentration of Polynuclear Aromatic Hydrocarbons in Complex Mixtures.- *Environ. Sci. Technol.* 26 (5) 983-990.
- Lee, C. M., Meyers, S. L., Wright Jr, C. L., Coates, J. T., Haskell, P.A., Falta Jr., R. W. (1998): NAPL compositional changes influence partitioning Coefficients.- *Environ. Sci. Technol.* 32(22), 3574-3578
- Lee, L.S.; Suresh, P.; Okuda, J. (1992): Equilibrium Partitioning of Polycyclic Aromatic Hydrocarbons from Coal Tar into Water.- *Environ. Sci. Technol.* 26 (11), 2110-2115.
- Loyek, D. (1998): Lösung und Lösungsraten polyzyklischer aromatischer Kohlenwasserstoffe aus verschiedenen Teer- und Creosotphasen.- Dissertation, Tübinger Geowissenschaftliche Arbeiten, Reihe C, Nr. 44; 81 S., Tübingen.

- Mariner, P.E., Jin, M., Studer, J. E., Pope, G.A. (1999): The first vadose zone partitioning interwell tracer test for nonaqueous phase liquid and water residual.- *Environ. Sci. Technol.* 33 (16), 2825-2828
- Meinardus, H. W., Dwarakanath, V., Ewing, J., Hirasaki, G. J., Jackson, R. E., Jin, M., Ginn, J. S., Londergan, J. T., Miller, C. A., Pope, G. A. (2002): Performance assessment of NAPL remediation in heterogeneous alluvium.- *J. Contam. Hydr.* 54, 173-193
- Miller, C.T.; Poirier-McNeill, M.M.; Mayer, A.S. (1990): Dissolution of Trapped NAPL: Mass Transfer Characteristics.- *Water Resour. Res.* 26 (11), 2783-2796.
- Molson, J. (2000): Numerical simulation of hydrocarbon fuel dissolution and biodegradation in groundwater, Ph.D. Thesis, Dept. of Earth Sciences, University of Waterloo
- Molson, J. (2001): BIONAPL/3D: A 3D model for groundwater flow, multi-component NAPL dissolution and biodegradation. User Guide. 46pp
- Mueller, J.G., P.J. Chapman, and P.H. Pritchard (1989) Creosote-contaminated sites. *Environ. Sci. Technol.*, 23(10):1197-1201
- Mukherji, S., Peters, C. A., Weber Jr., W. J. (1997): Mass transfer of polynuclear aromatic hydrocarbons from complex DNAPL mixtures.- *Environ. Sci. Technol.* 31(2), 416-423
- Nambi, I. M., Powers, S. E. (2000): NAPL dissolution in heterogeneous systems: an experimental investigation in a simple heterogeneous system.- *J. Contam. Hydr.* 44, 161-184
- Nelson, N. T., Brusseau, M. L. (1996): Field study of the partitioning tracer method for detection of dense nonaqueous phase liquid in a Trichlorethene-contaminated aquifer, *Environ. Sci. Technol.* 30 (9), 2859-2863
- Nelson, N. T., Brusseau, M. L., Carlson, T. D. (1999): A gas phase partitioning tracer method for the in situ measurement of soil water content. - *Water Resour. Res.* 35, (12), 3699-3707
- Nelson, N.T., Oostrom, M., Wietsma, T.W., Brusseau, M.L. (1999): Partitioning tracer method for the insitu measurement of DNAPL saturation: influence of heterogeneity and sampling method. - *Environ. Sci. Technol.* 33 (22), 4046-4053
- Noordman, W. H., De Boer, G. J., Wietzes, P., Volkering, F., Janssen, D. B. (2000): Assesment of the use of partitioning and interfacial tracers to determine the content and mass removal rates of nonaqueous phase liquids.- *Environ. Sci. Technol.* 34(20), 4301-4306
- Novakowski, K. S., Lapcevic, P. A., Voralek, J.W., Sudicky, E. A. (1998): A note on a method for measuring the transport properties of a formation using a single well.- *Water Resour. Res.* 34, (5), 1351-1356
- Piepenbrink, M., Ptak, T., Grathwohl, P. (2000): Partitioning and Interfacial Tracer Tests for NAPL source zone characterisation at a former gasification plant, in: Bjerg, P.L., Engesgard, P., Krom, Th. D. (eds.), *Groundwater 2000*, proceedings of the international conference on groundwater research, Copenhagen, Denmark, 6-8 June 2000. Balkema, Rotterdam., pp. 117-118.
- Piepenbrink, M., Ptak, T., Grathwohl, P. (2001a): Natural gradient partitioning and interfacial tracer tests for NAPL source zone characterisation at a former coal gasification plant. Conference pre-prints of the 3rd international Conference on Groundwater Quality, June 18-21, Sheffield, UK, pp. 122-124.
- Piepenbrink, M., Ptak, T., Grathwohl, P. (2001b): Field applicability of Partitioning and Interfacial Tracer Tests for NAPL source zone characterisation at a former gasification plant, in: Seiler, KP, Wohnlich, S. (eds), *New approaches in characterizing groundwater flow*, Volume 1. Swets & Zeitlinger, Lisse, pp. 159-163.

- Piepenbrink, M., Ptak, T., Grathwohl, P. (2001c): Validation of Partitioning and Interfacial Tracer Tests for NAPL source zone characterisation at former gasification plants, in: Wiesner, J (ed.), Sanierung und Entwicklung teerkontaminierter Standorte - Prospects and limits of natural attenuation at tar oil contaminated sites. Dechema, Frankfurt a. M., pp. 399-406.
- Powers, S.E.; Abriola, L.M.; Dunkin, J.S.; Weber, W.J.Jr. (1994): Phenomenological Models for Transient NAPL-Water Mass Transfer Processes.- J. Contam. Hydr. 16, 1-33.
- Ptak, T., M. Piepenbrink, E. Martac (2004): Tracer tests for the investigation of heterogeneous porous media and stochastic modelling of flow and transport—a review of some recent developments. Journal of Hydrology Vol. 294 Page 122–163
- Rao, P. S. C., Annable, M. D., Kim, H. (2000): NAPL source zone characterisation and remediation technology performance assessment : recent developments and applications of tracer techniques .- J. Contam. Hydr. 45, 63-78
- Rao, P. S. C., Annable, M. D., Sillan, R. K., Dai, D., Hatfield, K., Graham, W. D., Wood, A. L., Enfield, C. G. (1997): Field-scale evaluation of in situ cosolvent flushing for enhanced aquifer remediation. Water Res. Research 33 (12) 2673-2686
- Saripalli, K. P., Annable, M. D., Rao, P. S. C., (1997): Estimation of non-aqueous phase liquid (NAPL-) water interfacial areas in porous media following mobilization by chemical flooding, Environ. Sci. Technol. 31, 3384-3388
- Saripalli, K. P., Kim, H. K., Annable, M. D., Rao, P. S. C., (1997): Measurement of specific fluid-fluid interfacial areas of immiscible fluids in porous media, Environ. Sci. Technol. 31 (3), 932-936
- Saripalli, K. P., Rao, P. S. C., Annable, M. D. (1998): Determination of specific NAPL-water interfacial areas of residual NAPLs in porous media using the interfacial tracers techniques.- J. Contam. Hydrol. 30, 375-391.
- Schroth, M. H., Istok, J.D., Haggerty, R. (2001): In situ evaluation of solute retardation using single-well push-pull tests.- Advances in Water Resources 24 , 105-117
- Semprini, L., Hopkins, O. S., Tasker, B. R. (2000): Laboratory, Field and Modeling Studies of Radon-222 as a natural Tracer for monitoring NAPL Contamination.- Transport in Porous Media. 38, 223-240
- Setarge, B., Danzer, J., Klein, R., Grathwohl, P. (1999): Partitioning and interfacial tracers to characterize non-aqueous phase liquids (NAPLs) in natural aquifer material. Phys. Chem. Earth (B). 24(6) 501-510
- Sheely, C. Q. (1978): Description of field tests to determine residual oil saturation by single-well tracer method. – Journal of petroleum technology February 1978, 194-202
- Sillan, R. K., Annable, M. D., Rao, P. S. C., Dai, D., Hatfield, K., Graham, W. D., Wood, A. L., Enfield, C. G. (1998): Evaluation of in situ cosolvent flushing dynamics using a network of spatially distributed multilevel samplers. Water Res. Research 34 (9) 2191-2202
- Tang J. S. (1992): Interwell tracer tests to determine residual oil saturation to waterflood at Judy Creek BHL ‘A’ Pool.- The Journal of Canadian Petroleum Technology 31 (8), 61-70
- Tomich, J. F., Dalton, R. L., Deans, H. A., Shallenberger, L. K. (1973): Single well tracer method to measure residual oil saturation. – Journal of petroleum technology February 1973, 211-218
- Valocchi, A. J. (1985): Validity of the local equilibrium assumption for modelling sorbing solute transport through homogeneous soils.- Water Resour. Res. 21, (6), 808-820
- Vulava, V. M., Perry, E. B., Romanek, C. S., Seaman, J. C. (2002): Dissolved gases as partitioning tracers for determination of hydrogeological parameters.- Environ. Sci. Technol. 36 (2), 254-262

- Willson, C. S., Pau, O., Pedit, J. A., Miller, C. T. (2000): Mass transfer rate limitation effects on partitioning tracer tests.- *J. Contam. Hydr.* 45, 79-97
- Wilson, D. J., Burt, R. A., Hodge, D. S. (2000): Mathematical Modeling of column and field dense nonaqueous phase liquid tracer tests.- *Environmental Monitoring and Assessment* 60(4), 181-216
- Wilson, R. D., Mackay, D. M. (1995): Direct detection of residual nonaqueous phase liquid in the saturated zone using SF₆ as a partitioning tracer, *Environ. Sci. Technol.* 29, 1255-1258
- Wise, W.R. (1999): NAPL characterisation via partitioning tracer tests: quantifying effects of partitioning nonlinearities.- *J. Contam. Hydrol.* 36, 167-183.
- Wise, W.R., Dai, D., Fitzpatrick, E. A., Evans, L.W., Rao, P.S.C., Annable, M.D. (1999): Non-aqueous phase liquid characterisation via partitioning tracer tests: a modified Langmuir relation to describe partitioning nonlinearities.- *J. Contam. Hydrol.* 36, 153-165.
- Young, C. M., Jackson, Jin, M., Londergan, J. T., Mariner, P. E., Pope, G. A., Anderson, F. J., Houk, T. (1999): Characterization of a TCE DNAPL zone in alluvium by partitioning tracers. -*Groundwater Monitoring and Remediation* 19 (1), 84-94
- Zamfirescu, D. (2000). Release and fate of specific organic contaminants at a former gasworks site.- *Tübinger Geowissenschaftliche Arbeiten (TGA)*, C 53. 96 pp.
- Zamfirescu, D. and P. Grathwohl (2001): Occurrence and Attenuation of Specific Organic Compounds in the Groundwater Plume at a Former Gasworks Site. *J. Contam. Hydrol.* 53, 407-427.
- Zhang, Y., Graham, W. D. (2001): Partitioning tracer transport in a hydrogeochemically heterogeneous aquifer.- *Water Resour. Res.* 37, (8), 2037-2048
- Zhang, Y., Graham, W. D. (2001): Spatial characterization of a hydrogeochemically heterogeneous aquifer using partitioning tracers: optimal estimation of aquifer parameters.- *Water Resour. Res.* 37, (8), 2049-2063

Lebenslauf

Persönliche Daten:

Name: Piepenbrink
Vorname: Matthias
Geburtsdatum, -ort: 15.03.1972, Lörrach
Anschrift: Jahnstraße 2/1
72131 Ofterdingen

Schulbildung:

1978 - 1982 Grundschole Inzlingen
1982 - 1991 Hans-Thoma-Gymnasium Lörrach
14.06.1991 Abitur

Hochschulbildung:

WS 1992/93 Studienbeginn an der Eberhard-Karls-Universität Tübingen
Fachrichtung: Geologie; Diplom

11.01.1995 Vordiplom

21.10.1998 Diplom

01.1999 – 05.2002 Doktorand am Zentrum für Angewandte Geowissenschaften
Thema der Promotion: Characterization of complex non-aqueous phase liquids (NAPLs) in the subsurface environment: partitioning and interfacial tracer tests & numerical dissolution assessment
Eberhard-Karls-Universität, Tübingen
Betreuer: Prof. Dr. Peter Grathwohl
PD Dr.-Ing. habil. Thomas Ptak

seit 06.2002 „Associate Researcher“ am ZAG
Eberhard-Karls-Universität, Tübingen
Arbeitsgruppe: Prof. Dr. Peter Grathwohl